ISSN 1694-7398
journals.manas.edu.kg

June 2020
Volume 8, Issue 1

MANAS JOURNAL OF ENGINEERING

MJEN

BISHKEK 2020

KYRGYZ TURKISH MANAS UNIVERSITY
MANAS JOURNAL OF ENGINEERING (MJEN)

ISSN: 1694- 7398
Year: 2020
Volume: 8
Issue: 1
http://journals.manas.edu.kg
journals@manas.edu.kg

PUBLICATION PERIOD

Manas Journal of Engineering (MJEN) is published twice year, MJEN is a peer reviewed journal.

CORRESPONDENCE ADDRESS
Kyrgyz Turkish Manas University
Chyngyz Aitmatov Avenue 56 Bishkek, KYRGYZSTAN
URL: http://journals.manas.edu.kg
e-mail: journals@manas.edu.kg
Tel : +996 312 492763- Fax: +996 312 541935

KYRGYZ TURKISH MANAS UNIVERSITY
MANAS JOURNAL OF ENGINEERING (MJEN)

CONTENT

MANAS Journal of Engineering
ISSN 1694-7398 | e-ISSN 1694-7398

Volume 8 (Issue 1) (2020) Pages 1-10

Carbon nanotube supported direct borohydride fuel cell anode catalysts: the effect of catalyst loading

Hilal Demir Kıvrak[1,*], Aykut Caglar[1], Tulin Avcı Hansu[1,2], Omer Sahin[2]

[1]Department of Chemical Engineering, Faculty of Engineering, Van Yuzuncu Yil University, Van, Turkey, hilalkivrak@gmail.com, hilalkivrak@yyu.edu.tr, ORCID: 0000-0001-8001-7854, ORCID: 0000-0002-0681-1096

[2]Department of Chemical Engineering, Faculty of Engineering, Siirt University, Siirt, Turkey, ORCID: 0000-0001-5441-4696, ORCID: 0000-0003-4575-3762

ABSTRACT

Energy, vital and permanent need for human life and welfare, supplied by fossil fuels such as oil, coal, and natural gas through the world has been rising gradually. However, the employment of fossil fuels to supply energy need have several disadvantages such as shortage of fossil fuels and global warming caused via fossil fuel exhaust gases. To eliminate these disadvantages of fossil fuel consumption in energy generating systems, research studies are dedicated to the alternative energy sources such as fuel cells, batteries, solar energy, wind energy. Fuel cells are the most popular alternative energy devices and attributed great importance to recompense the rapidly increasing energy demand. Direct Borohydride Fuel Cells (DBFCs), known as a special group of an alkaline direct liquid fuel cell (DLFC). At present, monometallic CNT supported Pd electrocatalysts (Pd/CNT) are prepared at varying Pd loadings via sodium borohydride (NaBH4) reduction method to investigate their NaBH4 electrooxidation activities. These monometallic Pd/CNT catalysts are characterized by X-ray Diffraction (XRD), N2 adsorption-desorption, X-ray photoelectron spectroscopy (XPS), and Scanning Electron Microscopy-Energy Dispersive X-ray analysis (SEM-EDX). NaBH4 electrooxidation measurements are performed with cyclic voltammetry (CV), chronoamperometry (CA), and electrochemical impedance spectroscopy (EIS). The 30% Pd/CNT catalyst exhibits the highest electrochemical activity. By altering Pd loading, catalyst surface electronic structure changes significantly, leading to enhanced NaBH4 electrooxidation activity. As a conclusion, it is clear that Pd/CNT catalysts are good candidate as anode catalysts for direct borohydride fuel cells.

ARTICLE INFO

Research article

Received: 13.04.2020
Accepted: 27.05.2020

Keywords:
Pd/CNT,
fuel cell,
sodium borohydride,
catalyst,
loading

**Corresponding author*

1. Introduction

Energy is one of the most important needs for the daily life and development and survival of human society. The emissions from fossil fuels cause toxic and dangerous substances, leading to serious environmental problems. Increasing global energy consumption has been caused exhausting of fossil fuels, leading to the search for alternative energy resources [1, 2]. The importance of renewable energy sources has enhanced global energy demand owing to the effects of petroleum-based fuels such as environmental pollution and global warming [3]. Fuel cells are the most popular alternative energy devices and attributed great importance to recompense the rapidly increasing energy demand [4]. Considering fuel cell, the chemical energy of molecules is converted into electrical energy with high energy efficiency [5, 6].

Polymer electrolyte membrane (PEM) fuel cells are commonly regarded as a competent substitute to batteries for portable power devices. Hydrogen PEM (H_2-PEM) fuel cells [7], direct methanol fuel cells (DMFCs) [8, 9], direct ethanol fuel cells (DEFCs), direct alcohol fuel cells (DAFCs) [10, 11], and direct formic acid fuel cells (DFAFCs) [12, 13] are most commonly studied fuel cells in literature. The critical limitations for commercialization of H_2-PEM are the high cost of miniaturized H_2 containers, potential dangers in the transportation of H_2, and low gas-phase energy density of H_2. Although liquid-alcohols have superior energy density compared to H_2, the toxicity of methanol vapor is still a remaining concern for the commercialization of DMFCs for on-board systems. On the other hand, C-C bond breaking is difficult for other alcohols [14, 15]. Due to some limitations in alcohol fuel cells such as CO_2 generation, low

electrochemical activity, and crossover, the researchers concentrated on Direct Borohydride Fuel Cells (DBFCs), known as a special group of an alkaline direct liquid fuel cell (DLFC) [16-18]. This kind of fuel cell produces electricity via the oxidation of borohydride anion (BH_4^-) at the anode and oxygen reduction at the cathode shown as Eq. (1.1) and Eq. (1.2) [19-21].

$$BH_4^- + 8OH^- \longrightarrow BO_2^- + 6H_2O + 8e^- \quad (E^0 = -1.24\ V) \quad (1.1)$$

$$O_2 + 2H_2O + 4e^- \longrightarrow 4OH^- \quad (E^0 = 0.40\ V) \quad (1.2)$$

Nanomaterials have attained much attention due to versatile applications such as disease diagnostics, photocatalysis, energy, environment, and storage appliances [22-27]. DBFCs have enhanced performances, especially regarding mobile applications [17, 28, 29]. In order to improve DBFC performance, the anode catalyst is one of the important elements to enhance its catalytic performance [30, 31]. The catalytic electrooxidation of $NaBH_4$ has been widely investigated by using various catalysts such as Pt [32-36], Au [37-40], Pd [41-43], Ag [44], Co [45-47], Ni [18], and alloys such as Pt–Bi [48], Pd–Bi [48], Pt-Ni [16, 49], Pt-Au [50], Pd-Au [51], Ni-Co [52], Cu-Ag [53]. There numerous studies on the synthesis, the characterization of CNT supported Pd catalysts and the investigation of their $NaBH_4$ electrooxidation activities. However, the mechanism of $NaBH_4$ electrooxidation has not still understood. Thus, the detailed investigation of CNT supported Pd catalysts should be performed to understand the mechanism.

Herein, monometallic CNT supported Pd electrocatalysts (Pd/CNT) are prepared at varying Pd loadings via the $NaBH_4$ reduction method to investigate their $NaBH_4$ electrooxidation activities. The electrochemical performance of Pd metal charges ranging from 0.1-70% by weight on the support material is investigated. The surface properties and electrochemical performances of these catalysts were examined with different techniques. Particle size and distribution of the Pd/CNT catalyst were defined by using XRD and SEM-EDX analysis. N_2 adsorption-desorption analysis was applied to check the surface area of the Pd/CNT catalyst. XPS spectroscopy was used to examine the possible chemical state of Pd in the Pd/CNT. The electrochemical activity of these catalysts was investigated by CV, CA, and EIS. Pd/CNT catalyst can be a promising anode catalyst for DBFCs with its high electrocatalytic performance and stability.

2. Experimental

2.1. Materials and equipments

Potassium tetrachloropalladate (II) (K_2PdCl_4, 99.99%), sodium borohydride ($NaBH_4$, >99%), sodium hydroxide (NaOH, >98%), multi-walled carbon nanotube (MWCNT, 98%) were purchased from Sigma-Aldrich and used as received. Nafion 117 solution (5%) was obtained from Aldrich. Potentiostat, Ag/AgCl reference electrode, glassy carbon, and Pt wire electrodes were purchased from CH Instruments. Deionized water was distilled by the water purification system (Milli-Q Water Purification System). All glassware was washed with acetone and copiously rinsed with distilled water.

2.2. Preparation of catalysts and working electrodes

2.2.1. Preparation of monometallic catalysts

The Pd/CNT catalyst was synthesized with the $NaBH_4$ reduction method. The metal loading on the carbon support was varied at 0.1-70 wt% Pd metal precursor (K_2PdCl_4) was dissolved in pure water and then CNT was added. These mixtures were stirred for two hours. $NaBH_4$ was used for metal reduction. After adding $NaBH_4$, stirring was continued for half an hour and filtered. Finally, these catalysts were washed completely and dried at 85 ^oC for 12 hours [54-56].

2.2.2 Preparation of working electrodes

Glassy carbon electrode was polished by alumina before electrode preparation. 5 mg of catalyst was dispersed in 1 mL of Aldrich 5% Nafion solution. As a result, a catalyst ink was obtained. Following this, 5 µL of the catalyst ink was dropped on a glassy carbon electrode. Finally, the electrode was dried at room temperature to remove the solvent.

2.3. Characterization techniques

Monometallic 30% Pd/CNT catalyst was characterized by XRD, N_2 adsorption-desorption, SEM-EDX, and XPS measurements. XRD measurement of this catalyst was analyzed using a PANalytical Empyrean X-ray diffractometer device with Cu Kα radiation (λ = 1.54056 Å). N_2 adsorption-desorption analysis was conducted on a MicromeriticsTristar II 3020 equipped with surface area and porosity measurement analyzer that employed the BET method. XPS analysis was applied by the Specs-Flex device to determine the oxidation state of the Pd/CNT catalyst. SEM-EDX and mapping were analyzed employing the ZEISS SIGMA 300 to scan the surface of the Pd/CNT catalyst.

2.4. Electrochemical Measurements

The electrochemical measurements of monometallic Pd/CNT catalysts were performed with CHI 660 E electrochemical potentiostat in a three-electrode system. The counter electrode was Pt wire and Ag/AgCl electrode was served as the reference electrode. The glassy carbon electrode was employed as the working electrode. All electrochemical measurements were performed in the cell at room temperature. The cyclic voltammograms were recorded in a

potential range of -1.0~0.4 V versus Ag/AgCl at a sweep rate of 50 mV s^{-1} in 3 M NaOH + 0.1 M $NaBH_4$. Stability measurements of these catalysts were carried out in a 3 M NaOH + 0.1 M $NaBH_4$ solution with 600 s -0.4 V by CA. EIS as a dynamic method was used to examine the electrochemical behavior of catalysts. Then, Potentiostatic EIS measurements were recorded between 300 kHz and 0.04 Hz in 3 M NaOH + 0.1 M $NaBH_4$ at an amplitude of 5 mV at the -0.4 V electrode potential.

3. Results and discussion

3.1. Physical characterization

XRD pattern of the Pd/CNT catalyst was illustrated in Figure 1. Figure 1 shows the diffraction peaks at 2Θ value of 25.7º, 39.5º, 45.6º, 67.0º, 80.7º, and 85.0º corresponding the C (0 0 2), Pd (1 1 1), Pd (2 0 0), Pd (2 2 0), Pd (3 1 1), and Pd (2 2 2) planes, respectively (JCPDS card no: 87-0638). These planes approve the existence of metallic Pd with face center cubic structure [57]. XRD line corresponding to (111) plane was observed to be intense according to other planes. Therefore, the crystallite size of this plane was calculated utilizing the Scherrer equation. The crystallite size corresponding to (111) plane was found as 5.87 nm.

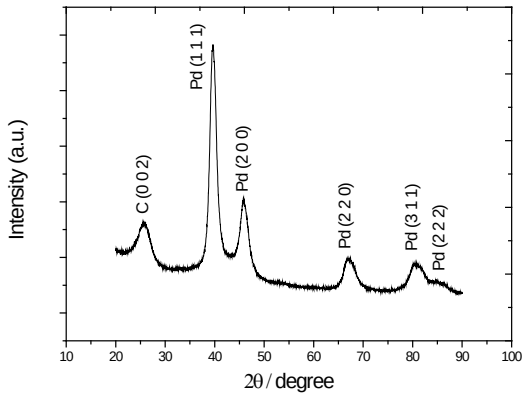

Figure 1. *XRD pattern of Pd/CNT catalyst.*

The N_2 adsorption-desorption analysis was used to characterize the BET surface area, average particle, and pore volume of the Pd/CNT catalyst and given in Figure 2. Union of Pure and Applied Chemistry (IUPAC) classifies hysteresis loops into H1, H2, H3, and H4 types [58]. Pd/CNT catalyst shows the V adsorption isotherms with an H1-type hysteresis loop which is usually connected to the pore duct with uniform size and regular shape [8, 59]. The average pore size, pore volume, and BET surface area of Pd/CNT were found as 24.5 nm, 0.93 cm^3/g, and 129.48 m^2/g, respectively.

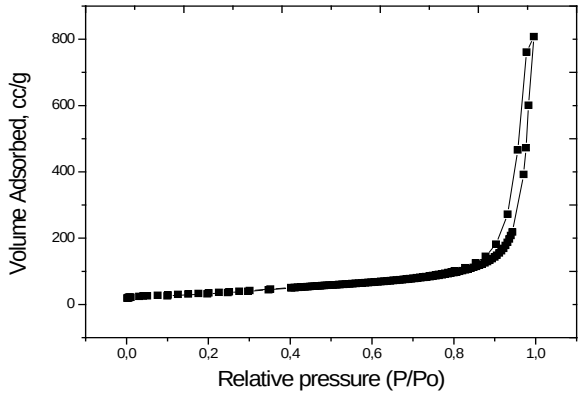

Figure 2. *N_2 adsorption-desorption isotherm of Pd/CNT catalyst.*

The possible chemical states of Pd in the Pd/CNT catalyst were defined via XPS and related spectra were illustrated in Figure 3. The deconvoluted Pd 3d spectra composed of six peaks at the presence of Pd^0 (Pd $3d_{5/2}$ at 335.7 eV and Pd $3d_{3/2}$ at 339.5 eV), PdO (Pd $3d_{3/2}$ at 341.0 eV), $Pd(OH)_x$ (Pd $3d_{5/2}$ at 336.3 eV and Pd $3d_{3/2}$ at 340.3 eV), and PdO_2 (Pd $3d_{5/2}$ at 337.4 eV). The elemental state (Pd^0) had a chemical state with a relative intensity of about 35% as well as the hydroxyl group.

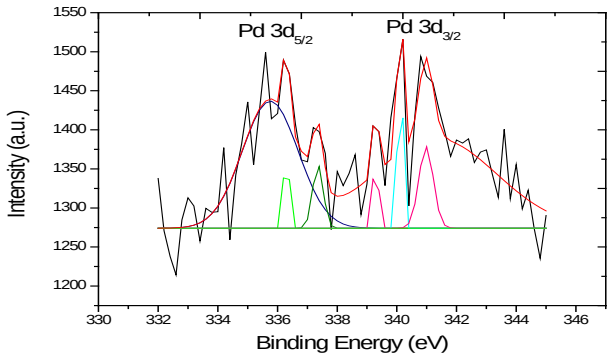

Figure 3. *XPS spectra of Pd/CNT.*

SEM-EDX and mapping images of the Pd/CNT catalyst was shown in Figure 4(a-e). This analysis was performed to set light to the formation and morphologies of the Pd/CNT catalyst. The Pd and carbon nanotube networks were plainly shown from Figure 4(a, b). In addition, it was observed that Pd metal was distributed homogeneously into the tube. The formation of the Pd/CNT catalyst was verified by mapping analysis in which turquoise and green particles indicate the Pd and carbon in Figure 4(c, d). The atomic and weight ratios from EDX results of Pd and carbon elements were given in Table 1. As shown in Table 1, the Pd metal was obtained on the carbon surface.

Table 1- *Atomic and weight elemental composition of the Pd/CNT catalyst.*

Element	Weight %	Atomic %
C	67.94	92.52
O	2.94	3.00
Pd	29.12	4.48

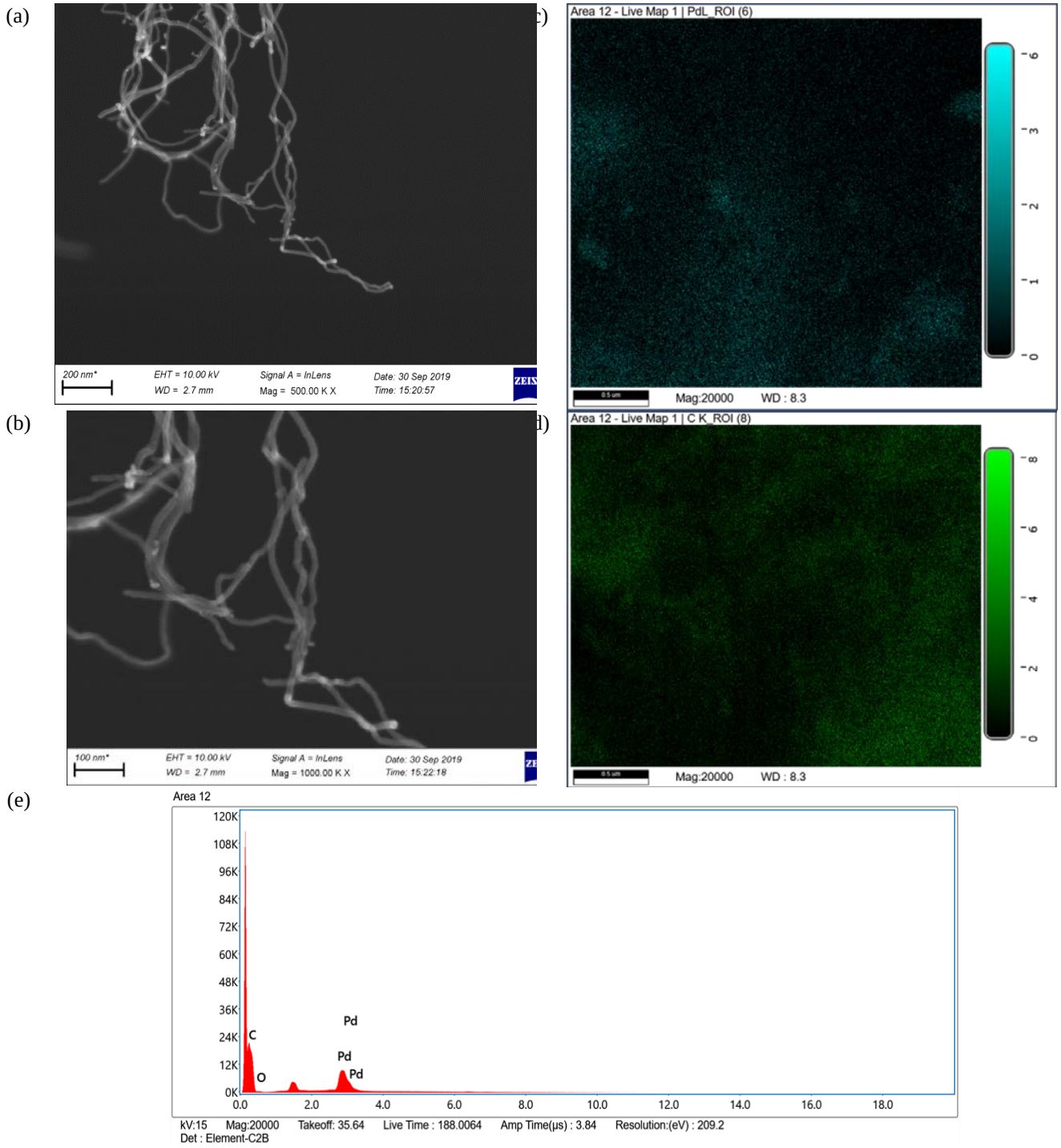

Figure 4. *SEM-EDX (a, b, e) and mapping images (Pd (c), C (d))of Pd/CNT catalyst.*

3.2. Electrochemical measurements

The electrochemical characterization of monometallic Pd/CNT electrocatalysts were evaluated by cyclic voltammetry at 3 M NaOH solution at 25 °C. Cyclic voltammograms were performed at -1.0 V ~ 0.4 V potential windows at 50 mV s^{-1} scan rate for monometallic Pd/CNT electrocatalysts. A comparison of the cyclic voltammetric behaviors of monometallic Pd/CNT electrocatalysts were presented in Figure 5a. The highest current value of hydrogen adsorption-desorption peaks was obtained for the 70% Pd/CNT catalyst. The electrochemical active surface area (ECSA) of the synthesized 0.1-70.0% Pd/CNT catalysts were obtained from the $Q/(0.424*Pd_m)$ equation. Q (mC) is an area of the reduction of PdO peak, the 0.424 (mC/cm^2) charge is the reduction charge value associated with a monolayer of PdO, and Pd_m is the Pd mass loading (mg). ECSA values of 0.1% Pd/CNT, 0.5% Pd/CNT, 1% Pd/CNT, 3% Pd/CNT, 5% Pd/CNT, 7% Pd/CNT, 10% Pd/CNT, 20% Pd/CNT, 30% Pd/CNT, 50% Pd/CNT, and 70% Pd/CNT catalysts were obtained as 551, 1336, 18, 115, 334, 216, 269, 280, 286, 309, and 260 m^2/g, respectively. On the other hand, activities of $NaBH_4$ electrooxidation reaction on monometallic Pd/CNT electrocatalysts were examined by CV measurements in 3 M NaOH + 0.1 M $NaBH_4$ at room temperature. As shown in Figure 5b, during the positive scan, $NaBH_4$ electrooxidation on monometallic Pd/CNT electrocatalysts began at about −0.8 V, while an oxidation peak appeared at -0.2 V. Cyclic voltammogram of monometallic Pd/CNT electrocatalysts revealed a peak located at around -0.3 V during the back scan, attributed to the electrocatalytic reaction of the interim product (BH_3OH^-) [31, 35]. 30% Pd/CNT catalyst exhibited better activity than the other monometallic Pd/CNT electrocatalysts. In addition, 30% Pd/CNT electrocatalyst displayed electrocatalytic activity with a maximum current density of 16.5 mA cm^{-2}. The purpose of adding wt% Pd metal precursor to the support material is to change the specific surface area and electronic properties of the surface. The 30% Pd/CNT catalyst has a high specific surface area and different surface electronic properties which provides more active sites for the reaction. This phenomenon is called as structure sensitivity. The exchange current density value of 16.5 mA cm^{-2} (7.9 A cm^{-2} mg^{-1}_{Pd}) appraised for $NaBH_4$ electrooxidation for 30% Pd/CNT catalyst was higher than those reported as 1.38 mA cm^{-2} for $NaBH_4$ electrooxidation on Pd/rGO-Fe_3O_4 catalyst by Martins et al [19]. In addition, this catalyst was higher than the current density of the Pd-rGO-C@TiC electrode (1.35 A cm^{-2} mg^{-1}_{Pd}) raported by Chen et al [43].

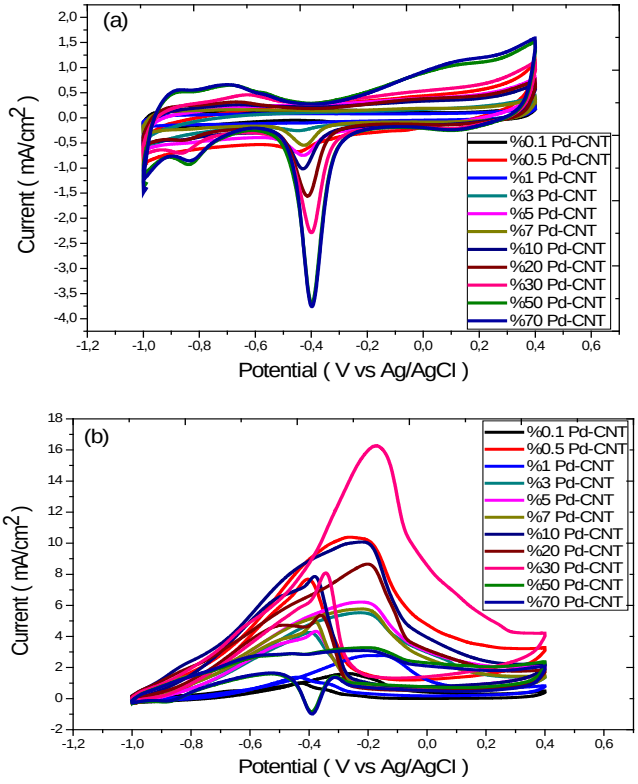

Figure 5. *Pd/CNT catalysts obtained (a) 3 M NaOH, (b) 3 M NaOH + 0.1 M $NaBH_4$ solution for cyclic voltammograms (scan rate: 50 mV s^{-1}).*

The stability and catalytic activity of 30% Pd/CNT catalysts at varying potentials were examined by using the CA method. Figure 6 shows the CA results of catalysts in the solution of 3 M NaOH + 0.1 M $NaBH_4$ at -0.4 V and -0.2 V potentials. The chronoamperometric curves display a sharp decrease in the first period owing to the accumulation of interim species at the surface of catalysts (Figure 6). As shown in Figure 6, the $NaBH_4$ electrooxidation of 30% Pd/CNT catalyst at -0.4 V indicates a higher initial current and a higher current at a longer time compared to other potentials. Furthermore, for the stability evaluation, the retention of the current value of 1000 s to the initial value was used by normalizing chronomaperommogram by dividing current values to initial current values and given in Figure 6b. Figure 6a and Figure 6b clearly shows that 30% Pd/CNT catalyst at -0.4 V potential has higher stability than the measurements at other potentials.

Nyquist plots obtained from EIS results were used to determine the $NaBH_4$ electrooxidation activity of 30% Pd/CNT catalyst. EIS measurements were performed between 300 kHz and 0.04 Hz in 3 M NaOH + 0.1 M $NaBH_4$ at an amplitude of 5 mV at the -0.4 V electrode potentials. According to the CV results, all catalysts have approximately -0.2 V peak currents. Therefore, CA analysis was taken at -0.2 and -0.4 V potentials. EIS measurements were taken at this potential as the best stability was achieved at -0.4 V. It is

understood that the image of the Nyquist plots is usually semicircle and the diameter of these semicircles is connected with the charge transfer resistance (R_{ct}) concerned with the electrocatalytic activity of electrocatalysts [60, 61]. As can be seen in Figure 7, since the 30% Pd/CNT catalyst has a smaller R_{ct} than compared to the 5% Pd/CNT, 7% Pd/CNT, 10% Pd/CNT, and 50% Pd/CNT catalysts, it indicates that the $NaBH_4$ electrooxidation reaction increases in the 30% Pd/CNT catalyst [62].

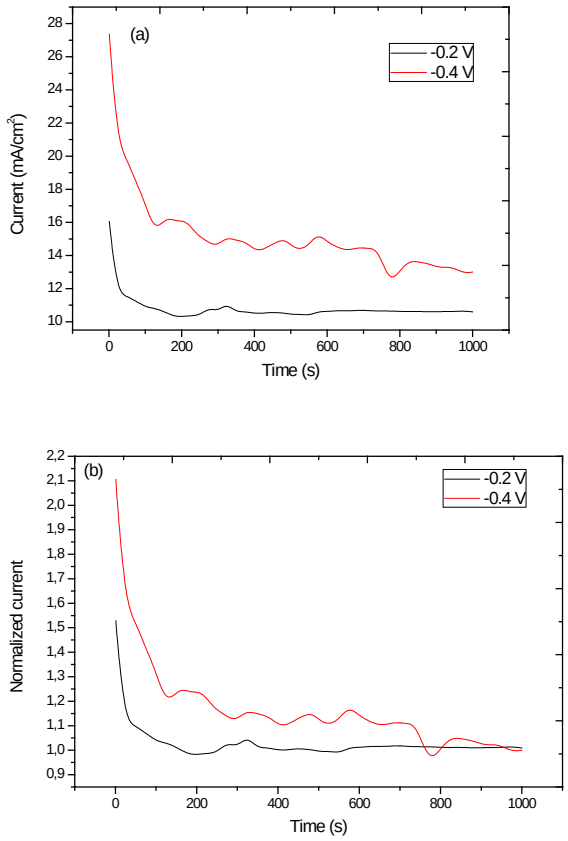

Figure 6. *(a) chronoamperomograms in solution of 3 M NaOH + 0.1 M $NaBH_4$ at -0.4 V and -0.2 V on 30% Pd/CNT catalyst (b) normalizing chronomaperommograms in solution of 3 M NaOH + 0.1 M $NaBH_4$ at -0.4 V and -0.2 V on 30% Pd/CNT catalyst.*

(a)

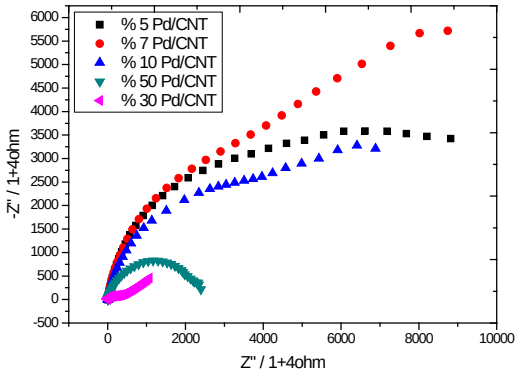

(b)

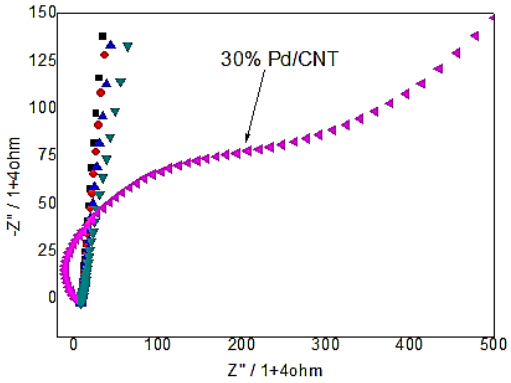

Figure 7. *Nyquist type EIS plots at -0.4 V potentials in 3 M NaOH + 0.1 M $NaBH_4$ on (a) Pd/CNT catalysts at various Pd loadings, (b) 30%Pd/CNT catalyst*

4. Conclusions

In this study, the monometallic Pd/CNT catalysts at varying 0.1-70.0% Pd loadings were prepared by the $NaBH_4$ reduction method. The 30% Pd/CNT catalyst was characterized via XRD, BET, SEM-EDX, and FTIR analyses. In addition, the monometallic Pd/CNT catalysts at varying 0.1 -70.0% were investigated by CV, CA, and EIS for $NaBH_4$ electrooxidation. The crystallite size corresponding to (111) plane is found as 5.87 nm for 30% Pd/CNT catalyst. The average pore size, pore volume, and BET surface area of Pd/CNT were found as 24.5 nm, 0.93 cm^3/g, and 129.48 cm^2/g, respectively. The 30% Pd/CNT catalyst has a high specific surface area and different surface electronic properties which provides more active sites for the reaction. This phenomenon is called as structure sensitivity [63]. An increase in Pd loading improves electrochemical activity until 30% Pd loading was reached. Further increase in Pd loading leads to a decrease in the electrocatalytic activity due to aggregation and blocking of the surface active sites. In this paper, the sample preparation method and its ultra-high electrocatalytic activity make Pd/CNT expected to be a promising electrode, which brings hope for the preparation of high-performance DBFCs [64].

Acknowledgments

The CHI 660E potentiostat employed in electrochemical measurements was purchased from the Scientific and Technological Research Council of Turkey (TUBITAK) project (project no: TUBITAK 113Z249). The chemicals were purchased from the Van YuzuncuYıl BAP project (project no: FBA-2018-7152). Characterization measurements were also purchased from Van Yuzuncu Yıl BAP project (project no: FBA-2018-7152).

References

[1]. Kurata M., Matsui N., Ikemoto Y., Tsuboi H., "Do determinants of adopting solar home systems differ between households and micro-enterprises? Evidence from rural Bangladesh", Renewable Energy, 129, (2018), 309-316.

[2]. Chia S.R., Ong H.C., Chew K.W., Show P.L., Phang S.-M., Ling T.C., Nagarajan D., Lee D.-J., Chang J.-S., "Sustainable approaches for algae utilisation in bioenergy production", Renewable Energy, 129, (2018), 838-852.

[3]. El-Nagar G.A., Derr I., Fetyan A., Roth C., "One-pot synthesis of a high performance chitosan-nickel oxyhydroxide nanocomposite for glucose fuel cell and electro-sensing applications", Applied Catalysis B: Environmental, 204, (2017), 185-199.

[4]. Hermann A., Chaudhuri T., Spagnol P., "Bipolar plates for PEM fuel cells: A review", International journal of hydrogen Energy, 30, (2005) 1297-1302.

[5]. Peighambardoust S.J., Rowshanzamir S., Amjadi M., "Review of the proton exchange membranes for fuel cell applications", International journal of hydrogen energy, 35 (2010) 9349-9384.

[6]. Hosseini H., Mahyari M., Bagheri A., Shaabani A., "Pd and PdCo alloy nanoparticles supported on polypropylenimine dendrimer-grafted graphene: a highly efficient anodic catalyst for direct formic acid fuel cells", Journal of Power Sources, 247, (2014) 70-77.

[7]. Brites Helú M.A., Fernandez W.V., Fernández J.L., "Ordered Array Electrodes Fabricated by a Mask-Assisted Electron-Beam Method as Platforms for Studying Kinetic and Mass-Transport Phenomena on Electrocatalysts", ChemElectroChem, 5, (2018) 2620-2629.

[8]. Ulas B., Caglar A., Kivrak A., Kivrak H., "Atomic molar ratio optimization of carbon nanotube supported PdAuCo catalysts for ethylene glycol and methanol electrooxidation in alkaline media", Chemical Papers, 73, (2019) 425-434.

[9]. Sahin O., Kivrak H., "A comparative study of electrochemical methods on Pt–Ru DMFC anode catalysts: The effect of Ru addition", International Journal of Hydrogen Energy, 38, (2013), 901-909.

[10]. Atbas D., Çağlar A., Kivrak H., Kivrak A., "Microwave Assisted Synthesis of Sn Promoted Pt Catalysts and Their Ethanol Electro-oxidation Activities", American Journal of Nanomaterials, 4, (2016), 8-11.

[11]. Sahin O., Duzenli D., Kivrak H., "An ethanol electrooxidation study on carbon-supported Pt-Ru nanoparticles for direct ethanol fuel cells", Energy Sources, Part A: Recovery, Utilization, and Environmental Effects, 38, (2016), 628-634.

[12]. Ulas B., Caglar A., Sahin O., Kivrak H., "Composition Dependent Activity of PdAgNi Alloy Catalysts for Formic Acid Electrooxidation", Journal of Colloid and Interface Science, 532, (2018), 47-57.

[13]. Caglar A., Sahan T., Cogenli M.S., Yurtcan A.B., Aktas N., Kivrak H., "A novel Central Composite Design based response surface methodology optimization study for the synthesis of Pd/CNT direct formic acid fuel cell anode catalyst", International Journal of Hydrogen Energy, 43, (2018), 11002-11011.

[14]. Chen C., Xu H., Shang H., Jin L., Song T., Wang C., Gao F., Zhang Y., Du Y., "Ultrafine PtCuRh nanowire catalysts with alleviated poisoning effect for efficient ethanol oxidation", Nanoscale, 11, (2019), 20090-20095.

[15]. Wang Y., Zheng M., Sun H., Zhang X., Luan C., Li Y., Zhao L., Zhao H., Dai X., Ye J.-Y., "Catalytic Ru containing Pt3Mn nanocrystals enclosed with high-indexed facets: Surface alloyed Ru makes Pt more active than Ru particles for ethylene glycol oxidation", Applied Catalysis B: Environmental, 253, (2019), 11-20.

[16]. Hosseini M.G., Rashidi N., Mahmoodi R., Omer M., "Preparation of Pt/G and PtNi/G nanocatalysts with high electrocatalytic activity for borohydride oxidation and investigation of different operation condition on the performance of direct borohydride-hydrogen peroxide fuel cell", Materials Chemistry and Physics, 208, (2018), 207-219.

[17]. Olu P.-Y., Barros C.R., Job N., Chatenet M., "Electrooxidation of NaBH4 in Alkaline Medium on Well-defined Pt Nanoparticles Deposited onto Flat Glassy Carbon Substrate: Evaluation of the Effects of Pt Nanoparticle Size, Inter-Particle Distance, and Loading", Electrocatalysis, 5, (2014), 288-300.

[18]. Zhang D., Wang G., Yuan Y., Li Y., Jiang S., Wang Y., Ye K., Cao D., Yan P., Cheng K., "Three-dimensional functionalized graphene networks modified Ni foam based gold electrode for sodium borohydride electrooxidation", International Journal of Hydrogen Energy, 41, (2016), 11593-11598.

[19]. Martins M., Metin Ö., Sevim M., Šljukić B., Sequeira C.A.C., Sener T., Santos D.M.F., "Monodisperse Pd nanoparticles assembled on reduced graphene oxide-Fe3O4 nanocomposites as electrocatalysts for borohydride fuel cells", International Journal of Hydrogen Energy, 43, (2018), 10686-10697.

[20]. Song C., Li B., Cheng K., Y K., Zhu K., Cao D., Wang G., "Synthesis and investigation of a high-activity catalyst: Au nanoparticles modified metalic Ti microrods for NaBH4 electrooxidation", International Journal of Hydrogen Energy, 43, (2018), 3688-3696.

[21]. Lafforgue C., Atkinson R.W., Swider-Lyons K., Chatenet M., "Evaluation of carbon-supported palladium electrocatalysts for the borohydride oxidation reaction in conditions relevant to fuel cell operation", Electrochimica Acta, 341, (2020), 135971.

[22]. Ajmal S., Bibi I., Majid F., Ata S., Kamran K., Jilani K., Nouren S., Kamal S., Ali A., Iqbal M., "Effect of Fe and Bi doping on LaCoO3 structural, magnetic, electric and catalytic properties", Journal of Materials Research and Technology, 8, (2019), 4831-4842.

[23]. Bibi I., Hussain S., Majid F., Kamal S., Ata S., Sultan M., Din M.I., Iqbal M., Nazir A., "Structural, dielectric and magnetic studies of perovskite [Gd1− xMxCrO3 (M= La, Co, Bi)] nanoparticles: photocatalytic degradation of dyes", Zeitschrift für Physikalische Chemie, 233, (2019), 1431-1445.

[24]. Majid F., Malik A., Ata S., Hussain Z., Bibi I., Iqbal M., Rafay M., Rizvi H., "Structural and Optical Properties of Multilayer Heterostructure of CdTe/CdSe Thin Films", Zeitschrift für Physikalische Chemie, 233, (2019), 1215-1231.

[25]. Majid F., Rauf J., Ata S., Bibi I., Yameen M., M. Iqbal, Hydrothermal Synthesis of Zinc Doped Nickel Ferrites: Evaluation of Structural, Magnetic and Dielectric Properties, Zeitschrift für Physikalische Chemie, 233, (2019), 1411-1430.

[26]. Majid F., Nazir A., Ata S., Bibi I., Mehmood H.S., Malik A., Ali A., Iqbal M.,"Effect of Hydrothermal Reaction Time on Electrical, Structural and Magnetic Properties of Cobalt Ferrite", Zeitschrift für Physikalische Chemie, (2019).

[27]. Aal R.M.A., Gitru M.A., Essam Z.M., "Novel synthetized near infrared cyanine dyes as sensitizer for dye sensitized solar cells based on nano-TiO2", Chemistry International, 3, (2017), 358-367.

[28]. Pramanik H., Rathoure A.K., "Electrooxidation study of NaBH4 in a membraneless microfluidic fuel cell with air breathing cathode for portable power application", International Journal of Hydrogen Energy, 42, (2017), 5340-5350.

[29]. Yang F., Cheng K., Ye K., Wei X., Xiao X., Guo F., Wang G., Cao D., "High performance of Au nanothorns supported on Ni foam substrate as the catalyst for NaBH4 electrooxidation", Electrochimica Acta, 115, (2014), 311-316.

[30]. Ye K., Ma X., Huang X., Zhang D., Cheng K., Wang G., Cao D., "The optimal design of Co catalyst morphology on a three-dimensional carbon sponge with low cost, inducing better sodium borohydride electrooxidation activity", RSC Advances, 6, (2016), 41608-41617.

[31]. D. Duan, Yin X., Wang Q., Liu S., Wang Y., "Performance evaluation of borohydride electrooxidation reaction with ternary alloy Au–Ni–Cu/C catalysts", Journal of Applied Electrochemistry, 48, (2018), 835-847.

[32]. Šljukić B., Milikić J., Santos D.M.F., Sequeira C.A.C., "Carbon-supported Pt0.75M0.25 (M=Ni or Co), electrocatalysts for borohydride oxidation", Electrochimica Acta, 107, (2013), 577-583.

[33]. Jin W., Liu J., Wang Y., Yao Y., Gu J., Zou Z., "Direct NaBH4–H2O2 fuel cell based on nanoporous gold leaves", International Journal of Hydrogen Energy, 38, (2013), 10992-10997.

[34]. Ojani R., Raoof J.-b., Valiollahi R., "Pt nanoparticles/graphene paste electrode for sodium borohydride electrooxidation", Journal of Solid State Electrochemistry, 17, (2013), 217-221.

[35]. Šljukić B., Milikić J., Santos D.M.F., Sequeira C.A.C., Macciò D., Saccone A., "Electrocatalytic performance of Pt–Dy alloys for direct borohydride fuel cells", Journal of Power Sources, 272, (2014), 335-343.

[36]. Oliveira R.C.P., Milikić J., Daş E., Yurtcan A.B., Santos D.M.F., Šljukić B., "Platinum/polypyrrole-carbon electrocatalysts for direct borohydride-peroxide fuel cells", Applied Catalysis B: Environmental, 238, (2018), 454-464.

[37]. Pe F.i, Wang Y., Wang X., He P.Y., Liu L., Xu Y., Wang H., "Preparation and Performance of Highly Efficient Au Nanoparticles Electrocatalyst for the Direct Borohydride Fuel Cell", Fuel Cells, 11, (2011), 595-602.

[38]. Santos D.M.F., Sequeira C.A.C., "Cyclic voltammetry investigation of borohydride oxidation at a gold electrode", Electrochimica Acta, 55, (2010), 6775-6781.

[39]. Olu P.-Y., Bonnefont A., Braesch G., Martin V., Savinova E. R., Chatenet M., "Influence of the concentration of borohydride towards hydrogen production and escape for borohydride oxidation reaction on Pt and Au electrodes – experimental and modelling insights", 2017.

[40]. Yan P., Zhang D., Cheng K., Wang Y., Ye K., Cao D., Wang B., Wang G., Li Q., "Preparation of Au nanoparticles modified TiO2/C core/shell nanowire array and its catalytic performance for NaBH4 oxidation", Journal of Electroanalytical Chemistry, 745, (2015), 56-60.

[41]. Cheng K., Xu Y., Miao R.R., Yang F., Yin J.L., Wang G.L., Cao D.X., "Pd Modified MmNi50.6Co10.2Mn5.4Al1.2 Alloy as the Catalyst of NaBH4 Electrooxidation", Fuel Cells, 12, (2012), 869-875.

[42]. Braesch G., Bonnefont A., Martin V., Savinova E.R., Chatenet M., "Borohydride oxidation reaction mechanisms and poisoning effects on Au, Pt and Pd bulk electrodes: From model (low) to direct borohydride fuel cell operating (high) concentrations", Electrochimica Acta, 273, (2018), 483-494.

[43]. Cheng K., Jiang J., Kong S., Gao Y., Ye K., Wang G., Zhang W., Cao D., "Pd nanoparticles support on rGO-C@TiC coaxial nanowires as a novel 3D electrode for NaBH4 electrooxidation", International Journal of Hydrogen Energy, 42, (2017), 2943-2951.

[44]. Sanli A.E., Aytaç A., Uysal B.Z., Aksu M.L., "Recovery of NaBH4 from BH3OH− hydrolyzed intermediate on the AgI surface treated with different electrochemical methods", Catalysis Today, 170, (2011), 120-125.

[45]. Zhang D., Ye K., Cao D., Wang B., Cheng K., Li Y., Wang G., Xu Y., "Co@MWNTs-Plastic: A novel electrode for NaBH4 oxidation", Electrochimica Acta, 156, (2015), 102-107.

[46]. Zhang D., Ye K., Cheng K., Cao D., Yin J., Xu Y., Wang G., "High electrocatalytic activity of cobalt–multiwalled carbon nanotubes–cosmetic cotton nanostructures for sodium borohydride electrooxidation", International Journal of Hydrogen Energy, 39, (2014), 9651-9657.

[47]. Guo S., Sun J., Zhang Z., Sheng A., Gao M., Wang Z., Zhao B., Ding W., "Study of the electrooxidation of borohydride on a directly formed CoB/Ni-foam electrode and its application in membraneless direct borohydride fuel cells", Journal of Materials Chemistry A, 5, (2017), 15879-15890.

[48]. Simões M., Baranton S., Coutanceau C., "Influence of bismuth on the structure and activity of Pt and Pd nanocatalysts for the direct electrooxidation of NaBH4", Electrochimica Acta, 56, (2010), 580-591.

[49]. Wang B., Zhang D., Ye K., Cheng K., Cao D., Wang G., Cheng X., "Plastic supported platinum modified nickel electrode and its high electrocatalytic activity for sodium borohydride electrooxidation", Journal of Energy Chemistry, 24, (2015), 497-502.

[50]. Iotov P.I., Kalcheva S.V., Kanazirski I.A., "On the enhanced electrocatalytic performance of PtAu alloys in borohydride oxidation", Electrochimica Acta, 108, (2013), 540-546.

[51]. Simões M., Baranton S., Coutanceau C., "Electrooxidation of Sodium Borohydride at Pd, Au, and PdxAu1−x Carbon-Supported Nanocatalysts", The Journal of Physical Chemistry C, 113, (2009), 13369-13376.

[52]. Guo M., Cheng Y., Yu Y., Hu J., "Ni-Co nanoparticles immobilized on a 3D Ni foam template as a highly efficient catalyst for borohydride electrooxidation in alkaline medium", Applied Surface Science, 416, (2017), 439-445.

[53]. Duan D., Liu H., Wang Q., Wang Y., Liu S., "Kinetics of sodium borohydride direct oxidation on carbon supported Cu-Ag bimetallic nanocatalysts", Electrochimica Acta, 198, (2016), 212-219.

[54]. Caglar A., Ulas B., Cogenli M.S., Yurtcan A.B., Kivrak H., "Synthesis and characterization of Co, Zn, Mn, V modified Pd formic acid fuel cell anode catalysts", Journal of Electroanalytical Chemistry, 850, (2019), 113402.

[55]. Caglar A., Kivrak H., "Highly active carbon nanotube supported PdAu alloy catalysts for ethanol electrooxidation in alkaline environment", International Journal of Hydrogen Energy, 44, (2019), 11734-11743.

[56]. Çağlar A., Aldemir A., Kivrak H., "Alcohol electrooxidation study on carbon nanotube supported monometallic, Pt, Bi, and Ru catalysts", Fullerenes, Nanotubes and Carbon Nanostructures, 26, (2018), 863-870.

[57]. Navaladian S., Viswanathan B., Varadarajan T.K., Viswanath R.P., "A Rapid Synthesis of Oriented Palladium Nanoparticles by UV Irradiation", Nanoscale Res Lett, 4, (2008), 181-186.

[58]. I.L.M. SIT, Characterızation of the structure and performance of Ce3+ exchanged lix molecular sieves, Materiali in tehnologije, 52, (2018), 423-428.

[59]. Ulas B., Caglar A., Kivrak H., "Determination of optimum Pd: Ni ratio for Pd x Ni 100-x/CNT s formic acid electrooxidation catalysts synthesized via sodium borohydride reduction method", International Journal of Energy Research, 43, (2019), 3436-3445.

[60]. Karuppasamy L., Chen C.-Y., Anandan S., Wu J.J., "Sonochemical fabrication of reduced graphene oxide supported Au nano dendrites for ethanol electrooxidation in alkaline medium", Catalysis Today, 307, (2018), 308-317.

[61]. Chen S., Xu H., Yan B., Li S., Dai J., Wang C., Shiraishi Y., Du Y., "Highly active electrooxidation of ethylene glycol enabled by pinecone-like Pd–Au–Ag nanocatalysts", Journal of the Taiwan Institute of Chemical Engineers, 83, (2018), 64-73.

[62]. Xu H., Song P., Yan B., Wang J., Gao F., Zhang Y., Du Y., "Superior ethylene glycol electrocatalysis enabled by Au-decorated PdRu nanopopcorns", Journal of Electroanalytical Chemistry, 814, (2018), 31-37.

[63]. Zhang J., Zhang D., Cui C., Wang H., Jiao W., Gao J., Liu Y., "A three-dimensional porous Co–P alloy supported on a copper foam as a new catalyst for sodium borohydride electrooxidation", Dalton Transactions, 48, (2019), 13248-13259.

[64]. Yin X., Wang Q., Duan D., Liu S., Wang Y., "Amorphous NiB alloy decorated by Cu as the anode catalyst for a direct borohydride fuel cell", International Journal of Hydrogen Energy, 44, (2019), 10971-10981.

MANAS Journal of Engineering
ISSN 1694-7398 | e-ISSN 1694-7398

Volume 8 (Issue 1) (2020) Pages 11-16

The concentration distribution of components and particles in the system: tomato-water-sodium nitrate and assessment of the oxidation-reduction potential at different temperatures

Damira Sambaeva[1], Timur Maimekov[2], Nurzat Shaykieva[3], Janarbek Izakov[3], Zarlyk Maimekov[3,*]

[1]Kyrgyz State University of Geology, Mining and Natural Resources Development, Bishkek, Kyrgyz Republic

[2]Moscow Institute of Physics and Technology, Dolgoprudny, Russia

[3]Kyrgyz-Turkish Manas University, Engineering Faculty, Department of Environmental Engineering, Bishkek, Kyrgyz Republic, zarlyk.maymekov@manas.edu.kg, ORCID 10000-0002-9117-262X

ABSTRACT

The paper considers a triple complex system of tomato, water and sodium nitrate. Taking into account the average macronutrient composition and moisture content of field and greenhouse tomatoes, physicochemical modeling of the system was carried out tomato-water-sodium nitrate. The hydrogen index of tomato was determined at various temperatures and it was noted that tomato medium was acidic. It is shown that with an increase in the content of sodium nitrate in the system: tomato - water - sodium nitrate within the temperature range from 278 to 293 K, the hydrogen index of tomato increases, i.e. the process of neutralizing the acidic medium based on sodium hydroxide proceeds. The calculated hydrogen value of tomato corresponds to the experimental values of pH = 3.3-4.38. The obtained results made it possible to determine the distribution of individual simple and complex cations and anions in water-salt solution, as well as to establish the values of redox potential, and thereby revealed the antioxidant nature of tomato.

ARTICLE INFO

Research article

Received: 25.12.2019
Accepted: 13.04.2020

Keywords:
Tomato,
sodium nitrate,
redox potential,
solution,
ions,
complex system

**Corresponding author*

1. Introduction

Currently, the study of oxidation process in biological systems, specifically deceleration aging process of human body are relevant task. Accordingly, an active search for antioxidants based on plant materials with the highest content of lycopene in order to limit the oxidation of biogenic elements carried out [1; 2; 3]. It should be noted here that lycopene is most often found in vegetables of red color (tomato, watermelon etc.) [4; 5]. Noted, that tomato (tomato from lat.) is a thermophilic plant and in tomato the amount of water is more than 90%., which grows well in fertile soils, using nitrogen, phosphorus, potassium, i.e. stimulating the process of bioremediation of technogenic soil [6; 7]. For example, the toxic effect of nitrate and sodium nitrite on germinating seeds and nitrogen in relation to tomatoes was considered and the chemical composition of the tomato [8; 9] was also given in studies [10; 11]. In the study [12; 13] the influence of various plant growth regulators and micronutrients on the content of micronutrients in tomatoes was studied; the effect of various soil pH on the growth of a tomato was considered in the

studies [14; 15]; in [16; 17; 18] the effect of nitrogen fertilizers on the content of nitrates in salad was indicated; the role of macronutrients and micronutrients in improving the quality of tomatoes was noted in [19]; influence of temperature, pH and food additives on the content of volatile products of tomatoes was given in [20; 21]; nutrients in tomato based on the use of vermicompost and chemical fertilizers are indicated in [22; 23]; the influence of potassium on the quality of tomato fruit was considered in [24; 25], and in [26; 27] the influence of fertilizers on the yield of some minerals in tomato were shown, and the efficiency of biohumus in the quantitative and qualitative growth of tomato plants; the reaction of foliar application of boron to vegetative growth, the quality of tomato yield were studied in [28], and in [29] the influence of zinc and boron on the growth, flowering and fruiting of tomatoes, as well as the effect of foliar application of ferrous sulfate and citric acid, and quality tomato plants; the

composition of tomato fruit were studied in [30]; the influence of boron, calcium and surface moisture on the quality of fresh tomatoes was considered in [31].

The brief review of the literature shows that the study of the influence of temperature, pH, concentration of mineral salts, including sodium nitrate [32; 33] on the activity of the bioremediation process of the soil-tomato-fertilizer system, is a very useful research.

2. Materials and methods

Physicochemical modeling of the system tomato-water-sodium nitrate was carried out by searching for potentially possible phases in equilibrium, distributing components and particles, and also the composition of the system by chemical elements while minimizing the isobaric-isothermal potential [34; 35; 36; 37]. The calculation included the use of macronutrient composition and the moisture content of the tomato, as well as the calculation of the thermodynamic characteristics of the system at various temperatures (278-298 K) and sodium nitrate concentrations (29.3-50 mg). The verification and comparison of various basic sources, as well as the processing, correction and visualization of the thermodynamic parameters of the system studied above, were carried out taking into account the molar ratio of all components over a wide range of temperature changes (P = 0.1 MPa). The thermodynamic parameters of the system (ΔG, ΔH, ΔS, ΔU), equilibrium compositions, pH, Eh, ionic strength (I) of the aqueous tomato solution were calculated. The concentration distribution of individual components and particles (cations and anions) in aqueous solution of tomato (Table 1-5). The humidity of the tomato (W_{H2O} = 935 g/kg) was determined by the express method based on the drying using humidity (OHAUS MB200) analyzer. The hydrogen value of the tomato was determined on the basis of the pH-meter (Denver Instruments) and was equal to pH = 3.64-4.38, and the content of the gluten in the field tomato ranged from 5.6 to 5.68 %, in the green house tomato from 5.76 to 6.03 %.

3. Results and discussion

It was noted that the tomato was a thermophilic plant; therefore, the physico-chemical modeling was carried out within the temperature range from 278 to 293 K and atmospheric air pressure. In the model calculations, only macronutrients of tomato (mg/kg) were taken into consideration: calcium-140, magnesium-200, sodium-400, potassium-2900, phosphorus-260, chlorine-570, sulfur-120; water content in tomato H_2O = 935 g/kg; the content of sodium nitrate in the system varied from 29.3 to 50 mg/l. The chemical composition of the tomato (per 100 g/g) was given according to the data of [38]: proteins-0.6, fats-0.2, carbohydrates-4.2, starch-0.3, ash-0.7, organic acids-0.5, mono- and disaccharides-3.5; microelements (per 100g/mg): iron-0.9, zinc-0.2, iodine-2μg, copper-110μg, manganese-0.14, selenium-0.4 μg, fluorine-20 μg, molybdenum-7 μg, boron-115 μg, cobalt-6 μg. Table 1 shows the data obtained at the optimal temperature of growth of a tomato equal to 20 °C.

Table 1. *Physicochemical and thermodynamic parameters of the system: tomato-water-sodium nitrate.*

Temperature, K	*Pressure, MPa*	*Volume, m^3*	*Mass, kg*	*Density, kg/m^3*
293.15	0.1	0.0293	0.98	33.58
G, MJ	*H, MJ*	*S, kJ/K*	*U, MJ*	*Cp, kJ*
-12.92	-15.44	4.01	-15.44	1.78
C_{NaNO3}, mg/l	*Eh, B*	*pH*	*Ion strength*	*TDS, mg/kg sol*
29.3	-0.53	3.36	10	1092.73

Table 2. *Phase parameters of the system: tomato-water-sodium nitrate.*

Name phase	*Volume, m^3*	*Mole quantity*	*Mass, kg*	*Density, kg/m^3*	*Weight %*
AqueousSol.	$3.79 \cdot 10^{-6}$	$2.38 \cdot 10^{-4}$	$7.61 \cdot 10^{-3}$	$2.01 \cdot 10^{3}$	0.77283
Liquid	$2.93 \cdot 10^{-2}$	$5.27 \cdot 10^{-2}$	$9.74 \cdot 10^{-1}$	33.2	98.90978
Sulfur (S)	$5.84 \cdot 10^{-8}$	$3.74 \cdot 10^{-6}$	$1.20 \cdot 10^{-4}$	$2.05 \cdot 10^{3}$	0.01218
KCl	0	$4.03 \cdot 10^{-5}$	$3.00 \cdot 10^{-3}$	0	0.30519

Table 3. *Distribution of chemical elements of the system: tomato-water-sodium nitrate.*

Chemical elements	*Chemical component*	*Molality*	*mg/kg sol*	*Chemical potential*
Ca	0.003493	1.28	$5.13 \cdot 10^{4}$	-105505
Mg	0.008229	3.01	$7.32 \cdot 10^{4}$	-79752
Na	0.017744	6.50	$1.49 \cdot 10^{5}$	-48403
K	0.074172	12.4	$4.85 \cdot 10^{5}$	-53759
P	0.008394	3.07	$9.52 \cdot 10^{4}$	-3488
Cl	0.046658	2.32	$8.23 \cdot 10^{4}$	-43934
S	0.003742	0	0	38
N	0.000345	0.126	$1.77 \cdot 10^{3}$	-40802
C	1	22.2	$2.67 \cdot 10^{5}$	51310
H	103.8314	28.9	$2.91 \cdot 10^{4}$	8173
O	53.90142	53.7	$8.58 \cdot 10^{5}$	-73828

Table 4. *Distribution of components and particles of the system: tomato-water-sodium nitrate.*

Components and particles	*Molality*	*Mole quantity*	*mg/kg sol*	*Coeff. activity*
AqueousSol				
CO_2	$4.01 \cdot 10^{-5}$	$1.10 \cdot 10^{-7}$	$1.77 \cdot 10^{-3}$	6.8897
Ca^{+2}	0.589	$1.61 \cdot 10^{-3}$	23.6	19.322
$CaCl^{+}$	0.69	$1.88 \cdot 10^{-3}$	52.1	5.1448
$CaOH^{+}$	$7.79 \cdot 10^{-11}$	$2.13 \cdot 10^{-13}$	$4.45 \cdot 10^{-9}$	3.764
Cl^{-}	$5.09 \cdot 10^{-6}$	$1.39 \cdot 10^{-8}$	$1.81 \cdot 10^{-4}$	$4.9 \cdot 10^{4}$
HCO_2^{-}	22.2	$6.07 \cdot 10^{-2}$	1.00	$1.5 \cdot 10^{4}$
$H_2PO_2^{-}$	$2.89 \cdot 10^{-5}$	$7.89 \cdot 10^{-8}$	$1.88 \cdot 10^{-3}$	$1.0 \cdot 10^{4}$
$H_2PO_3^{-}$	3.07	$8.39 \cdot 10^{-3}$	$2.49 \cdot 10^{2}$	$3.4 \cdot 10^{3}$
HCO_3^{-}	$3.02 \cdot 10^{-12}$	$8.25 \cdot 10^{-15}$	$1.84 \cdot 10^{-10}$	1.1
HPO_3^{-2}	$5.28 \cdot 10^{-9}$	$1.44 \cdot 10^{-11}$	$4.22 \cdot 10^{-7}$	$1.2 \cdot 10^{9}$
HPO_4^{-2}	$2.47 \cdot 10^{-15}$	$6.73 \cdot 10^{-18}$	$2.37 \cdot 10^{-13}$	$1.0 \cdot 10^{10}$
K^{+}	12.4	$3.39 \cdot 10^{-2}$	$4.85 \cdot 10^{2}$	0.2817
$Mg(HCO_3)$	$3.15 \cdot 10^{-5}$	$8.60 \cdot 10^{-8}$	$2.69 \cdot 10^{-3}$	15.515
Mg^{+}	1.53	$4.18 \cdot 10^{-3}$	37.1	3.4
$MgCl^{+}$	1.48	$4.05 \cdot 10^{-3}$	88.7	1.6
$MgOH^{+}$	$1.25 \cdot 10^{-9}$	$3.41 \cdot 10^{-12}$	$5.16 \cdot 10^{-8}$	100
NH_4^{+}	$1.26 \cdot 10^{-1}$	$3.45 \cdot 10^{-4}$	2.28e	0.197
Na^{+}	6.35	$1.73 \cdot 10^{-2}$	$1.46 \cdot 10^{2}$	1.2706
H^{+}	$6.04 \cdot 10^{-3}$	$1.65 \cdot 10^{-5}$	$6.09 \cdot 10^{-3}$	0.0494
H_2O	38.5	$1.05 \cdot 10^{-1}$	1.90	1
Liquid				
CO_2	-	$9.39 \cdot 10^{-1}$	4.24	1
H_2O	-	51.5	95.34	0.0052
S	-	$3.74 \cdot 10^{-3}$	3.84	1
KCl	-	$4.03 \cdot 10^{-2}$	96.16	1

Table 5. *Gases parameters of the system: tomato-water-sodium nitrate.*

Components	*Fugacity*	*Log fugacity*	*Partial pressure*	*Log partial pressure*	*Coeff. fugacity*
NH_3	$4.19 \cdot 10^{-10}$	-9.38	$4.19 \cdot 10^{-10}$	-9.3	1
CO_2	$1.78 \cdot 10^{-2}$	-1.75	$1.78 \cdot 10^{-2}$	-1.7	1
N_2	$9.85 \cdot 10^{-62}$	-61.0	$9.85 \cdot 10^{-62}$	-61	1
O_2	$1.00 \cdot 10^{-70}$	-110	$1.00 \cdot 10^{-70}$	-110	1
H_2O	$4.26 \cdot 10^{-3}$	-2.37	$4.26 \cdot 10^{-3}$	-2.3	1

The hydrogen index of a tomato (Table 1-5, Figure 1) at different temperatures was equal to: 278K, pH = 3.34; T = 283 K, pH = 3.35; T = 288 K, pH = 3.36; T = 293 K, pH = 3.36; T = 298 K, pH = 3.37, i.e. the medium was acidic (Figure 1). Antioxidation nature of the aqueous solution of the tomato was caused by the values of the oxidation-reduction potential of the tomato (Eh, B): T = 278 K, Eh = -0.540; T = 283 K, Eh = -0.535; T = 288 K, Eh = -0.529; T = 293 K, Eh = -0.523; T = 298 K, Eh = -0.518, where Eh <0 and the oxidizing medium. It was noted that with increasing temperature, the acidity of the tomato decreases (Figure 2). Negative values of the thermodynamic parameters ΔG, ΔH, ΔU (Table 1-5) of the system indicate the progress of the ion transport process in phases (the ionic strength was I = 10), while the amount of dissolved substances in 1 kg aqueous tomato solution was (TDS, mg / kg): T = 278.15K, TDS = 1098.0; T = 283.15 K, TDS = 1092.7; T = 288.15 K, TDS = 1087.5; T = 293.15 K, TDS = 1082.4; T = 298.15K, TDS = 1077.7.

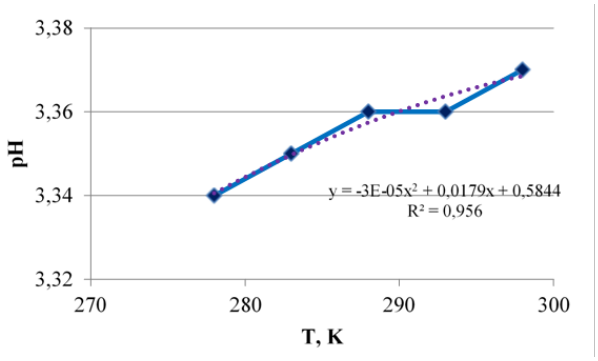

Figure 1. *The change in the pH of an aqueous tomato solution depending on temperature, $NaNO_3$ content of 29.3 mg/l.*

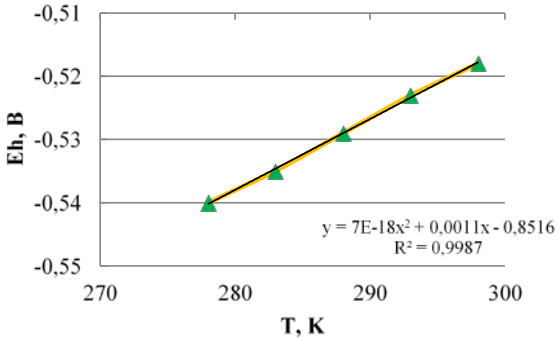

Figure 2. *Change in the redox potential of an aqueous tomato solution depending on temperature, $NaNO_3$ content of 29.3 mg/l.*

With the increase of sodium nitrate in the system: tomato (macroelements) - water - sodium nitrate within the temperature range from 278 to 293 K the hydrogen index of the tomato increases, i.e. the process of neutralizing the acidic medium based on sodium hydroxide proceeds: $NaNO_3$ - 29.3 mg/l, pH = 3.34-3.37; $NaNO_3$ - 29.5 mg/l, pH = 3.63-3.66; $NaNO_3$ -29.6 mg/l, pH = 3.87-3.94; $NaNO_3$ - 29.7 mg/l, pH = 4.31-4.47; $NaNO_3$ - 30 mg/l, pH = 4.76-4.89; $NaNO_3$ - 35 mg/l, pH = 4.77-4.89; $NaNO_3$ - 40 mg/l, pH = 4.77-4.89; $NaNO_3$ - 45 mg/l, pH = 4.77-4.9; $NaNO_3$ - 50 mg/l, pH = 4.78-4.9. It should be noted that the calculated hydrogen value of a tomato determined on the basis of the model compiled corresponds to the experimental pH values measured by the Denver instrument (pH = 3.3-4.38). The total weight balance in the phases was 100% (Table 1-5), and thus confirm the adequacy of the calculated results obtained on the basis of the proposed model of the system: tomato-water-sodium nitrate.

It can be seen from Table 6 that as the temperature of the aqueous tomato solution increases, the concentrations of $CaOH^{+}$, Cl^{-}, $H_2PO_2^{-}$, HCO_3^{-}, HPO_3^{2-} increase, and such particles as Ca^{+2}, $Mg(HCO_3)^{+}$ decrease slightly. Concentrations of $CaCl^{+}$,HCO_2^{-}, $H_2PO_3^{-}$, HPO_4^{2-}, K^{+}, Mg^{+2}, $MgCl^{+}$, $MgOH^{+}$, NH_4^{+}, Na^{+}, $NaCl^{+}$, $H^{+}$and H_2O remain constant.

Table 6. *Concentration distribution of cations and anions in an aqueous tomato solution as a function of temperature. The content of $NaNO_3$ = 29.3 mg/l.*

Particle distribution in moles	*Temperature, K*			
	278.15	*288.5*	*293.15*	*298.15*
Ca^{+2}	$1.8\cdot10^{-3}$	$1.67\cdot10^{-3}$	$1.61\cdot10^{-3}$	$1.55\cdot10^{-3}$
$CaCl^{+}$	$1.7\cdot10^{-3}$	$1.82\cdot10^{-3}$	$1.88\cdot10^{-3}$	$1.94\cdot10^{-3}$
$CaOH^{+}$	$6.1\cdot10^{-14}$	$1.43\cdot10^{-13}$	$2.13\cdot10^{-13}$	$3.12\cdot10^{-13}$
Cl^{-}	$3.4\cdot10^{-9}$	$8.91\cdot10^{-9}$	$1.39\cdot10^{-8}$	$2.13\cdot10^{-8}$
HCO_2^{-}	$6.0\cdot10^{-2}$	$6.07\cdot10^{-2}$	$6.07\cdot10^{-2}$	$6.07\cdot10^{-2}$
HCO_3^{-}	$4.7\cdot10^{-15}$	$6.7\cdot10^{-15}$	$8.25\cdot10^{-15}$	$1.01\cdot10^{-14}$
$H_2PO_2^{-}$	$1.1\cdot10^{-8}$	$5.03\cdot10^{-8}$	$7.89\cdot10^{-8}$	$1.24\cdot10^{-7}$
$H_2PO_3^{-}$	$8.9\cdot10^{-3}$	$8.39\cdot10^{-3}$	$8.39\cdot10^{-3}$	$8.39\cdot10^{-3}$
HPO_3^{2-}	$4.2\cdot10^{-12}$	$9.76\cdot10^{-12}$	$1.44\cdot10^{-11}$	$2.09\cdot10^{-11}$
HPO_4^{2-}	$3.2\cdot10^{-18}$	$5.39\cdot10^{-18}$	$6.73\cdot10^{-18}$	$8.26\cdot10^{-18}$
K^{+}	$3.3\cdot10^{-2}$	$3.37\cdot10^{-2}$	$3.39\cdot10^{-2}$	$3.41\cdot10^{-2}$
$Mg(HCO_3)^{+}$	$1.7\cdot10^{-7}$	$1.09\cdot10^{-7}$	$8.6\cdot10^{-8}$	$6.95\cdot10^{-8}$
Mg^{+2}	$4.3\cdot10^{-3}$	$4.25\cdot10^{-3}$	$4.18\cdot10^{-3}$	$4.1\cdot10^{-3}$
$MgCl^{+}$	$3.8\cdot10^{-3}$	$3.98\cdot10^{-3}$	$4.05\cdot10^{-3}$	$4.13\cdot10^{-3}$
$MgOH^{+}$	$1.2\cdot10^{-12}$	$2.46\cdot10^{-12}$	$3.41\cdot10^{-12}$	$4.67\cdot10^{-12}$
NH_4^{+}	$3.4\cdot10^{-4}$	$3.45\cdot10^{-4}$	$3.45\cdot10^{-4}$	$3.45\cdot10^{-4}$
Na^{+}	$1.7\cdot10^{-2}$	$1.74\cdot10^{-2}$	$1.73\cdot10^{-2}$	$1.73\cdot10^{-2}$
$NaCl^{+}$	$2.5\cdot10^{-4}$	$3.42\cdot10^{-4}$	$3.95\cdot10^{-4}$	$4.52\cdot10^{-4}$
H^{+}	$1.6\cdot10^{-5}$	$1.64\cdot10^{-5}$	$1.65\cdot10^{-5}$	$1.66\cdot10^{-5}$
H_2O	$1.0\cdot10^{-1}$	$1.04\cdot10^{-1}$	$1.05\cdot10^{-1}$	$1.07\cdot10^{-1}$

With increasing sodium nitrate content in the aqueous tomato solution, the concentrations of $CaOH^{+}$, $H_2PO_2^{-}$, HCO_3^{-}, HPO_3^{2-}, HPO_4^{2-}, $Mg(HCO_3)^{+}$, $MgOH^{+}$, H^{+}were increased, and such particles as Ca^{+2}, $CaCl^{+}$, Cl^{-}, HCO_2^{-}, $H_2PO_3^{-}$, K^{+}, Mg^{+2}, $MgCl^{+}$, NH_4^{+}, Na^{+}, $NaCl^{+}$, and H_2O change a little or remain constant (Table 7).

Table 7. *Concentration distribution of cations and anions in an aqueous solution of a tomato depending on the content of sodium nitrate. Temperature is 293 K.*

Particle distribution in moles	*Concentration of sodium nitrate in an aqueous solution of tomato, mg/l*							
	29.3	*29.5*	*29.7*	*30.0*	*35.0*	*40.0*	*45.0*	*50.0*
Ca^{+2}	$1.61\cdot10^{-3}$	$1.61\cdot10^{-3}$	$1.61\cdot10^{-3}$	$1.61\cdot10^{-3}$	$1.57\cdot10^{-3}$	$1.53\cdot10^{-3}$	$1.48\cdot10^{-3}$	$1.44\cdot10^{-3}$
$CaCl^{+}$	$1.88\cdot10^{-3}$	$1.88\cdot10^{-3}$	$1.88\cdot10^{-3}$	$1.88\cdot10^{-3}$	$1.83\cdot10^{-3}$	$1.79\cdot10^{-3}$	$1.74\cdot10^{-3}$	$1.69\cdot10^{-3}$
$CaOH^{+}$	$2.13\cdot10^{-13}$	$4.15\cdot10^{-13}$	$2.51\cdot10^{-12}$	$6.66\cdot10^{-12}$	$6.54\cdot10^{-12}$	$6.42\cdot10^{-12}$	$6.3\cdot10^{-12}$	$6.18\cdot10^{-12}$
Cl^{-}	$1.39\cdot10^{-8}$	$1.39\cdot10^{-8}$	$1.39\cdot10^{-8}$	$1.39\cdot10^{-8}$	$1.39\cdot10^{-8}$	$1.38\cdot10^{-8}$	$1.38\cdot10^{-8}$	$1.37\cdot10^{-8}$
HCO_2^{-}	$6.07\cdot10^{-2}$	$6.07\cdot10^{-2}$	$6.07\cdot10^{-2}$	$6.06\cdot10^{-2}$	$6.04\cdot10^{-2}$	$6.01\cdot10^{-2}$	$5.99\cdot10^{-2}$	$5.97\cdot10^{-2}$
HCO_3^{-}	$8.25\cdot10^{-15}$	$1.61\cdot10^{-14}$	$9.72\cdot10^{-14}$	$2.58\cdot10^{-13}$	$2.60\cdot10^{-13}$	$2.60\cdot10^{-13}$	$2.62\cdot10^{-13}$	$2.64\cdot10^{-13}$
$H_2PO_2^{-}$	$7.89\cdot10^{-8}$	$4.07\cdot10^{-8}$	$6.73\cdot10^{-9}$	$2.53\cdot10^{-9}$	$2.51\cdot10^{-9}$	$2.49\cdot10^{-9}$	$2.47\cdot10^{-9}$	$2.44\cdot10^{-9}$
$H_2PO_3^{-}$	$8.39\cdot10^{-3}$	$8.39\cdot10^{-3}$	$8.39\cdot10^{-3}$	$8.39\cdot10^{-3}$	$8.39\cdot10^{-3}$	$8.39\cdot10^{-3}$	$8.39\cdot10^{-3}$	$8.39\cdot10^{-3}$
HPO_3^{2-}	$1.44\cdot10^{-11}$	$2.81\cdot10^{-11}$	$1.69\cdot10^{-10}$	$4.52\cdot10^{-10}$	$4.55\cdot10^{-10}$	$4.62\cdot10^{-10}$	$4.62\cdot10^{-10}$	$4.66\cdot10^{-10}$
HPO_4^{2-}	$6.73\cdot10^{-18}$	$2.56\cdot10^{-17}$	$9.35\cdot10^{-16}$	$6.61\cdot10^{-15}$	$6.72\cdot10^{-15}$	$6.95\cdot10^{-15}$	$6.95\cdot10^{-15}$	$7.07\cdot10^{-15}$
K^{+}	$3.39\cdot10^{-2}$	$3.38\cdot10^{-2}$	$3.38\cdot10^{-2}$	$3.38\cdot10^{-2}$	$3.37\cdot10^{-2}$	$3.37\cdot10^{-2}$	$3.36\cdot10^{-2}$	$3.35\cdot10^{-2}$
$Mg(HCO_3)^{+}$	$8.6\cdot10^{-8}$	$1.67\cdot10^{-7}$	$1.02\cdot10^{-6}$	$2.7\cdot10^{-6}$	2.69e-06	$2.67\cdot10^{-6}$	$2.67\cdot10^{-6}$	$2.67\cdot10^{-6}$
Mg^{+2}	$4.17\cdot10^{-3}$	$4.17\cdot10^{-3}$	$4.17\cdot10^{-3}$	$4.17\cdot10^{-3}$	$4.13\cdot10^{-3}$	$4.08\cdot10^{-3}$	$4.04\cdot10^{-3}$	$3.99\cdot10^{-3}$
$MgCl^{+}$	$4.05\cdot10^{-3}$	$4.05\cdot10^{-3}$	$4.05\cdot10^{-3}$	$4.05\cdot10^{-3}$	$4.01\cdot10^{-3}$	$3.96\cdot10^{-3}$	$3.92\cdot10^{-3}$	$3.87\cdot10^{-3}$
$MgOH^{+}$	$3.41\cdot10^{-12}$	$6.64\cdot10^{-12}$	$4.01\cdot10^{-10}$	$1.07\cdot10^{-10}$	$1.06\cdot10^{-10}$	$1.06\cdot10^{-10}$	$1.06\cdot10^{-10}$	$1.05\cdot10^{-10}$
NH_4^{+}	$3.45\cdot10^{-4}$	$3.47\cdot10^{-4}$	$3.49\cdot10^{-4}$	$3.53\cdot10^{-4}$	$4.12\cdot10^{-4}$	$4.71\cdot10^{-4}$	$5.29\cdot10^{-4}$	$5.88\cdot10^{-4}$
Na^{+}	$1.73\cdot10^{-2}$	$1.73\cdot10^{-2}$	$1.73\cdot10^{-2}$	$1.74\cdot10^{-2}$	$1.74\cdot10^{-2}$	$1.75\cdot10^{-2}$	$1.75\cdot10^{-2}$	$1.76\cdot10^{-2}$
$NaCl^{+}$	$3.95\cdot10^{-4}$	$3.95\cdot10^{-4}$	$3.95\cdot10^{-4}$	$3.95\cdot10^{-4}$	$3.96\cdot10^{-4}$	$3.97\cdot10^{-4}$	$3.98\cdot10^{-4}$	$3.99\cdot10^{-4}$
H^{+}	$1.65\cdot10^{-5}$	$8.46\cdot10^{-6}$	$1.40\cdot10^{-6}$	$5.26\cdot10^{-7}$	$5.2\cdot10^{-7}$	$5.14\cdot10^{-7}$	$5.08\cdot10^{-7}$	$5.04\cdot10^{-7}$
H_2O	$1.05\cdot10^{-1}$	$1.05\cdot10^{-1}$	$1.05\cdot10^{-1}$	$1.05\cdot10^{-1}$	$1.05\cdot10^{-1}$	$1.04\cdot10^{-1}$	$1.04\cdot10^{-1}$	$1.04\cdot10^{-1}$

Thus, the synergistic effect of temperature and sodium nitrate were observed only in such complex pair particles as $CaOH^{+}$, $H_2PO_2^{-}$, HCO_3^{-}, HPO_3^{2-}, where their content grows in an aqueous solution of tomato due to their low migration, and

apparently due to the significant partial pressure of carbon dioxide and the chemical potential of the phosphorus-containing particles in the system. (Table 1-5).

4. Conclusions

Physicochemical modeling of the system: tomato-water-sodium nitrate was carried out. In the calculations, the macronutrient composition and humidity of the tomato were used at various temperatures and concentrations of sodium nitrate. The hydrogen index of a tomato was calculated at various temperatures, and it was noted that the medium of tomato was acidic. With an increase in the sodium nitrate content in the system: tomato - water - sodium nitrate within the temperature range from 278 to 293 K, the hydrogen index of the tomato increases, i.e. the process of neutralizing the acidic medium based on sodium hydroxide proceeds. The calculated hydrogen value of the tomato corresponds to the experimental values of pH = 3.3-4.38. The oxidation-reduction potential (Eh, B) of the tomato-water-sodium nitrate system at different temperatures was established, and it was confirmed that the medium was oxidizing (Eh <0). It was noted that with increasing temperature, the acidity of the tomato decreases. As the temperature of the aqueous tomato solution increases, the concentrations of $CaOH^+$, Cl^-, $H_2PO_2^-$, HCO_3^-, HPO_3^{2-} increase, and such particles as Ca^{+2}, $Mg(HCO_3)^+$ decrease slightly. Concentrations of $CaCl^+$,HCO_2^-, $H_2PO_3^-$, HPO_4^{2-}, K^+, Mg^{+2}, $MgCl^+$, $MgOH^+$, NH_4^+, Na^+, $NaCl^+$, H^+ and content of H_2O remain practically constant. With increasing sodium nitrate content in the aqueous tomato solution, the concentrations of $CaOH^+$, $H_2PO_2^-$, HCO_3^-, HPO_3^{2-}, HPO_4^{2-}, $Mg(HCO_3)^+$, $MgOH^+$, H^+ are increased, and such particles as Ca^{+2}, $CaCl^+$, Cl^-, HCO_2^-, $H_2PO_3^-$, K^+, Mg^{+2}, $MgCl^+$, NH_4^+, Na^+, $NaCl^+$and H_2O change little or remain constant. The synergistic effect of temperature and sodium nitrate was observed only in such complex pair particles as $CaOH^+$, $H_2PO_2^-$, HCO_3^-, HPO_3^{2-}, where their content grows in an aqueous solution of tomato due to their low migration, and apparently due to the significant partial pressure of carbon dioxide and the chemical potential of the phosphorus-containing particles in the system.

References

[1] Adeniyi H., Ademoyegun O. “Effects of different rates and sources of fertilizer on yield and antioxidant components of Tomato”. African Journal, 7(2), (2012), 135-138.

[2] Oguntibeju O.O., Truter E.J., Esterhuyse A.J. “The Role of Fruit and Vegetable Consumption in Human Health and Disease Prevention”. Diabetes Mellithus – Insight and Perspectives, (2013), 117 – 130.

[3] Slunkhe D.K., Jadhav S.J., Yu M.H. “Quality and nutritional composition of tomato fruit as influenced by certain biochemical and physiological changes”. Qual.Plant. Plant Foods Hum. Nutr., 24, (1974), 85.

[4] Alvarez M. A. B., Gagne S., Antoun H. “Effect of compost on rhizosphere microflora of the tomato and on the incidence of plant growth-promoting rhizobacteria”. App.Environ. Microbial, 61, (1995). 194-199.

[5] Aoun A.B., Lechiheb B., Benyahya L., Ferchich A. “Evaluation of fruit quality traits of traditional varieties of tomato (Solanum lycopersicum) grown in Tunisia”. African Journal of Food Science, 7, (2013), 350-354.

[6] Wang Z.H., Zong Z.Q., Li S.X., Chen B.M. “Nitrate accumulation in vegetables and its residual in vegetable fields”. Environ. Sci., 23, (2002), 79–83.

[7] Phipps R.H., Cornforth I.S. “Factors affecting the toxicity of nitrite nitrogen to tomatoes”. Plant and Soil, 33, (1970), 457.

[8] Ranjan D., Rabha B.K., Ahmed F. “Effect of some plant growth regulators and micronutrients mixture on physio morphic character of tomato”. Ann.Agric.Res.New Series, 26 (4), (2005), 476-480.

[9] Sanyal D., Kar P.L., Longkukar M. “Effect of growth regulators on the physico-chemical composition of tomato (Lycopersicon esculentum Mill.)”. Adv. Hort. & Forestry, 4, (1995), 67-71.

[10] Krumbien A., Auerswald H. “Characterization of aroma volatiles in tomatoes by sensory analyses”. Nahrung, 42(6), (1998), 395-399.

[11] Gajbhiye N. D. “Toxic Effect of Sodium Nitrate on Germinating Seeds of Vigna radiate”. International Journal of Biotechnology and Bioengineering, 7(10), (2013), 1006.

[12] Bokade N. “Effect of growth regulators on growth and yield of summer tomato”. J. Maharashtra Agric. Univ., 31(1), (2006), 64-65.

[13] Desai S.S., Chovatia R.S., Singh V. “Effect of different plant growth regulators and micronutrients on fruit quality and plant micronutrient content of tomato”. International Journal of Agricultural Sciences, 10 (1), (2014), 130-133.

[14] Bosco F., Capolongo A., Ruggeri B. “Effect of temperature, pH, ionic strength, and sodium nitrate on activity of LiPs: Implications for bioremediation”. Bioremediation Journal, 6 (1), (2010), 65-76.

[15] Hojhabrian M. “Effect of different soil pHs on the growth and proceeds of Tomatoes”. Journal of Novel Applied Sciences, 3 (2), (2014), 145-147.

[16] Fan X.H., Li Y.C. “Nitrogen release from slow-release fertilizers as affected by soil type and temperature”. Soil Sci. Soc. Amer. J, 74, (2010), 1635–1641.

[17] Yanar D., Geboloğlu N., Yanar Y., Aydin M., Çakmak P. “Effect of different organic fertilizers on yield and fruit quality of ındeterminate tomato (Lycopersicon esculentum)”. Scientific Research and Essays, 6, (2011), 3623-3628.

[18] Liu C.W., Sung Y., Chen B.C., Lai H.Y. “Effects of Nitrogen Fertilizers on the Growth and Nitrate Content of Lettuce (Lactuca sativa L.)”. Int. J. Environ. Res. Public Health, 11, (2014), 4427-4440.

[19] Ejaz M., Waqas R., Butt M., Rehman S., Manan A. “Role of macronutrients and micronutrients in enhancing the quality of tomato”. IJAVMS, 5 (4), (2011), 401-404.

[20] Xu Y., Barringer S. “Comparison of tomatillo and tomato volatile compounds in the headspace by selected ion flow tube mass spectrometry”. Journal of Food Science, 75(3), (2010), 268-273.

[21] Patana-anake P., Barringer S. “The Effect of Temperature, pH, and Food additives on Tomato Product Volatile Levels”. International Food Research Journal, 22(2), (2015), 561-571.

[22] Mukta S., Rahman M.M., Mortuza M.G. “Yield and nutrient content of tomato as influenced by the application of vermicompost and chemical fertilizers”. J. Environ. Sci. & Natural Resources, 8 (2), (2015), 115-122.

[23] Dabire C., Sereme A., Parkouda C., Somda M.K., “Traore A. S. Influence of organic and mineral fertilizers on chemical and biochemical compounds content in tomato (solanum lycopersicum) var. mongal F1”. Journal of Experimental Biology and Agricultural Sciences, 4 (6), (2016), 631-636.

[24] Kazeniac S.J., Hall R.M. “Flavor chemistry of tomato volatiles”. Journal of Food Science, 35(5), (1970), 519-530.

[25] Çolpan E., Zengin M., Özbahçe A. “The effects of potassium on the yield and fruit quality components of stick tomato”. Horticulture, Environment and Biotechnology, 54, (2013), 20-28.

[26] Makinde A.I., Jokanola O.O., Adedeji J.A., Awogbade A.L., Adekunle A.F. “Impact of Organic and Inorganic Fertilizers on the Yield, Lycopene and Some Minerals in tomato (Lycopersicum esculentum Mill) Fruit”. European Journal of Agriculture and Forestry Research, 4, (2016), 18-26.

[27] Abduli M.A., Amiri L., Madadian E., Gitipour S., Sedighian S. “Efficiency of vermicompost on quantitative and qualitative growth of tomato plants”. International Journal of Environmental Research, 7(2), (2013), 467-472.

[28] Naresh B. “Response of foliar application of boron on vegetative growth, fruit yield quality of tomato var. Pusa-Ruby”. Indian Journal of Hill Farming, 15(1), (2002), 109-112.

[29] Yadav P.V.S., Abha T., Sharma N.K. “Effect of zinc and boron on growth, flowering and fruiting of tomato (Lycopersicon esculentum, Mill)”. Haryana Journal of Horticultural Science, 30(1/2), (2001), 105-107.

[30] Davies G.M., Hobes G. “The constituent of tomato fruit the influence of environment nutrition and genotypes”. Critical Review Food Sci. & Nutr., 15, (1981), 205-280.

[31] Huang J.S., Snapp S.S. “The effect of boron, calcium, and surface moisture on shoulder check, a quality defect in freshmarket tomato”. J. American Soc. Hort. Sci., 129(4), (2004), 599 – 607.

[32] Santamaria P. “Nitrate in vegetables: Toxicity, content, intake and EC regulation”. J. Sci. Food Agr., 86, (2006), 10–17.

[33] Petersen A., Stoltze S. “Nitrate and nitrite in vegetables on the Danish meaket: content and intake”. Food Addit. Contam., 16, (1999), 291–299.

[34] Karpov I.K., Chudnenko K.V., Kulik D.A., Bychinskyi V.A. “The convex programming minimization of five thermodynamic potential other than Gibbs energy in geo-chemical modeling”. American J. Science., 302, (2002), 281-311.

[35] Helgeson H.C., Delany J.M., Nesbitt H.W., Bird D.K. “Summary and critique of the thermodynamic properties of rock-forming minerals”. American J. Science., (1978), 278-A: 1-229.

[36] Maimekov Z.K., Abdykadyrova R.E., Sambaeva D.A., Isaev A.D., Izakov J.B., Maymekov T.Z. “Physicochemical modeling of a heterogeneous complex system: soil-water-sodium nitrate and ecological assessment of the concentration distribution of components and particles in a slurry solution”. Science, New technologies and Innovations of Kyrgyzstan-Bishkek, 1, (2018), 18-23.

[37] Karpov I.K., Chudnenko K.V., Kulik D.A. “Modeling chemical mass transfer in geochemical processes: Thermodynamic relations, conditions of equilibria, and numerical algorithms”. American J. Science., 297, (1997), 767-806.

[38] Bekseev Sh. G. “Early vegetable growing. Breeding, cultivation, seed growing”, 1st edition. Nauka, St. Peterburg. (2006), 131-140.

MANAS Journal of Engineering
ISSN 1694-7398 | e-ISSN 1694-7398

Volume 8 (Issue 1) (2020) Pages 17-21

Detection of some antioxidant enzyme activities in apricot fruit grown in Van region from Turkey

Mustafa Bilici[1,2]

[1]Van Yuzuncu Yil University, Faculty of Medicine, Medical Education, 65080,Van, Turkey

[2]Van Yuzuncu Yil University, Faculty of Science, Department of Chemistry,Van, Turkey, mustafabilici@yyu.edu.tr, ORCID: 0000-0002-8689-6463

ABSTRACT

In this study, it was aimed to determine antioxidant enzyme activity in apricot fruit. The antioxidant property of this fruit is quite high. Its structure contains many vitamins, minerals and enzymes. For this purpose, it is aimed to determine the activity of superoxide dismutase (SOD) which is one of the enzyme activities thought to be present in apricot fruit. Furthermore, oxidative stress indicator and the level of malondialdehyde (MDA) were determined. SOD and MDA values of the apricot samples were determined to be 0.076 U/ml and 1.579 mmol/l, respectively (($p \leq 0.05$). In this study, antioxidant enzyme activity and lipid peroxidation were determined by spectrophotometric method. Then, the results obtained were analyzed by using multidimensional statistical methods and the results were discussed in a multidimensional manner.

ARTICLE INFO

Research article

Received: 01.05.2020
Accepted: 22.05.2020

Keywords:
Apricot,
fruit,
antioxidant enzyme,
oxidative stress,
MDA

1. Introduction

The reactive molecules formed during the transformation of nutrients into energy form provided that they use oxygen are called free radicals. Oxygen is a quite necessary molecule for the maintenance of life and also forms intermediates that act as sources of free radicals and are highly reactive. These molecules formed cause damage to protein, lipid and DNA-like cell groups. Antioxidant defense systems have been developed to control the formation of free radicals in aerobic structures and to prevent the bad effects of these molecules [1,2]. Sometimes, antioxidant defense systems cannot completely prevent the harmful effects of free radicals, which results in oxidative stress [3]. In some studies that have been recently carried out in pathogen-plant interaction, it has been shown that catalase, ascorbate peroxidase, superoxide dismutase-like enzymes that destroy the toxic side effects of reactive oxygen molecules have effects [4].

In this study, the fact that the antioxidant properties of the above-mentioned enzymes are quite high is clearly seen in our analysis results. The inoculation of plants with pathogens or the application of microbial signals of cell culture leads to the rapid generation of hydrogen peroxide, which is one of the reactive oxygen species [5]. The organism structure tries to keep free radicals occurring as the normal product of the physiological activities of plants at a level as the oxidant-antioxidant balance with a very sensitive structure that the plant first gain. The disruption of this balance structure leads to oxidative stress. The biggest barrier to oxidative damage is the big difference between the oxygen concentration in the atmosphere (150mmHg) and the oxygen concentration in the tissue structure (30mmHg). In addition to this advantage, endogenous antioxidant systems and antioxidants which are called exogenous are also available [6,7].

Fruits are a rich source of phenolic and polyphenolic compounds that are responsible especially for their protection against oxidative stress. The close interest in the possible protective effects of dietary antioxidants against human degenerative diseases has led to the investigation of food components [8]. Apples, blueberry and apricot are the members of ***ericaceae*** family. Apricot that can be very easily distinguished from other fruits with the help of its different colors is grown in many regions in Turkey and in many regions in America and northern Europe in the world. That's exactly for this reason apricot fruit with many different species is called by different names according to its types in different regions. It is also of great importance to distinguish well according to this type of fruit which is called by the names Şekerpare, Iğdır, Malatya, Hacıhaliloğlu, Kabaaşı and Soğancı apricot to take advantage of its benefits. Some of the other apricot varieties grown in Turkey are Hasanbey, Çataloğlu, Çöloğlu, Alyanak, Şalak (Aprikoz), Şekerpare, Tokaloğlu-

Erzincan, Tokaloğlu-Yalova, Tokaloğlu-Konya Ereğli, Şam, Turfanda İzmir, İri, Bitirgen, İmrahor, Karacabey, Çiğli, Sakıt 2, Mahmudun Eriği, Adilcevaz-5, Turfanda Eskimalatya, Çekirge 52, Hacıkız, İsmailağa, Ethembey, Kuru Kabuk varieties. There are also some foreign apricot varieties which can be listed as Paviot, Canino, Stark Early Orange, Hungarian Best, Cafona, Precoce de Colomer, Polonais, San Castrese, Boccuccia, Wilson Delicious, Luizet, Fracasso, Royal, Perfection. Furthermore, apricot fruit contains antioxidants that fight cancer. Strong antioxidants in apricot fruit decrease the risk of developing various types of cancer. Antioxidants protect your cells against the damage of free radicals and environmental pollutants. This is very important to prevent the growth of tumors. Apricot fruit also contains folic acid. They are nutrients that help repair and synthesize DNA and also prevent the mutation of malignant cells. They strengthen the bones and teeth, protect the heart health, and in addition to these, they are also perfect for improving circulation and oxygenation of cells. They are also known to be good for diabetes, eye health and kidney disorders. When all these characteristics are taken into consideration, apricot fruit is a very important plant for human health. [9,10]

Superoxide dismutase (SOD, EC 1.15.1.1) is an enzyme that catalyses the conversion of the superoxide (O_2^-) radical to oxygen (O_2) and hydrogen peroxide (H_2O_2). Superoxide is a by-product of oxygen metabolism and, if not regulated orderly, leads to formation of cell damage [11]. H_2O_2 is also harmful for living cells and can be degraded by other enzymes. Therefore, SOD is an important antioxidant defense in nearly all living cells. One exception is Lactobacillus plantarum and related lactobacilli, which use a different mechanism to prevent damage from reactive O_2^-. Irwin Fridovich and Joe McCord at Duke University discovered the enzymatic activity of superoxide dismutase in 1968. SODs were previously known as a group of metalloproteins with unknown function; for example, CuZnSOD was known as erythrocuprein (or hemocuprein, or cytocuprein) or as the veterinary anti-inflammatory drug "Orgotein". Likewise, Brewer (1967) identified a protein that later became known as superoxide dismutase as an indophenol oxidase by protein analysis of starch gels using the phenazine-tetrazolium technique [12].

Free radicals that occur during normal metabolism or pathologically cause many damages in cells and tissues. Since oxidative damage caused by free oxygen radicals affects biomolecules such as protein, lipid and nucleic acid, some clinical tests for oxidative products of these biomolecules are used to demonstrate oxidative stress [13]. Hydroperoxides are the first stable products formed during the peroxidation of unsaturated lipids. The decomposition of lipid hydroperoxides forms a complex mixture of secondary peroxidation products such as hydrocarbon gases (ethane, pentane) and aldehydes (malondialdehyde, MDA). It is reported that MDA increases the permeability of cell membranes, affects ion exchange of membranes, disrupts intracellular ion balance, causes enzyme activities to deteriorate, breaks DNA structure. It is known that it may cause endothelial dysfunction and consequently atherosclerosis, causing disruption between antioxidants and free radicals [14,15].

In this study, superoxide dismutase (SOD), the antioxidant enzyme of apricot fruit and the level of malondialdehyde (MDA), which is the end product of lipid peroxidation, were examined.

2. Material and method

In this study, fruit samples were taken for the processes performed to determine antioxidant enzyme activity, and for the methods and antioxidant enzyme activities. Then, the processes of obtaining extracts were performed for antioxidant enzyme analyses. Apricots samples (***Prunus armeniaca***) were collected in Van region from Turkey.

2.1. Preparation of Apricot Extracts;

Apricot samples were cut into small pieces, frozen in liquid nitrogen and crushed in a blender. The apricot samples obtained were subjected to extraction with three different solvents (diethyl ether, ethanol, water) with different polarities (4,3; 24,3; 78,5 dielectric constant, respectively). For this purpose, 10 g of fruit samples was taken and extracted for 400 minutes with 250 mL diethyl ether in soxhlet apparatus. After extraction, diethyl ether was removed at 40 °C' in a rotary evaporator (ether extract). After the fruit residues obtained at the end of diethyl ether extraction were treated for eight times with 150/min revolution in the stirrer and one hour periods until the solution became colourless with 50 mL ethanol in the dark, they were filtered, and the filtrates were combined. Ethanol in the sample was removed at 40 °C' in a rotary evaporator (ethanol extract). Fruit residues from ethanol extraction were dried and then boiled for 10 minutes by mixing with distilled water (200 mL) with a volume of up to 20 times of it, and the filtrate was frozen after the filtration process. The frozen samples were kept in freeze dryer at 0.04 mbar -50 °C for 96 hours, and then the water was removed (water extract). Furthermore, after 10 grams of crashed fruit samples were boiled with distilled water (200 mL) with a volume of up to 20 times of them for 10 minutes and filtered, they were frozen and lyophilized (hot water extract). All extracts obtained were stored at +4 °C. The samples were preserved at -18 °C in cases where they were not used for a long time.

2.2. Determination of Superoxide Dismutase (SOD) Activity (Manual Method)

To determine the SOD activity of the apricot samples, the reactive solution sample was prepared according to literature [16]. The sample volume and blind volume were adjusted as indicated Table 1. After it was waited at a room temperature of 25˚C for 20 minutes, 50 µl of blind and 50 µl of samples from $CuCl_2$ were added to it. After pipetting was performed as indicated in 1, blind and sample tubes were read

spectrophotometrically against bidistilled water at 560 nm. The SOD activity of the sample was calculated accordingly to equation given below:

Inhibition, %: [(Blind OD – Sample OD) / Blind OD] x 100

1 Unit SOD: is the enzyme activity inhibiting Nitroblue tetrazolium reduction by 50%.

Activity = (inhibition, %) / (50 x 0.1)

Activity was calculated in U/ml [16].

Table 1. *SOD Activity Determination Method:*

	Blind	Sample
Reactive	1.425 µl	1.425 µl
Sample	-	50 µl
Bidistilled	-	100 µl
Xanthine oxidase	25 µl	25 µl

2.3. Determination of Malondialdehyde (MDA) Level

To determine the MDA level of the samples, the reactive solutions were prepared according to published procedure [17]

2.4. Experimental Procedure

200 ul of sample was taken in a tube. 800 µl of phosphate buffer and 25 µl of BHT solution and 500 µl of 30% TCA were added to it. The tubes were mixed in vortex and kept in the ice bath for 2 hours after their caps were closed. The tubes were cooled to room temperature. Then, after the caps of the tubes were removed, they were centrifuged at 2000 rpm for 15 minutes. 1 ml of the supernatant obtained from centrifugation (filtrate) was taken and transferred to other tubes. 75 µl EDTA, 25 µl TBA were added to filtrates 1 ml of which was taken. The tubes were mixed in vortex and kept in hot water bath at (70˚C) for 15 minutes. Then, it was cooled to room temperature, and their absorbance was read in UV/Vis spectrophotometer at 532 nm.

Calculation of Malondialdehyde (MDA) level:
C= F x 6.41 x A
C= concentration
F= dilution factor
A= absorbance
Level calculation; it was calculated as µmol/L [18].

3. Results

The experimental results for SOD and MDA are given in the Table 2. The trials were given according to statistical value as a result of 5 different groups and 3 repeated analyses ($p \leq 0.05$). Duncan and ANOVA statistical methods were used. Based on these results obtained, it was observed that apricot fruit had quite high values in terms of antioxidant enzyme activity compared to many other fruits (Apple, Pear, Quince Cranberry. Strawberry, etc.).

Table 2. *In this study, SOD activity values, the antioxidant enzyme apricot contains, and MDA values, which are the lipid peroxidation products, are given below.*

	Result
SOD (Superoxide Dismutase)	0.060 U/mI
MDA (Malondialdehyde Acid)	1.579 mmol/I

4. Discussion

The active oxygen derivative has at least 4 different roles in the plant.

1. Active oxygen first causes hypersensitive cell death.
2. Active oxygen has a direct lethal effect against the disease factor.
3. It plays a role in lignification. It is important for strengthening the cell wall.
4. Active oxygen acts as a stimulant molecule in the plant [19].

Hydrogen peroxide formed in the plant cell after the infection of the cause of disease or other active oxygen species have the signal effect on the plant's endurance mechanism.

Antioxidant groups are divided into two groups as enzymatic and non-enzymatic. We can define the substances that can prevent or delay the oxidation of substances with oxidization potential such as lipid, protein, DNA and carbohydrate, which are contained in the living cell, as antioxidants. They are present in fewer amounts in the tissues compared to oxidizable substrates [20,21]. In this study carried out on apricot fruit, it was found that antioxidant enzyme SOD (Superoxide Dismutase) was 0.06 U/mI and MDA was 1.579 mmol/I. The systems that prevent the formation of ROS may be different. The antioxidants that capture and neutralize ROSs such as mitochondrial cytochrome oxidase, which reduces ROSs are the systems detoxifying radicals such as flavonoids, alpha tocopherol, ascorbic acid, methionine, uric acid, beta carotene, reduced glutathione, mucus [22]. In accordance with these explanations in this study, it is seen that the increase in the consumption of apricot fruit according to the values of SOD and the values of the lipid peroxidation product MDA will be beneficial (due to high antioxidant enzyme activities) with respect to decreasing oxidative stress and removing radicals from the body or reducing their harmful effects for human health.

In apricot fruit, it was determined that SOD (Superoxide Dismutase) was 0.06 U/ml and MDA (Malondialdehyde acid) was 1.579 mmol/I. These values mean that the antioxidant values of apricot fruit are quite high compared to many other plants and fruits. This also shows the richness of the fruit in terms of the antioxidant which is effective in the removal of

radical compounds resulting from metabolic activities in living creatures, and that it is also an important factor especially in reducing the risk of cancer. On the other hand, it is also known to be effective on the prevention of the formation of Alzheimer's disease, which has a significant effect on brain function [23]. In the literature studies carried out, it is seen that apricot fruit protects the body against high levels of oxidative stress when it is considered that the DPPH Radical removal activity of blueberry is 52.5% and its reducing power value that is an indicator of antioxidant activity is 0.170 [10]. Recently, the tendency to the use of plant-derived natural antioxidants has gained importance in the treatment of many diseases [24]. In another study, total antioxidant capacity in apricot juice was determined by using FRAP method and it was reported to have higher antioxidant properties than orange, peach and cherry. In the literature studies, in both plant and human studies, it was reported that superoxide dismutase (SOD) enzyme activity increased in some plants, however, it decreased in various diseases in people [25].

5. Conclusion

In conclusion, it is seen that the investigation of apricot samples in Turkey in terms of the antioxidant substances, they contain natural nutrition in terms of human health are important and will help in fighting against diseases and adding value to national economy.

References

[1] Tosun İ., Yüksel S., "Üzümsü meyvelerin antioksidan kapasitesi", Gıda, 28(3), (2003), 305-311

[2] Akkuş İ., "Serbest Radikaller ve Fizyopatolojik Etkileri", Mimoza Yayınları, Konya, 1995, 68

[3] Yılmaz İ., "Antioksidan içeren bazı gıdalar ve oksidatif stress", İnönü Üniversitesi Tıp Fakültesi Dergisi, 17(2), (2010), 143-153

[4] Derviş E., "Oral antioksidanlar. Dermatoz", 2(1), (2011), 263-267

[5] Güler E., Dedeakayoğulları H., Kılınç A., Yalçın A.S., "Oksidatif stresin belirlenmesinde yeni bir yaklaşım", 23.ulusal biyokimya kongresi, 2011

[6] Mavi A., "İnsan eritrosit ve lökositlerinden süperoksit dismutaz enzimininsaflaştırılması ve bazı ilaçların enzim üzerine etkilerinin incelenmesi", Ph.D. dissertation, Institute of Natural Sciences, Atatürk University, 2005.

[7] Becker A., "Controlling als Praxis: Eine structurationsTheoretische Perspektive auf Controlling", In E. Scherm & G. Pietsch (Hrsg.), Controlling: Theorien und Konzeptionen. 2004, pp. 753-777

[8] T.C Orman ve Su İşleri Bakanlığ Orman Genel Müdürlüğü Yayınları Maviyemiş Likapa Eylem Planı 2015-2019

[9] Uruk T., Kahraman S., "Yaban Mersini (Vaccinim myrtillus) Antioksidan aktivitesinin araştırılması", Iğdır.Üniversitesi Fen Bilimleri Enst.Der., 71(4), (2017), 77-83

[10] Mot C.A., Dumitrescu S.R., Sarbu C.,."Rapid and effective evaluation of the antioxidant capacity of propolis extracts using DPPH bleaching kinetic profiles, FT-IR and UV-VIS spectroscopic data", Journal of Food Composite and Analysis, 24, (2011), 516-522

[11] Hayyan M., Hashim M.A., Al Nashef I.M., "Superoxide Ion, Generation and Chemical Implications", Chem. Rev., 116 (5), (2016), 3029–3085.

[12] Brewer G.J., "Achromatic regions of tetrazolium stained starch gels: inherited electrophoretic variation", American Journal of Human Genetics., 19 (5), (Sep 1967), 674–80.

[13] Therond P., Bonnefont-Rousselot D., Davit-Spraul A., Conti M., Leqrand A., "Biomarkers of oxidative stress: an analytical approach", Curr Opin Clin Nutr Metab Care, 3, (2000), 373-84

[14] Sargowo, D., Ovianti, N., Susilowati, E., Ubaidillah, N., Nugraha, A. W., Proboretno, K. S., Failasufi M., Ramadhan F., Wulandari H., Waranugrah Y., Putri, D. H. "The role of polysaccharide peptide of Ganoderma lucidum as a potent antioxidant against atherosclerosis in high risk and stable angina patients", Indian heart journal, 70(5), (2018), 608-614

[15] Erçin U., Bilgihan A., Erkan A.F., Yücel, H.б "New Parameters of Coronary Artery Diseases: Oxidative Stress Markers", Journal of Turkish Clinical Biochemistry, 17(1), (2019), 48-55

[16] Sun. Y., Oberley LW., Li Y., "A simple method for clinical assay of superoxide dismutase", Clin Chem. Mar, 34(3), (1988), 497-500

[17] Gutteridge J.M., "Lipid peroxidation and antioxidants as biomarkers of tissue damage", Clin Chem. Dec;41(12 Pt 2), (1995), 1819-28.

[18] Bergmeyer J., Grabl M., "Methods of Enzymatic Analysis (Third Edition), Germany, 1983, 190-302

[19] Stadtman E.R., "Importance of individuality in oxidative stress and aging", FreeRadical Biology and Medicine, 33, (2002), 597-604

[20] Çaylak E, "Hayvan ve bitkilerde oksidatif stres ile antioksidanlar. Biyokimya", AD, Çankırı Karatekin

Üniversitesi 18200 Tıp Araştırmaları Dergisi, 9(1) , (2011), 73-83

[21] Gutteridge J.M.C.,"Lipid peroxidation and antioxidants as biomarkers of tissue damage", Clin. Chem., 41, (1995), 1819-1828

[22] Rice-Evans C., , Re R, Pellegrini N., Proteggente A., Pannala A., Yang M., "Antioxidant activity applying an improved ABTS radical cation decolorization assay", Free Radic. Biol. Med., 26, (1999), 1231-1237

[23] Skrovankova S., Sumezynki P., Mlcek J., Jurikova T., Sochor J., "Bioactive Compounds and Antioxidant Activity in Different Types of Berries", Int.J.Mol.Sci.16, (2015), 24673-24706

[24] Haznedaroğlu M.Z., Öztürk T. Konyalıoğlu S., "Salvia smyrnaea boiss. uçucu yağının antioksidan ve antimikrobiyal aktivitesi", Bitkisel İlaç Hammaddeleri Toplantısı, Bildiriler, 2002. Eskişehir.

[25] Tosun İ., Üstün Ş., "An investigation about antioxidant capacity of fruit nectars", Pakistan Journal of Nutrition, 2(3), (2003), 167-169

MANAS Journal of Engineering
ISSN 1694-7398 | e-ISSN 1694-7398

Volume 8 (Issue 1) (2020) Pages 22-27

Ferrocene as a leaving group; Unexpected rearrangement reactions for the synthesis of 2,3-diarylnapthoquinones

Nevroz Aslan Ertas[1,2] Arif Kivrak[1,*]

[1]Department of Chemistry, Faculty of Sciences, Van Yüzüncü Yil University, 65000, Van, Turkey, akivrak@yyu.edu.tr, ORCID: 0000-0003-4770-2686

[2]Department of Molecular Biology and Genetics, Faculty of Sciences, Van Yüzüncü Yil University, 65000, Van, Turkey

ABSTRACT

In general, Suzuki-Miyaura coupling reaction between aryl bromide and arylboronic acids form the new C-C bond in the presence of Pd-catalyst. In the present study, 2-bromo-3-ferrocenyl-1,4-naphthoquinone 2 intermediate is synthesized by starting from 2,3-dibromo-1,4-naphthoquinone via Suzuki-Miyaura Coupling reaction. Then, it is investigated that the reaction between 2 and arylboronic acids give a new rearrangement reaction involving free radicals. Ferrocene structure displays critical roles for the formation of 2,3-diaryl-1,4-naphthoquinones. This reaction could be first example for the radical C-C bond cleavage reactions including ferrocene.

ARTICLE INFO

Research article

Received: 29.05.2020
Accepted: 19.06.2020

Keywords:
Ferrocene,
naphthoquinone,
rearrangement reactions,
mechanism,
substitution reactions

*Corresponding author

1. Introduction

Design and synthesis of new biologically important organic compounds have been gained crucial importance over the last decades. In fact, 1,4-naphthaquinone and their derivatives have been well known organic structures in medicinal and material chemistry.[1] They have two carbonyl groups increasing the activities of naphthaquinones.[2] Moreover, naphthoquinone based structures show different kinds of biological properties. They have been used as antiviral,[3] cardiovascular,[4] antibacterial,[5] antiparasitic,[6] anticancer,[6] and radical scavenging[7] agents. Some of napthaquinones have critical roles for the treatments of some diseases like anticancer[4]. For example, Daunorubicin,[8] Doxorubicin,[9] Mitomycin[10], and Mitoxantron[11] are commercially available naphthaquinone based drugs in the markets. Many naphthaquinone derivatives are isolated from nature.[12] Napthaquinones have been also used as oxidizing agents in organic reactions for the formation of more complex structures.[13]

Ferrocene structure, consisting of two cyclopentadien and an iron, has been used for the preparation of novel organic compounds since 1951.[14] Ferrocene have many vital properties in organic reactions such as; neutral, highly stable and non-toxic compound. Therefore, not only biologically active ferrocene based organic molecules[15] but also high conductive ferrocene based organic materials[16] have been designed and synthesized in last decades. It was reported that ferrocene moities increases biological activities[17] or creates different biological properties. Ferrocenyl aspirin, ferroquine, and ferrocifen are commercial drugs consisting of ferrocene on the structures (Scheme 1).[18]

There are different kinds of ferrocene based organic molecules in literature. If organic molecules are modified with ferrocene moieties, they can be change properties and create new activities [14, 19, 20]. Ferrocene have higher redox properties, with lower oxidation potential, so it may be oxidized easily to form the Fe (+3) isomers. Recently, we synthesized new ferrocene based molecules for optoelectronic and sensor applications (Figure 1).[16, 21] Structure **1** may be new generation small organic structures for organic solar cells, and compound 2 displayed higher sensor activities for the detection of peroxides (Fig. 1).[16] Moreover, Compound 2 has high stability and reproducibility than Pd-based electrochemical sensors.[22]

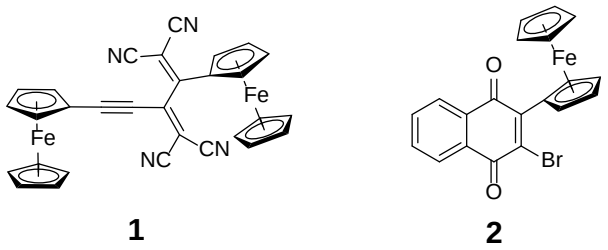

Figure 1. *Previously synthesized ferrocene based molecules.*

In the lights of previous studies, we thought that new ferrocenyl naphthoquinones may be synthesized by using Pd-catalyzed cross coupling reactions. Hence, Pd-catalyst cross coupling reaction was applied for elaboration reactions. Suzuki-Miyaura reactions are most known coupling reactions to form the new carbon-carbon bond between aryl/alkylboronic acids and halogenated aromatics. Suzuki-Miyaura coupling reactions need to aryl halide, aryl/alkyl boronic acids, weak bases and Pd-catalyst. On the other hand, there are a variety of modified reaction procedure in literature. Generally, carbon-carbon bonds between ferrocene moieties and aromatic compounds are very strong, so it is not possible to broken these carbon-carbon bonds. Moreover, there is not any study about ferrocene which was used as a leaving group in literature. In the present study, we investigated a new rearrangement reaction involving free radicals between 2-bromo-3-ferrocene-1,4-naphthoquinone 2 and arylboronic acids. Ferrocene structures played very unique roles for the formation of 2,3-diaryl-1,4-napthquinones (Fig. 2).

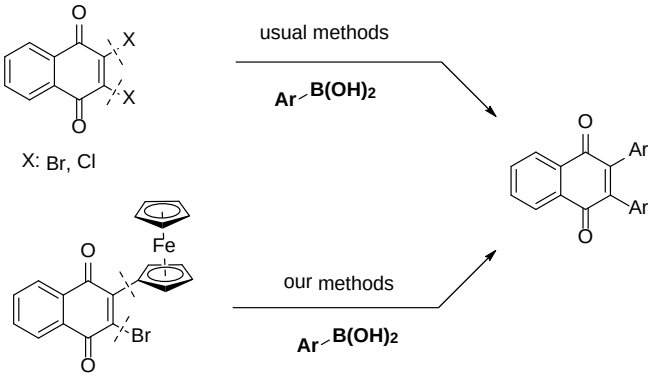

Figure 2. *Synthesis of 2,3-diaryl-1,4-naphthoquinone.*

2. Results and discussion

Naphthoquinone derivatives have been well known organic structures for a variety of applications. They have critical roles not only biological applications, but also material sciences. Recently, we synthesized novel ferrocene based naphthoquinone derivatives, and found its electrochemical properties, there are a few studies about the synthesis of ferrocene based naphthoquinones.[20] In the present study, ferrocenyl-naphthoquinone was prepared by using Suzuki-Miyaura cross-coupling reaction [24] under the mild reaction conditions. There are different kinds of modified Suzuki-Miyaura coupling procedure between boronic acids and halo-substituted aromatics in literature.[25] Our previous study, 2,3-dibromo-1,4-naphthoquinone was reacted with ferroceneboronic acid, under reflux for overnights to gave the 2-bromo-3-ferrocenyl-1,4-naphthoquinone 2 (38% yield) and 2,3-diferrocenyl-1,4-naphthoquinone 5 (17% yield) [16] (Fig. 3**)**.

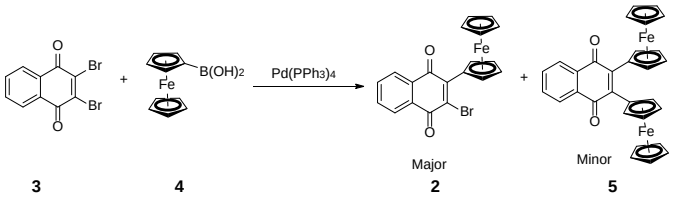

Figure 3. *Synthesis of 2-bromo-3-ferrocenyl-1,4-naphthoquinone **2**.*

After isolation of structure 2, we tried to synthesized 2-aryl-3-ferrocenyl- naphthoquinone (7 and 10) derivatives via Suzuki-Miyaura reactions. When 2-bromo-3-ferrocene-1,4-naphthoquinone 2 was underwent to react with phenylboronic acid 6 with Pd-catalyst under reflux for 24 hours, desired compound 7 was not formed. Unexpectedly, we isolated only 2,3-diphenyl-1,4-naphthoquinone 8 in 49% yield (Fig. 4). The same reaction condition was repeated for the synthesis of compound 10 by the reaction between 2-bromo-3-ferrocene-1,4-naphthoquinone 2 and p-tolylboronic acid 9, 80% yields of compound 11 was isolated after purification (Fig. 4). Unexpectedly, we did not obtain our desired products (7 and 10).

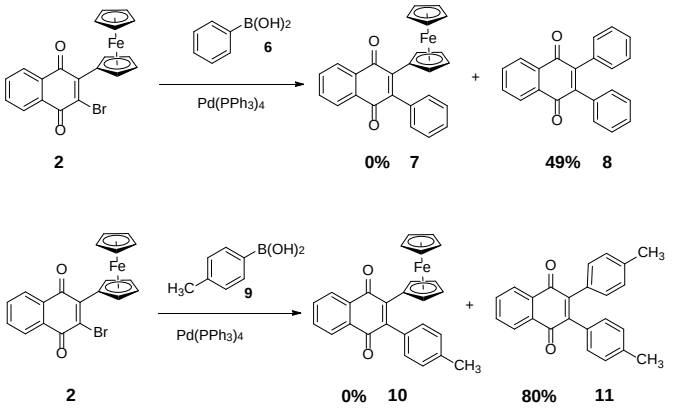

Figure 4. *The reaction between compound **2** and arylboronic acids.*

There are different reaction methodologies for the formation of 2,3-diaryl-1,4-naphthoquinone derivatives in literature. In general, 2,3-diaryl-1,4-naphthoquinones are obtained via Suzuki-Miyaura or Stille cross coupling reactions between 2,3-dibromo/chloro-1,4-naphthoquinones and $ArB(OH)_3$/$ArSnBu_3$. [26] [27] [23] They are also prepared

from the Fischer carbene complex with alkynes.[28] [29] Moreover, Patil et *al*. was reported that oxidative arylation of naphthoquinones using *o*-iodoxybenzoic acid and phenylhydrazines formed the 2,3-diaryl-1,4-naphthoquinones.[30] A new method for the direct arylation of quinones was demonstrated by Baran et *al*. by using arylation agents as $AgNO_3/K_2S_2O_8$ and arylboronic acids for the preparation of arylated quinones.[31] Then, it was found that $FeS/K_2S_2O_8$ catalyst was to be formed the mono-susbtituted quinones under mild reaction conditions.[32] Different kind of boronic acids were undergone to coupling reactions with 1,4-benzoquinone. In 2013, Komeyama et *al.* investigated the direct arylation reactions of benzoquinones with arylboronic acids in the presence of $FeSO_4/ K_2S_2O_8$ catalyst system.[33] Related with these studies, $Fe(acac)_2$, $Fe(NO_3)_3$ and $Mn(OAc)_3$ were also used as a catalyst for the preparation of 2-aryl-1,4-naphthoquinone by the reaction between 1,4-naphthoquinone and arylboronic acids.[34] The direct arylation of quinones with arylboronic acids without any metal catalyst was tested in the presence of $K_2S_2O_8$ by Ilangovan et *al*.[35] They improved that arylboronic acids turned to corresponding aryl radicals before addition of quinones. Therefore, this formation could be important for the proposing reaction mechanism for the formation of 2,3-diaryl-1,4-naphthoquinone derivatives.

The possible reaction mechanism was proposed for the formation of 2,3-diaryl-1,4-naphthoquinones (Fig. 5). Firstly, Suzuki-Miyaura cross coupling reaction between compound 2 and arylboronic acids in the presence of Pd-catalyst was carried out. Oxidative addition, transmetallation and reductive elimination reactions gave the coupled intermediate 15. After formation of intermediate 15, ferrocene moieties may be activated radical reactions, because it was improved that Fe-catalyst help to generation of radical intermediates for the direct arylation of naphthaquinones. As shown in Figure 5, ferrocene may be oxidized to +3, this electron combine with arylboronic acids to form hypothetical intermediates 17. Then, cleavage of the aryl-boron bond produces the nucleophilic aryl radical 18. Subsequent, this radical attack to intermediate 16 for the formation of intermediate 19. Then the final product 20 was obtained by the rearrangement reaction and cleavage C-C bonds between ferrocene and naphthaquinone (Fig. 5).

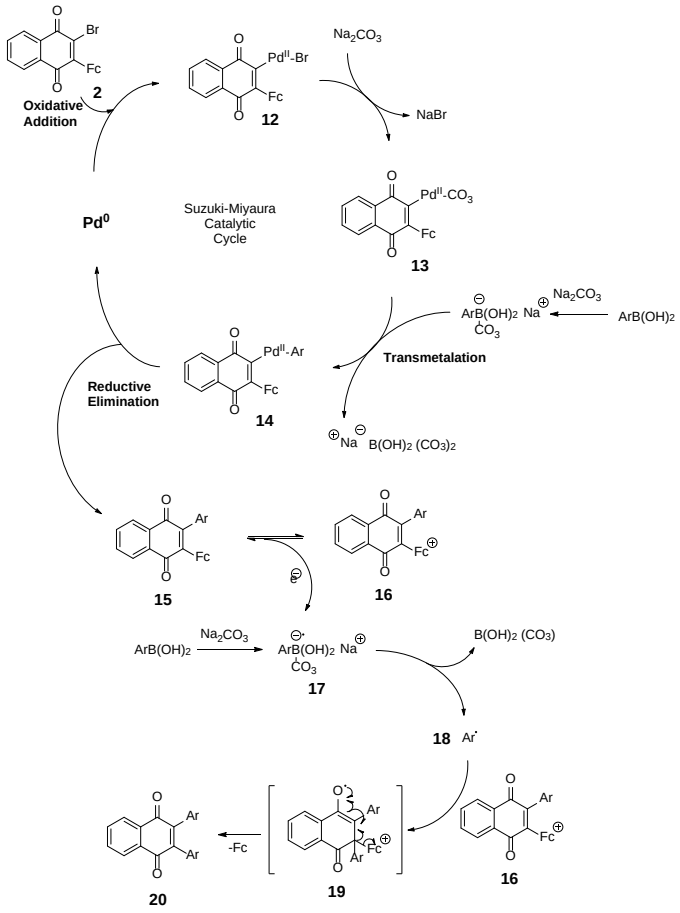

Figure 5. *The plausible reaction mechanism.*

The effects of two ferrocene moieties was also tested for the formation 2,3-diaryl-1,4-naphthaquinones. When diferrocenyl-1,4-naphthaquinone was allowed to react with arylboronic acids by using same reaction conditions (Fig. 6), only starting compound was recovered.

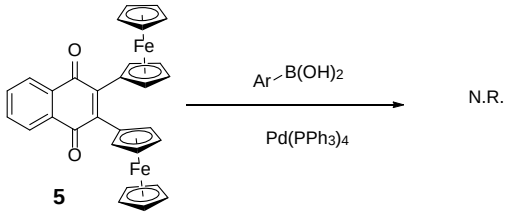

Figure 6. The reaction between 2,3-diferrocenyl-1,4-naphhaquinones.

3. Conclusions

Herein, new rearrangement reactions between 2-bromo-3-ferrocenyl-1,4-naphthoquinone 2 and arylboronic acids was investigated. In the first part, we prepared 2-bromo-3-ferrocenyl-1,4-naphthoquinone 2 by using Suzuki-Miyaura coupling reactions between 2,3-dibromo-1,4-naphthoquinone

and ferrocene boronic acid. Then, new rearrangement reactions involving radical intermediates for the formation of 2,3-diaryl-1,4,-naphthaquinone derivatives was investigated. It could be first example for the C-C bond cleavage of ferrocene structure and naphthoquinones in literature. According to proposed mechanism, ferrocene played very unique roles for the formation of arylation of napthaquinones as a leaving group. As a result, this study could also be useful for the design of novel rearrangement reactions for future chemical synthesis applications.

4. Experimental

2. 1. Synthesis of 2-bromo-3-ferrocenyl-1,4-naphthoquinone

2,3-Dibromo-1,4-naphthoquinone (200 mg, 0.63 mmol) and ferroceneboronic acid (303.4 mg, 1.32 mmol) were stirred in dioxane at room temperature. Then, $Pd(PPh_3)_4$ (34.6 mg, 0.03 mmole), potassium carbonate (552 mg, 3.98 mmole) and water (2 mL) were added under argon atmospheres. The mixture was stirred under reflux at 90 ^oC for 24 hours. The reaction mixture extracted with EtOAc (3x25 mL). The combined organic layers were dried over anhyd. $MgSO_4$ and organic solvent was removed under reduced pressure. Compounds was purified by flash chromatography on silica gel using EtOAc/Hexane (1:19) as the eluent to afford 2,3-diferrocenyl-1,4-naphthoquinone (17%) and 2-bromo-3-ferrocenyl-1,4-naphthoquinone (38%). The spectral data were in agreement with those reported previously for this compound. [16]

2.2. The reaction between 2-bromo-3-ferrocenyl-1,4-naphthoquinone 2 and boronic acids

2.2.1. Synthesis of 2,3-diphenylnaphthalene-1,4-dione 8

2-Bromo-3-ferrocenyl-1,4-naphthoquinone (52 mg, 0.12 mmol), phenylboronic acid (32 mg, 0,25 mmol), $Pd(PPh_3)_4$ (7 mg, 5%) and potassium carbonate (105 mg, 0,75 mmol) were stirred in dioxane/water (16/2 mL) under argon atmospheres. The resulting mixture was undergone to MW irradation at 120 ^oC for 45 minutes. After reaction was over, reaction mixture extracted with EtOAc (3x25 mL). The combined organic layers were dried over anhyd. $MgSO_4$ and organic solvent was removed under reduced pressure. Product was purified by flash chromatography on silica gel using EtOAc/Hexane (1:19) as the eluent to afford 2,3-diphenylnaphthalene-1,4-dione **8** (49% yield). 1H NMR (400 MHz, $CDCl_3$) δ 8.2 (m, 2H), 7.79 (m, 2H), 7.23 (m, 6H), 7.07 (m. 4H); 13C NMR (100 MHz, $CDCl_3$) δ 184.8, 145.8, 133.8, 133.2, 132.1, 130.5, 128.2, 127.6, 126.6. The spectral data were in agreement with those reported previously for this compound.[23]

2.2.2. Synthesis of 2,3-di-p-tolylnaphthalene-1,4-dione 11.

2-Bromo-3-ferrocenyl-1,4-naphthoquinone (52 mg, 0.12 mmol) and p-tolylboronic acid (34 mg, 0,25 mmol) $Pd(PPh_3)_4$ (7 mg, 5%) and potassium carbonate (105 mg, 0,75 mmol) were stirred in dioxane/water (16/2 mL) under argon atmospheres. The resulting mixture was undergone to MW irradation at 120 ^oC for 45 minutes. After reaction was over, reaction mixture extracted with EtOAc (3x25 mL). The combined organic layers were dried over anhyd. $MgSO_4$ and organic solvent was removed under reduced pressure. Product was purified by flash chromatography on silica gel using EtOAc/Hexane (1:19) as the eluent to afford 2,3-di-p-tolylnaphthalene-1,4-dione **11** (80% yield). ^1H NMR (400 MHz, $CDCl_3$) δ 8.2 (m, 2H), 7.77 (m, 2H), 7.05 (d, J = 8 Hz, 4H), 6.99 (d, J = 8.1 Hz, 4H); ^{13}C NMR (100 MHz, $CDCl_3$) δ 184.9, 145.4, 138.0, 133.7, 132.2, 130.5, 130.4, 128.4, 126.5, 21.3. The spectral data were in agreement with those reported previously for this compound.[23]

Acknowledgment

We want to express our thanks to the Scientific and Technical Research Council of Turkey (TUBİTAK-114Z042) for financial supports of Microwave Reactor and Van Yüzüncü Yil University (FBA-2019-7910) for financial supports of chemicals. N. A. also thanks to YÖK 100/2000 for scholarships.

References

[1] Semwal R.B., Semwal D.K., Combrinck S., Cartwright-Jones C., Viljoen A., “Lawsonia inermis L. (henna): Ethnobotanical, phytochemical and pharmacological aspects”, Journal of Ethnopharmacology, 155, (2014), 80-103

[2] Carbas B.B., Kivrak A., Zora M., Onal A.M., “Synthesis of a novel fluorescent and ion sensitive monomer bearing quinoxaline moieties and its electropolymerization”, Reactive & Functional Polymers, 71, (2011), 579-587

[3] Devaux C.A., Rolain J-M., Colson P., Raoult D., “New insights on the antiviral effects of chloroquine against coronavirus: what to expect for COVID-19?”, International Journal of Antimicrobial Agents, 55(5), (2020),105938

[4] Abbas G., Hassan Z., Al-Harrasi A., Khan A., Al-Adawi A., Ali M., “Synthesis, biological evaluation, molecular docking and structure-activity relationship studies of halogenated quinone and naphthoquinone derivatives”, Journal of Molecular Structure, 1195, (2019), 462-469

[5] Amani A M., “Synthesis, Characterization and Antibacterial and Antifungal Evaluation of Some Para-Quinone Derivatives”, Drug Research, 64(8), (2014), 420-423.

[6] Jardim G.A.M., da Cruz E.H.G., Valenca W.O., Lima D.J.B., Cavalcanti B.C., Pessoa C., Rafique J., Braga A.L., Jacob C., da Silva E.N., "Synthesis of Selenium-Quinone Hybrid Compounds with Potential Antitumor Activity via Rh-Catalyzed C-H Bond Activation and Click Reactions", Molecules, 2018, 23.

[7] Michalik M., Poliak P., Lukes V., Klein E., "From phenols to quinones: Thermodynamics of radical scavenging activity of para-substituted phenols", Phytochemistry, 166, (2019), 112077.

[8] Zangeneh M.M., Zangeneh A., Pirabbasi E., Moradi R., Almasi M., "Falcaria vulgaris leaf aqueous extract mediated synthesis of iron nanoparticles and their therapeutic potentials under in vitro and in vivo condition", Applied Organometallic Chemistry, 33(12), (2019), e5246

[9] Yu N., Li X., Wen M., Geng P., Ren X.L., Wang Z.J., Chen Z.G., "Doxorubicin-Loaded Bi-PEG Nanoparticles as Novel Chemo-Photothermal Nanoagents for Efficiently Killing Cancer Cells", Journal of Nanoscience and Nanotechnology, 20, (2020), 2032-2039

[10] Moaven O., Votanopoulos K.I., Shen P., Mansfield P., Bartlett D.L., Russell G., McQuellon R., Stewart J.H., Levine E.A., "Health-Related Quality of Life After Cytoreductive Surgery/HIPEC for Mucinous Appendiceal Cancer: Results of a Multicenter Randomized Trial Comparing Oxaliplatin and Mitomycin", Annals of Surgical Oncology, 27, (2020), 772–780

[11] Ishikawa T., "Recent advances in pharmacogenomics of ABC transporters involved in breast cancer therapy", Pharmacogenomics, 13, (2012), 633-636

[12] Tietze L.F., Bell H.P., Chandrasekhar S., "Natural product hybrids as new leads for drug discovery", Angewandte Chemie-International Edition, 42, (2003), 3996-4028

[13] Fang G.D., Gao J., D. Dionysiou D., Liu C., Zhou D.M., "Activation of persulfate by quinones: free radical reactions and implication for the degradation of PCBs", Environmental Science & Technology, 47, (2013), 4605-4611

[14] Zora M., Kivrak A., Kelgokmen Y., "A novel one-pot synthesis of ferrocenyl-substituted 1, 2, 4-oxadiazoles", Journal of Organometallic Chemistry, 759, (2014), 67-73.

[15] Santos M., Bastos P., Catela I., Zalewska K., Branco L.C., "Recent Advances of Metallocenes for Medicinal Chemistry", Mini-Reviews in Medicinal Chemistry, 17, (2017), 771-784

[16] Aslan-Ertas N., Kavak E., Salma F., Celik-Kazici H., Kivrak H., Kivrak A., "Synthesis of Ferrocene Based Naphthoquinones and its Application as Novel Non-enzymatic Hydrogen Peroxide", Electroanalysis, 32 (6), (2020), 1178-1185

[17] Wang X.Y., Li Q., Xu J.J., Wu S., Xiao T.F., Hao J., Yu P., Mao L.Q., "Rational Design of Bioelectrochemically Multifunctional Film with Oxidase, Ferrocene, and Graphene Oxide for Development of in Vivo Electrochemical Biosensors", Analytical Chemistry, 88, (2016), 5885-5891.

[18] Guyon L., Lepeltier E., Gimel J.C., Calvignac B., Franconi F., Lautram N., Dupont A., Bourgaux C., Pigeon P., Saulnier P., Jaouen G., Passirani C., "Importance of Combining Advanced Particle Size Analysis Techniques To Characterize Cell-Penetrating Peptide–Ferrocifen Self-Assemblies", Journal of Physical Chemistry Letters, 10, (2019), 6613-6620

[19] Kivrak A., Zora M., "Efficient one-pot synthesis of cyanoferrocene from ferrocenecarboxaldehyde using NH2OH· HCl/KI/ZnO/CH3CN system", Journal of Organometallic Chemistry, 692, (2007), 2346-2349

[20] Yucel B., Sanli B., Soylemez H., Yilmaz I., "Synthesis and electro-spectroelectrochemistry of ferrocenyl naphthaquinones", Tetrahedron, 67, (2011), 1406-1421

[21] Carbas B.B., Kivrak A., Kavak E., "Electrosynthesis of a new indole based donor-acceptor-donor type polymer and investigation of its electrochromic properties", Materials Chemistry and Physics, 188, (2017), 68-74

[22] Sahin O., Kivrak H., Kivrak A., Kazici H.C., Alal O., Atbas D., "Facile and Rapid Synthesis of Microwave Assisted Pd Nanoparticles as Non-Enzymatic Hydrogen Peroxide Sensor", International Journal of Electrochemical Science, 12, (2017), 762-769

[23] Hassan Z., Ullah I., Ali I., Khera R.A., Knepper I., Ali A., Patonay T., Villinger A., Langer P., "Synthesis of tetraaryl-p-benzoquinones and 2,3-diaryl-1,4-naphthoquinones via Suzuki-Miyaura cross-coupling reactions", Tetrahedron, 69, (2013), 460-469

[24] Cho C.H., Jung D.I., Neuenswander B., Larock R.C., "Parallel Synthesis of a Desketoraloxifene Analogue Library via Iodocyclization/Palladium-Catalyzed Coupling", Acs Combinatorial Science, 13, (2011), 501-510

[25] Algso M.A.S., Kivrak A., "New strategy for the synthesis of 3-ethynyl-2-(thiophen-2-yl) benzo [b] thiophene derivatives", Chemical Papers, 73, (2019), 977-985

[26] Yoshida S., Kubo H., Saika T., Katsumura S., "Synthesis of 2,3-Diarylquinone by Palladium Catalyzed Cross-Coupling of Dibromoquinones with

Heteroarylstannanes", Chemistry Letters, (1996), 139-140.

[27] Best W.M., Sims C.G., Winslade M., "Palladium-Catalysed Cross Coupling of Arylboronic Acids with 2-Chloro-1,4-naphthoquinones: The Synthesis of 2-Aryl- and 2,3-Bisaryl-1,4-naphthoquinones", Australian Journal of Chemistry, 54, (2001), 401-404

[28] Davies M.W., Johnson C.N., Harrity J.P.A., "Synthesis of Novel Quinone Boronic Ester Derivatives via a Highly Regioselective Cr-Mediated Benzannulation Reaction and Their Application in Pd-Catalyzed Coupling Processes", Journal of Organic Chemistry, 66, (2001), 3525-3532

[29] Hsung R.P., Xu Y.C., Wulff W.D., "The Effects of Phosphine Ligands on the Benzannulation Reaction of Molybdenum Carbene Complexes with Alkynes", Tetrahedron Letters, 36, (1995), 8159-8162

[30] Patil P., Nimonkar A., Akamanchi K.G., "Aryl-Free Radical-Mediated Oxidative Arylation of Naphthoquinones Using o-Iodoxybenzoic Acid and Phenylhydrazines and Its Application toward the Synthesis of Benzocarbazoledione", Journal of Organic Chemistry, 79, (2014), 2331-2336

[31] Fujiwara Y., Domingo V., Seiple I.B., Gianatassio R., Del Bel M., Baran P.S., "Practical C−H Functionalization of Quinones with Boronic Acids", Journal of the American Chemical Society, 133, (2011), 3292-3295

[32] Wang J., Wang S., Wang G., Zhang J., Yu X.Q., "Iron-mediated direct arylation with arylboronic acids through an aryl radical transfer pathway", Chemical Communications, 48, (2012), 11769-11771

[33] Komeyama K., Kashihara T., Takaki K., "FeSO4-promoted direct arylation of benzoquinones with ArB(OH)2 or ArBF3K", Tetrahedron Letters, 54, (2013), 1084-1086

[34] Wang Y.J., Zhu S., Zou L.H., "Recent Advances in Direct Functionalization of Quinones", European Journal of Organic Chemistry, (2019), 2179-2201

[35] Ilangovan A., Polu A., Satish G., "$K_2S_2O_8$-mediated metal-free direct C–H functionalization of quinones using arylboronic acids", Organic Chemistry Frontiers, 2, (2015), 1616-1620

MANAS Journal of Engineering
ISSN 1694-7398 | e-ISSN 1694-7398

Volume 8 (Issue 1) (2020) Pages 28-36

Modelling occupational health and safety risks among unskilled workers in construction industry

Hezekiah Oluwole Adeyemı[1,*], Olatilewa Rapheal Abolade[2], Ajibola Oluwafemi Oyedejı[2], Olanrewaju Bilikis Olatunde[1]

[1]Department of Mechanical Engineering, Olabisi Onabanjo University, Ago-Iwoye, Nigeria,
deyemi.hezekiah@oouagoiwoye.edu.ng, olatunde.bilikis@oouagoiwoye.edu.ng, ORCID: 0000-0002-5815-7321

[2]Department of Computer Engineering, Olabisi Onabanjo University, Ago-Iwoye, Nigeria,
abolade.raphael@oouagoiwoye.edu.ng, oyedeji.ajibola@oouagoiwoye.edu.ng

ABSTRACT

To enhance workers' protection in construction tasks, Occupational Health and Safety Risks (OHSR) needs to be properly recognized, assessed and controlled. This study modelled Health and Safety Risk (HSR) among unskilled workers in construction works. Data were collected from 150 subjects in 12 construction sites located in Southwest Nigeria. Variables considered to play key roles in HSR causation were measured with the questionnaire. All variables that correlated significantly ($p \leq 0.05$) to HSR on the tasks were noted by Spearman's rho correlation (Src) using SPSS software. The model prediction was adjusted by R2 and was validated by comparison with Human Professionals' Predictions (HPP). Model Cook's distance and its closeness to being normally distributed were evaluated. 37 attributes variables were initially collated with 13 predictor variables remained in the optimum model. Wrong work-methods, lack of work-control and harsh outdoor environment ranked among the strongest positive β coefficients (0.217, 0.127 and 0.126 respectively). The maximum coefficient of the adjusted R2 determination was 0.708. The histogram of the residuals suggested closeness to being normally distributed and 0.930 as the maximum Cook's distance. Comparison between the OHSR model and the HPP had strong Src strength. The OHSR showed a statistically significantly higher level of hazards' rating compared to HPP. OHSR model was developed and the performance was rated good, satisfied the study's objectives. The author recommended the development of measures at reducing β coefficients of all the predictor variables to minimize workplaces OHSR.

ARTICLE INFO

Research article

Received: 19.07.2019
Accepted: 27.05.2020

Keywords:
Unskilled, safety, model, predictor, variables, occupation

**Corresponding author*

1. Introduction

Unskilled workers can also be referred to as labourers, low-skill workers, semi-skilled workers, low-qualified workers or menial workers [1]. Labourers fall among the group of workers that require no special training or experience for performing some works adequately. This group of workers perform physically demanding labour and assist skilled workers at construction, maintenance, and repair project sites [2]. Studies have shown that the unskilled workers are much more exposed to all categories of challenging physical activities than other sets of workers [3, 4, 5, 6]. Labourers have less autonomy, assigned less responsibility, and as a result, can be subject to lower job satisfaction [5]. According to the Bureau of Labour Statistics [7], labourers can be found on almost all construction sites, performing a wide range of tasks from the very easy to the hazardous. They can be found at building, highway, and heavy construction sites, residential and commercial sites, tunnel and shaft excavations, and demolition sites.

In construction works, the duties of labourers are to prepare worksites, digging and backfilling trenches and tunnel and shaft excavations, dismantle concrete and masonry retaining and bearing walls, use hand tools (e.g., shovels, picks, sledgehammers), mix and pour concrete, load and unload materials and equipment from trucks, help lift and place materials, assist skilled trades workers by readying and supplying needed tools, equipment, and materials [8]. Physical abilities common with the unskilled labourers include ability to lift heavy loads, walk and stand for extended periods of time, quickly bend, stretch, twist, or reach out with one's body, arms, and/or legs, move one's hands and arms to grasp or manipulate objects, access difficult to enter spaces (e.g. trenches, tunnels, cramped quarters), operate applicable hand tools, power tools, and equipment.

2. Literature review

There have been several studies conducted in the construction industry with a focus on the technique of enhancing workers' safety. Fabián and Gloria [9] presented the safety trends through an exploratory study which covered the year 1930 to 2016 and reported on the need for further possible efforts at zeroing down hazards in the industry. Peter et al. [10] identified factors such as management commitment, workers' involvement and strict enforcement of safety regulation as a way forward to enhancing safety in the industry. Omobolanle and Johnsmall [11] suggested the need for specific, strictly monitored and legislation to promote an occupational health and safety culture that would provide continuous health and safety performance improvement on projects. Chunlin et al. [12] detailed the need for allocation of sufficient personal protective equipment among workers and more effort from the relevant authorities at organizing unannounced site visits more frequently to improve the safety performance. Amick et al. [13] described the need to encourage occupational injury reporting and reduce risks through training and hazard identification and control strategies.

The association between some contributory factors and accidents among different groups of workers in construction sites, as highlighted by Yahya et al. [14], are grouped under; individual characteristics (e.g. age and experience, drug abuse), site condition (e.g. hazardous operation, weather, equipment, welfare service), workgroup (e.g. teamwork), supervision (e.g. safety engagement, effective enforcement), project management (e.g. safety leadership and communication). These factors create stress and anxiety and have negative consequences on workers' health and lifestyle [5], making them vulnerable to injuries and illnesses related to outdoor weather conditions, loud noise, fumes or dust, oily or wet environment, hazardous conditions (e.g., construction sites, heavy machinery) to mention few. Many who work as labourers for even a short period may suffer from permanent work injuries such as hearing loss, back injuries, eye injury, head injury, missing fingernails and skin scars [15]. These are usually caused as a result of their inexperience and lack of health and safety training [16]. Most of the tools used by labourers in construction works are often very heavy and there is little mechanical help for lifting and carrying, most especially, on small construction and renovation sites. Long hours of work are typical and these hours increase fatigue and stress, both of which contribute to traumatic injuries and musculoskeletal injuries [17]. Low-qualified workers have low-paid jobs and non-standard forms of contractual agreements, meaning that they often suffer from job insecurity.

Occupational Safety and Health [18], mentioned that the responsibility for promoting occupational health among workers rests with the management. The managements are to conduct assessments on all activities that may be hazardous to health, take appropriate measures to eliminate hazards or reduce risks, implement effective protective measures and provide information, training and supervision to safeguard the health of employees. The employees on their part should also comply with work regulations and instructions and carefully read and understand relevant information, carefully and properly use any material, tool, device and Personal Protective Equipment (PPE) provided and avoid taken harmful substances e.g. alcohol, cigarette.

Workplace hazards' prevention begins with having a clear understanding of those factors that play key roles in their causation and then formulate and implement an effective measure, on occupational health management, to reduce and control the hazards [18, 19]. In line with this view, this study attempted to model Occupational Health and Safety Risks (OHSR) among the unskilled workers.
The objectives were to identify the major factors that contribute to safety risk on the job, develop and validate a linear regression equation (model) capable of forecasting the safety level among the group of workers.

3. Materials and methods

3.1. Study Area and Subjects

The primary data for this study was collected among the low-qualified workers popularly refered to as labourers while performing some physical tasks among which are; cleaning building sites, unloading and loading equipment and supplies from trucks, building or dismantling scaffolding, mixing, pouring and spreading materials(concrete), helping tradespersons (such as bricklayers, cement finishers), installing utility piping, placing concrete, performing selective demolition, performing excavation work among others. Fifteen (15) construction sites located in Abeokuta and Lagos, the Southwest states of Nigeria were used for the study. Abeokuta is the largest city and capital of Ogun State in southwest Nigeria. It is situated 64 miles north of Lagos by railway or 81 miles by water. Lagos State is located on the southwestern part of Nigeria [20].

3.2. Data Collection Procedures

A mixed-methods research which involved qualitative and quantitative approaches was used in this study. The method helped to uncover the relationships between the measured variables through quantitative research with the use of questionnaire. The meanings among the participants were conveyed through a qualitative research approach. The questionnaire was designed to determine the more important variables that contribute to the focal problem, OHSR among the unskilled labourers. Respondents were requested to provide information related to their opinions on each of the identified attributes capable of influencing OHSR. The 150 subjects, involved in the study, were asked to rate the extent to which each of the variables can contribute to OHSR on a five scale point (1 represented 'not important contributor' and

5 represent 'very important contributor'). The semi-structured interview was conducted and interpreted, by personnel trained, in English, Pidgin and Yoruba languages as applicable to each subject. Each of the interview sessions lasting about 45minutes on average were taped and later transcribed. Before the interview commenced, all potential volunteers agreed, and consents were taken in oral and/or written form after they were informed that their participation in the study was voluntary. The purpose of the study and the confidentiality of the information provided were emphasized.

3.3. Development of Occupation Health and Safety Risk Model

This correlation design study proposed a multiple linear regression model to predict safety risk. Among all the primary variables collated, the predictor variables were identified after filtered out those variables that did not correlate significantly ($p \leq 0.05$) to the level of OHSR reported by the workers using Spearman's correlation analysis. The details of the subjects' responses were input into Statistical Package for the Social Sciences (SPSS) software [21] and an iterative process was performed. The prediction of the model was done by the adjusted R^2. The optimum model was selected through accepted regression modelling practices which included; maximizing the adjusted R^2, minimizing model variances, and inclusion of only variables that have been proven to be statistically significant through F-test ($p \leq 0.0001$) procedures.

3.4. Model Estimation and Diagnostics

The safety risk level was measured on Likert type 5-point scale from 1 to 5, where 1 = very low, 2 = low risk, 3=medium risk, 4= high risk, and 5= very high risk [22]. The other variables were measured on a 5-point scale of 1 to 5, where 1 = not important contributor and 5 = very important contributor. The calculation of the predicted safety risk level (Y) for any case was written as:

$$Y = a + b_1X_1 + b_2X_2 + b_3X_3 + \ldots + b_xX_x$$

Where Y = the predicted level of OHSR, a= intercept, b_1 to b_x = the predictor variables of the optimum model, X = the value of the coefficient of the variables.

The histogram of the residuals which suggests closeness to being normally distributed was conducted. Cook's distance value was also computed to find out the maximum value. According to Field [23], a good model should have its Cook's distance less than 1.0 value.

3.5. Model Validation

To test the quality of the model, the responses, of 15 randomly selected subjects, to predictor variables (in the optimum model) were used to compute the outcome, OHSR level using the model generated linear regression equation. The calculated ratings for each subject were given linguistic interpretations using a 5 point scale describing OHSR likelihood occurrences (1=Not likely, 2= Low, 3= Mild, 4= High, 5= Extremely high). These values and their linguistic interpretations were compared, for correlation strength, with the average ratings and the interpretations (to the same test data) suggested by two human ergonomics professionals drawn from academics environment using the same 5 points scale. Spearman's rho was used for significance tests of correlation coefficients at a *p*-value of 0.01. The independent sample t-test was also used to analyse the means of the unrelated groups (the model, and the human professional, mean values) at $p < 0.05$.

4. Results and discussion

4.1. Identified Attributes that Play Key Roles in OHSR Causation.

Table 1 shows the attributes identified as having tendencies of contributing to OHSR. These attributes were subdivided into health, environment, motivation, personal, work practices, equipment related and others. The highest rating (mean value of workers' reported safety risk level) (4.8) for each of the category of the attributes was found in the environment and the work practice related groups of attributes.

Table 1. *Mean ratings of identified attributes capable of influencing occupational health and safety risk among labourers*

RANK	REF.	ATTRIBUTES	MEAN SCORE
	A	**HEALTH-RELATED**	
1	VA-1	Poor use or lack of PPE	3.2
2	VA-2	Poor safety program	3.5
3	VA-3	Poor medical consideration	3.0
4	VA-4	Lack of health and training program	4.5
5	VA-5	Poor access to safety promotional program	4.2
6	VA-6	Poor access to safety information	4.5
	B.	**ENVIRONMENT RELATED**	
7	VB-1	Harsh outdoor environment	4.8
8	VB-2	Exposure to hazards	4.5
9	VB-3	Inhalation of harmful substances	4.4
	C.	**MOTIVATION**	
10	VC-1	Unattractive wages	3.5
11	VC-2	Lack of incentives	2.5
12	VC-3	Penalty and punishments	2.0
	D.	**PERSONAL**	
13	VD-1	Poor feeding	2.5
14	VD-2	Inadequate water intake	3.0
15	VD-3	Technical incompetence	2.5
16	VD-4	Inexperience	2.5
17	VD-5	Substances intake	3.0
18	VD-6	Weak adaptation to work environment	3.0
19	VD-7	Cultural background differences	2.0
	E.	**WORK PRACTICES**	
20	VE-1	High work-load	4.5
21	VE-2	Wrong work-methods	4.8
22	VE-3	Harsh supervision	3.0

23	VE-4	Unsafe work practices	2.5
24	VE-5	Lack of work control	2.6
25	VE-5	Inadequate rest	4.5
26	VE-6	Excessive grip force	3.8
27	VE-8	No provision for rest places	4.0
	F.	**EQUIPMENT**	
28	VF-1	Wrong tools	4.5
29	VF-2	Poor handling of tools/equipment/plants	4.5
30	VF-3	Weak equipment's hazard information	3.
	G.	**OTHERS**	
31	VG-1	Job insecurity	2.5
32	VG-1	Communication barriers	2.5
33	VG-1	Psychosocial environment/job title	3
34	VG-1	Poor safety inspections	3.0
35	VG-1	Lack of occupational health programs	3.0
36	VG-1	Communication and understanding of in-house rules and regulations	2.5
37	VG-1	Insurance policies	3.0

4.2. Predictor variables in the optimum multiple regression OHSR modelling

Given the large number of predictor variables in Table 1, Table 2 shows the reduced number of predictor variables that correlated significantly ($p \leq 0.05$) to the safety risk level identified through Spearman's correlation analysis. The partial *F* statistic of the independent variables was checked to identify and remove any of the variables that became insignificant. This was done, using the 'enter method on SPSS software linear regression platform, until the 13th model when no insignificant variables remained. The predictor variables are; poor use of PPE (VA-1), inadequate water intake (VD-2), poor access to safety promotional program (VA-5), no provision for rest place (VE-8), exposure to environmental hazards (VB-2), inhalation of harmful substances (VB-3), poor safety program (VA-2), substances intake (VD-5), high work load (VE-1), wrong work-methods (VE-2), lack of work control (VE-5), harsh outdoor environment VB-1), wrong tools (VF-1).

Table 2. *Coefficient for dependent variable 'occupational health and safety risk'*

Model 13	Unstandardized Coefficients		Stand. Coeff.	T	Sig.
	B	Std. Error	Beta		
(Constant)	1.080	.077		13.975	.000
Poor use PPE (VA-1)	.070	.020	.069	3.454	.001
Inadequate water intake (VD-2)	-.106	.050	-.020	-2.109	.037
Poor access to safety promotional program (VA-5)	.124	.035	.124	3.541	.001
No provision for rest places (VE-8)	-.069	.027	-.076	-2.531	.013
Exposure to environmental hazards (VB-2)	.061	.024	.064	2.532	.012
Inhalation of harmful substances (VB-3)	.052	.023	.057	2.233	.027
Poor safety program (VA-2)	.068	.030	.065	2.246	.026
Substance intake (VD-5)	.041	.017	.047	2.381	.019
Excessive use (VE-1)	.117	.027	.115	4.419	.000
Wrong work-methods (VE-2)	.217	.035	.227	6.266	.000
Lack of work control (VE-5)	.127	.029	.148	4.332	.000
Harsh outdoor environment VB-1)	.126	.035	.123	3.580	.000
Wrong tools (VF-1)	.088	.028	.083	3.152	.002

Fig. 1 shows the percentage contributions of all the predictor variables to OHSR in the model with two variables (VF-8 and VD-2) having a negative β coefficient, all others are positive as predictor VE-2 emerged the highest (21.7%) contributor.

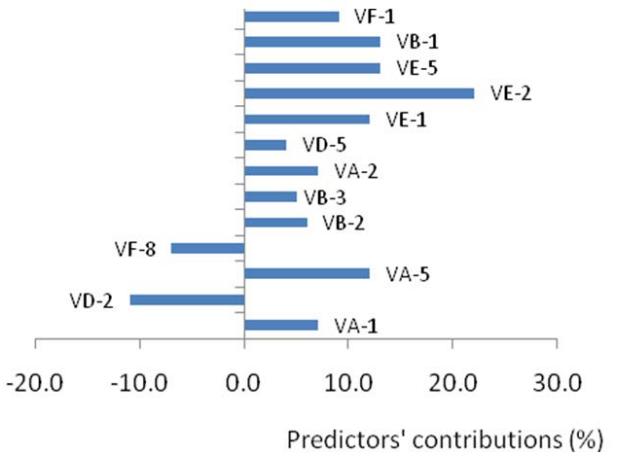

Figure 1. *Showing the percentage contributions of the predictor variables in the optimum model*

ANOVA result which assessed the overall significance of the model emerged ($F_{13,136} = 13.863$, $p < 0.0001$. Hence since $p < 0.05$ the model is significant. The adjusted R square value of 0.708 derived from the optimum model shows that the model accounts for 70.8% of variance in the outcome variable. This suggested a very good model. Because the constant (beta zero) is included, the "unstandardized coefficients were used to generate the equation for the regression line:

$$\begin{aligned} Y = {} & 1.080 + .070(VA-1) - .106(VD-2) \\ & + .124(VA-5) - .069(VE-8) \\ & + .061(VB-2) + .052(VB-3) \\ & + .068(VA-2) + .041(VD-5) \\ & + .117(VE-1) + .217(VE-2) \\ & + .127(VE-5) + .126(VB-1) \\ & + .088(VF \\ & - 1) \end{aligned} \quad (1)$$

Using this model, given values for all the predictor variables, the user can come up with a prediction for the "OHSR level".

4.3. Cook's Distance

The maximum value of the model Cook's distance was 0.930 with a standard deviation of 0.017. Since this value is less than the value of 1.0, it appears there is no major problematic case in the sample.

4.4. Normal Probability-Probability (P-P) Plot

Figure 2 described how closely the two data sets (the predictor and the OHSR variables) agreed. From the plot, most of the data points didn't fall exactly on the regression equation line. The residual, the vertical distance between a data point and the regression line, are minimal with some at zero points. The positive ones (above the regression line) have however appeared more than the negative (below the regression line). However, in the overall, there does not appear to be a severe problem with non-normality of residuals.

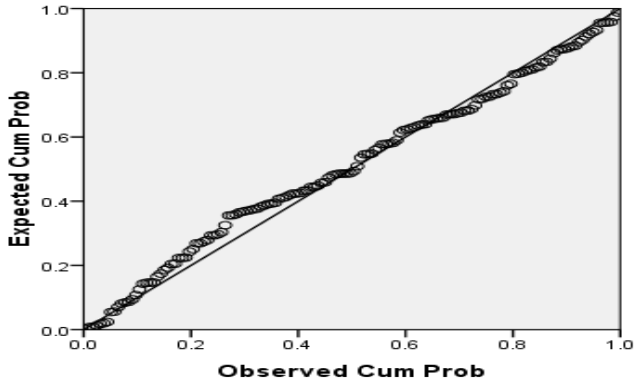

Figure 2. *Normal P-P plot of regression standard residual*

4.5. Model validation

Table 3 displays the results of 15 tested scenarios randomly selected from the numerous primary data collected. All the 13 predictor variables in the optimum model, the values of the predictors as reported by the subjects, the model result and the HEPP predicted values with linguistic interpretations are shown.

4.5.1. Percentages of similarity between OHSR model and HEPP

From Table 3, 60% of the total linguistic interpretations are the same (samples 2,3,5,6,7,8,9, and 14, 15) for all the samples. Whereas 40% had the model linguistic interpretations higher in level than those of the HEPP. However, in all the cases where the model predicted a higher level of OHSR occurrence, they are neighbourhood rankings. Figure 3 shows the relationship between the predicted values by the two sources (OHSR model and HEP). In the majority of the numeric values, those of HEP generally fall below that of the model.

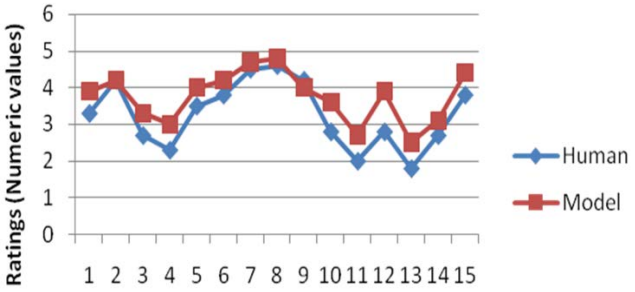

Figure 3. *Comparison of the OHSR model and the HEP values*

4.5.2. Statistic Test

a. Correlation

After comparing the result of predicted values of the model (using equation 1) with that of human professional subjective

average ratings for correlation strength using Spearman's rho, a significant correlation of r = 0.965, p<0.01 was derived, suggesting a very strong correlation.

Table 3. *Percentages of similarity between OHSR model and HEPP*

Samples	a	B	c	d	e	f	g	h	i	j	k	L	m	HEP predictions		Model Predictions	
														Val.	Inter.	Val.	İnter
1	3	1	3	4	4	4	4	5	5	1	1	5	2	3.3	Mild	3.9	High
2	2	2	2	5	5	4	5	2	3	4	2	5	3	4.2	High	4.2	High
3	4	4	4	5	4	1	4	1	2	2	1	5	2	2.7	Mild	3.3	Mild
4	2	2	3	5	2	1	4	1	4	2	1	4	1	2.3	Low	3.0	Mild
5	2	2	2	4	4	5	4	2	2	3	2	4	5	3.5	High	4.0	High
6	2	2	2	3	5	3	5	1	3	4	3	3	4	3.8	High	4.2	High
7	3	3	3	4	2	3	3	2	5	5	2	5	4	4.5	E.H.	4.7	E.H.
8	2	2	2	4	5	5	5	5	5	4	4	4	4	4.6	E.H.	4.8	E.H.
9	3	3	3	5	4	2	4	3	3	3	2	5	4	4.2	High	4.0	High
10	3	1	3	5	4	1	4	1	5	1	2	5	2	2.8	Mild	3.6	High
11	4	4	4	4	1	1	5	1	1	1	1	4	1	2.0	Low	2.7	Mild
12	1	1	4	3	5	2	5	3	1	3	2	4	3	2.8	Mild	3.9	High
13	3	3	3	5	3	1	3	1	2	1	1	3	1	1.8	Low	2.5	Mild
14	2	2	2	5	2	3	3	1	3	2	3	2	2	2.7	Mild	3.1	Mild
15	4	3	4	5	2	3	2	3	3	4	4	4	3	3.8	High	4.4	High

a = VA-1, b = VD-2, c = VA-5, d = VE-8, e = VB-2, f = VB-3, g = VA-2, h = VD-5, I = VE-1, j = VE-2, k = VE-5, l = VB-1, m = VF-1,

b. Independent samples t-test

The t-test to determine the mean difference between the Model values and HEP values found that the Model predicted higher values of risk level (3.7533 ± 0.233) compared to HEP (3.2667 ± 0.18097), t (28) = -1.648, p = 0.197. Since p>0.05, there is no significant difference between groups.

A multiple linear regression model was carried out to model Occupational Health and Safety Risk (OHSR) among the unskilled workers. The model was suitable for predicting the outcome (F = 13.863, df = 18, p<.001). The coefficients for the explanatory variables are as presented in Table 2.

The predictor variables after the 13th iterative process include; poor use of PPE (VA-1), inadequate water intake (VD-2), poor access to safety promotional program (VA-5), no provision for rest shade (VE-8), exposure to environmental hazards (VB-2), inhalation of harmful substances (VB-3), poor safety program (VA-2), substances intake (VD-5), excessive use (VE-1), wrong work-methods (VE-2), lack of work control (VE-5), harsh outdoor environment VB-1) and using wrong tools (VF-1). Among the predictor variables, use of wrong work-methods had the strongest value (0.217) of the coefficient.

The regression parameters can be used to calculate the value of safety risk from the entire model or part. Considering the effects of using 'wrong work-methods', the predicted safety level when VE-2 = 1 (work method close to normal) is 1.080 + (.217*1) = 1.287. By comparing the predicted safety risk value when using 'wrong work methods' is considered 'unergonomics' (VE-2 = 5) is 1.080 + (.217*5) = 1.287= 2.165. There is therefore roughly a 1.0 score point gap between the highest and lowest rank of 'using the wrong work-methods' category alone which is a substantial difference in safety level. The VE-2 predictor has a positive β coefficient of 0.217 in the model, hence the risk of OHS increased with using unergonomics methods.

Veronica et al. [24] mentioned that workers in severe harsh outdoor environments are at risk of a range of heat-related illnesses. According to Occupational Safety and Health Administration [8], heat-related illness include majorly; heatstroke, heat exhaustion (with weakness, headache, and profuse sweating, among others, as symptoms), heat cramps (involuntary spasms of large muscle groups as symptoms), heat syncope (symptoms include fainting or lightheadedness) and heat rash (red bumps on the skin, feeling of the skin as symptoms). Working under harsh outdoor environment (VB-

1) was linked with positive β coefficient of 0.126 in the model and the increase of which will worsen the model predicting the outcome. Maintenance of productivity in hot environments without compromising workers' safety is however possible through the adoption of a flexible management approach, worker rotation or work-rest cycling [25].

Intake of substances (VD-5) is a predictor variable in the model with a positive β coefficient of 0.041. Injury is linked with substance (drug, alcohol etc.) intake, even minimal amounts use while working may increase a worker's risk of being injured on the job [26]. For all substances intake, the risk of injury increased with increasing rates of current and lifetime use [27]. As reported by America's Medicine Cabinet [28], while medications can help keep the body healthy, they also can cause serious problems when used incorrectly. Taking medications, the wrong way is an extremely costly and dangerous problem. It increases the chances of severe medical complications or even death. Drinking too much or at the wrong time of alcohol, as reported by Health and Safety Executive [29], can be harmful.

Exposure to harmful substances (VB-3) contributed a positive β coefficient of 0.053 to the outcome of the model. Dust, concrete crusted clothing and variety of oils, greases among others, can lead a worker to the potential for becoming sick, ill and disabled. By extension, such hazardous substance can be unknowingly brought back to the worker's home which can be unintentionally poisoning the total family. Construction Safety Council [30] stated that controlling a hazard at its source is the best way to protect workers. However, when engineering, work practices and administrative controls do not provide sufficient protection, employers must provide PPE to their employee and ensure its proper use. Poor use or lack of PPE (VA-1) was connected to positive β coefficient of 0.070 in the model and this value increased the output. The purpose of using PPE is to shield or isolate individuals from physical or biological hazards. When the right PPE is used in physical tasks, hazards are reduced. The use of filtering face-pieces, half-face respirators among others can be used to prevent dust, mists and other hazardous materials.

Workplace health promotion programs are employer-sponsored initiatives directed at improving the health and well-being of workers [31]. Such health programs enable workers to increase control over their health and its determinants, and thereby improve their health. Health promotion programs may include among others, awareness programs to make health information available and accessible to employees, lifestyle/behaviour change programs, and encouraging employees to take simple steps to reduce stress [32]. In a developing country like Nigeria, most of the low-qualified workers are illiterate who may not properly read the content of safety poster and instructions. In addition, labourers are often neglected in safety management intervention program. This is evident with the positive β coefficient of 0.041 contributions to the model output of poor access to safety promotional program (VA-5).

Using the wrong tools (VF-1) is an important positive predictor significant in the model. As mentioned by the Labour Institute and the United Steelworkers International Union [33], not having the proper tool to use and the proper training on how to use various tools can result in a worker being injured. As mentioned by the majority of the subjects studied, some of the common hand tools they use (e.g. shovel, digger, cutlass etc.) were self-provided some of which were improvised and may not be right for the various tasks been used for. As reported by the University of California [34], if a tool which does not fit is used in a way it was not intended, injury such as carpal tunnel syndrome, tendonitis or muscle strain resulting from repetitive movements, performed over time, can be developed.

There is the need for the development of ergonomics measures capable of reducing the values of the β coefficient of all predictor variable in the model. Such measure may include management's commitment at minimizing hazards from the source and enforcement of safe work practice regulations, the involvement of low-skilled workers in safety programs and training, provision and enforcement of necessary PPE usage on the construction sites among other measures. These measures will enhance the occupational health and safety of the group of workers.

5. Conclusion

This study evaluated significant predictor variables that contribute to the Occupational Health and Safety Risk (OHSR) among the low-qualified workers in construction tasks. The OHSR level among the group of workers can be predicted through the developed model presented in Table 1 or with the regression equation 1. The model used 13 variables which include; lack of appropriate PPE, inadequate water intake, poor access to safety promotional program, no provision for rest shade, exposure to environmental hazards, inhalation of harmful substances, poor safety program, intake of harmful substances, excessive use, wrong work-methods, lack of work control, harsh outdoor environment and using wrong tools. The predictor variables have positive β confident except 'water intake' and lack of rest places. The result of the developed model was suitable for predicting the outcome. The author recommended the development of ergonomics measures at reducing β coefficients of all predictor variables to minimize OHSR among the group of workers.

References

[1]. Davos K. "Matching Skills and Labour Market Needs: Building Social Partnerships for Better Skills and Better Jobs," World Economic Forum Global Agenda Council on Employment, Switzerland, (2014).

[2]. Machin S. “The Changing Nature of abour Demand in the New Economy and Skill-Biased Technology Change,” Oxford Bulletin of Economics & Statistics, (63 Special Issue), (2001), 753-776.

[3]. Ahonen E. Q., Benavides F. G., Benach J. “Immigrant Populations, Work and Health - A Systematic Literature Review,” Scand J Work Environ Health, 33(2), (2007), 96-104.

[4]. Garcia A., Lopez-Jacob M., Agudelo-Suarez A., Ruiz-Frutos C., Ahonen E. “Condiciones de trabajo y salud en inmigrantes (proyecto ITSAL): entrevistas a informantes clave,” Gaceta Sanitaria, (2009), 91-98.

[5]. Alice B., Tony Z., Kerina T., Gicsuillermo H. “Occupational Health and Safety Risks for the Most Vulnerable Workers,” Milieu Ltd, Brussels, (2011).

[6]. EU Occupational Safety and Health Authority, “Hazards and Risks Associated with Older Workers,” Occupational Safety and Health Authority, (2011).

[7]. Bureau of Labour Statistics, “Occupational Outlook Handbook,” Bureau of Labour Statistics, (2010).

[8]. Occupational Safety and Health Authority, “Code of Practice for the Construction Industry,” Occupational Safety and Health Authority, (2006).

[9]. Sanchez F. A. S., Pelaez G. I. C. “Occupational Safety and Health in Construction: A Review of Applications and Trends,” Industrial Health, 55(3), (2017).

[10]. Peter O., John U. E., Okechuhwu F., Okechukwu E. “Building Construction Workers' Health and Safety Knowledge and Compliance on Site,” Journal of Safety Engineering, 5(1), (2016), 17-26.

[11]. Omobolanle A., Johnsmall W. “Impact of Occupational Health and Safety Legislation on Performance Improvement in the Nigerian Construction Industry,” Procedia Engineering, 196, (2017), 785-791.

[12]. Chunlin W., Xiaowei L., Tao W., Yue W., Bibek S. “Safety Challenges and Improvement Strategies of Ethnic Minority Construction Workers: A Case Study in Hong Kong,” International Journal of Occupational Safety and Ergonomics, 26(1), (2020), 80-90.

[13]. Amick III B. C., Hogg-Johnson S., Latour-Villamil D., Saunders R. “Protectin Construction Worker Health and Safety in Ontario, Canada: Identifying a Union Safety Effect,” Journal of Occupational and Environmental Medicine, 57(12), (2015), 1337-1342.

[14]. Yahya K., Hassan A., Ebrahim H., Narmin H., Hamid B., Amir H. B. “Factors Influencing Unsafe Behaviours and Accidents on Construction Sites: A Review,” Internationl Journal of Occupational Safety and Ergonomics, 20(1), (2014), 111-121.

[15]. Bureau of Labour Statistics, “Construction Labourers' : Occupational Outlook Handbook,” U.S. Department of Labour, (2008).

[16]. Health and Safety Executives, “Employers' Perspections of the Health and Safety of Young,” Health and Safety Executives, (2015).

[17]. Occupational Outlook Handbook, “Bricklayers and Stonemasons,” (1998).

[18]. Occupational Safety and Health Branch Labour Department, “Occupational Health Guide- Good Health is Good Future,” Occupational Safety and Health Authority, (2005).

[19]. Hinze J., Pederson C., Fredley J. “Identifying Root Causes of Construction Injuries,” Journal of Construction Engineering and Management, 124(1), (1998), 67-71.

[20]. Akomeno U. O., Rasheed A. A. “The Lagos Megacity,” (2016).

[21]. Statistical Package for Social Sciences (SPSS), “SPSS Regression Models,” IBM SPSS, (2007).

[22]. Adeyemi H. O., Adejuyigbe S. B., Ismaila S. O. “Low Back Pain Assessment Application for Construction Workers,” Journal of Engineering, Design and Technology, 13(3), (2015), 419-434.

[23]. P. Field, Discovering Statistics using IBM SPSS Statistics: And Sex and Drugs and Rock 'n' Roll, 4th ed., London: Sage, (2013).

[24]. Veronica M., Graham B., John D. S., Jens T. “Self-pacing as a Protective Mechanism against the Effects of Heat Stress,” Ann. Occup. Hyg., 55(5), (2011), 548-555.

[25]. Brake D. J., Bates G. P. “Deep Body Core Temperatures in Industrial Workers under Thermal Stress,” J Occup Environ Med, 44, (2002), 125-135.

[26]. R. Ramchand, A. Pomeroy and J. Arkes, “Effects of Substance Use on Workplace Injuries,” RAND Corporation, Santa Monica, (2009).

[27]. Shipp E. M., Tortolero S. R., Cooper S. P., Baumler E. G., Weller N. F. “Substance Use and Occupational Injuries Among High School Students in South Texas,” American Jurnal of Drug and Alcohol Abuse, 31(2), (2005), 253-265.

[28]. America's Medicine Cabinet, “Use Medicines Safely,” ISMP America's Medicine Cabinet, (2010).

[29]. Health and Safety Executive, “A Guide for Employers on Alcohol at Work,” Health and Safety Executive, (2011).

[30]. Construction Safety Council, “Health Hazards in Construction Workbook,” Construction Safety Council, Illinois, (2012).

[31]. Goetzel R. Z., Shechter D., Ozminkowski R. J., Marmet P. F., Tabrizi M. J. “Promising Practices in Employer Health and Productivity Management Efforts: Findings from a Benchmarking Study,” Journal of Occupational and Environmental Medicine, 49(2), (2007), 111-130.

[32]. Cook T., Campbell D. “Impact of Work Site Health Promotion on Health Care Costs and Utilization,” Journal of Community Medicine, 16, (2009), 99-117.

[33]. Labour Institute and the United Steelworkers International Union Under Grant Number SH-17045-08-60-F-42, “Lessons Learned,” 9(23), (2009), 1-14.

[34]. University of California, “Shop, Tool and Electrical Safety,” University of California, California, (2012).

MANAS Journal of Engineering
ISSN 1694-7398 | e-ISSN 1694-7398

Volume 8 (Issue 1) (2020) Pages 37-48

Fault analysis and prediction of power distribution networks on 11kV Feeders: A case study of Eleweeran and Poly Road 11kV Feeders, Abeokuta

Omowumi G. Olasunkanmı[1], Ajibola O. Oyedejı[2,*], Ayodeji A. Okubanjo[3]

[1]Department of Electrical and Electronics Engineering, Olabisi Onabanjo University, Ago-Iwoye, Nigeria.
grace.olasunkanmi@oouagoiwoye.edu.ng, ORCID: 0000-0002-4797-588X

[2]Department of Computer Engineering, Olabisi Onabanjo University, Ago-Iwoye, Nigeria.
oyedeji.ajibola@oouagoiwoye.edu.ng, ORCID: 0000-0002-0180-492X

[3]Department of Electrical and Electronics Engineering, Olabisi Onabanjo University, Ago-Iwoye, Nigeria.
okubanjo.ayodeji@oouagoiwoye.edu.ng, ORCID: 0000-0003-1908-0365

ABSTRACT

Distribution system, a vital link between the bulk power system and end users, accounts for 90% of power service interruptions. This study analyses faults occurring on power distribution network using Eleweeran and Poly Road 11 kV feeders in Abeokuta as case studies. Faults data, between 2014 and 2018, are collected for selected feeders using fault log books. Trend analysis of faults data is accomplished using MATLAB software with associated statistical measures (mean median mode, standard deviation, coefficient of correlation) determined. Reliability figure is thereafter computed for each of the two feeders. The mean and median of both actual and predicted fault values during the period under consideration are similar for the two feeders. The reliability index on Eleweeran 11 kV feeders showed that 2015 was the worst with failure rate of 1.55 and reliability figure of 0.21% while it was at its best in 2017 (failure rate of 1.07 and reliability of 0.34%). In the case of Poly Road 11 kV feeder, the highest failure rate of 0.62 with corresponding reliability of 0.54% was recorded in 2016 while in 2018 the failure rate was about 0.49 and reliability of 0.61%.

ARTICLE INFO

Research article

Received: 19.07.2019
Accepted: 27.05.2020

Keywords:
Distribution system,
power system,
faults,
reliability

**Corresponding author*

1. Introduction

Electric power systems are complex interconnected and most spatially extended technical systems, which are often prone to faults because of harsh environment they are exposed to. Power system or its sub-systems can be analysed through determination of the system voltages and currents under normal and abnormal conditions [1]. Generation, transmission and distribution are the three main stages involved in electric power system [2].

However, among these stages, the performance and maintenance of the distribution networks, which basically connect the generation centres to the end users, have received little attention in the field of power system [3]. The reasons for this are, the generating stations and the transmission systems are capital intensive and that the inadequacy of the generation and transmission are often associated with widespread catastrophic consequences for both the society and environment. A distribution system, however, is relatively cheaper compared to other two because its effects are localized. Therefore, less effort has been put to the evaluation and assessment of performance of this stage of electric power system [3]. The distribution system is the nearest stage to the customers and may be very prone to fault occurrence which may be human-induced or natural [4].

On the other hand, analysis of the customer failure statistics of most utilities shows that the distribution system contributes the most to the unavailability of supply to customers. Hence, the distribution systems account for about 90% of customers supply reliability problems [3]. Since the primary purpose of the system is to satisfy customer requirements and, proper functioning and longevity of the system are essential requisites for continued satisfaction, it is necessary that both demand and supply considerations are appropriately viewed and included in the systems. Therefore, improving the distribution system reliability through checkmating of the

system against possible and frequent faults occurrence (supply interruptions) has become a topical issue in the electric power industry due to its high impact on the cost of electricity and its high correlation with customer satisfaction [5].

Electric power is a vital element in any modern economy. Availability of reliable power supply at a reasonable cost is crucial for economic growth and development of any country. Electric power utilities throughout the world therefore endeavour to meet customer demands as much as economically at reasonable service reliability. To meet customer demands, power utility company has to evolve with the distribution system upgraded periodically to meet operation and maintenance performance indicator [3].

A fault in power system is described as any failure that causes interruptions of power supply [6-7]. Generally, faults occurring in power systems are traceable to natural events or by accidents where a phase establishes a connection with another phase, the ground or both in some cases [1]. In some cases, faults may be as a result of deterioration in insulation, damages by wind or sabotage or vandalism by human [1].

Power system faults can be temporary or permanent. A temporary fault occurs when the actuation of protective systems allows the circuit to be re-energized (fault clearing) after a reclosing operation. Examples of temporary faults are the insulation breakdown by the interaction between components and external agents (lightning strikes, wind, transient tree contacts, etc.) during a short period of time. Permanent faults require repair or replacement of the damaged components. Examples of permanent faults include insulators damage by flashover, underground cable breakdown and surge arrester damage [4, 7]. The fault phenomenon can affect system's reliability, security, and energy quality [6]. Any reliable electric power system should serve consumers without awkward interruptions in power supply voltage, but in Nigeria today, consumers of the electric power supply are subjected to unplanned outages on a regular basis which influence customer satisfaction [8].

The study of the effect of active failure on the power system reliability is important [9-10]. A new method for power system reliability assessment by using the fault tree analysis (FTA) approach was designed and the results identify the reliability measures connected to particular loads and the reliability measures connected to the power system as a whole: the probability of failed power delivery to selected loads, the importance measures of components corresponding to selected loads and the importance measures of components corresponding to the whole power system [11].

In [12], the reliability assessment of power equipment on the 33/11kV Anglo-Jos distribution substation of the Jos Electricity Distribution company was studied using the FTA technique. The study showed that 11kV liberty dam feeder had the highest occurrence of failure with the 110V DC battery bank having the highest mean time to repair [12].

In this study, the main focus is on analysis of faults that are associated with Eleweeran and Poly Road 11kV distribution feeders controlled by Ibadan Electricity Distribution Company (IBEDC), Abeokuta Business Unit in Ogun State as well as determining the reliability of the feeders in order to make useful suggestions on how to improve the service level of these feeders.

2. Material and methods

It is well-known that distribution systems are affected by stochastic events such as faults on lines, sudden failures of power plants and random variations in demand. Probabilistic methods are therefore essential for a sound assessment of the reliability of power systems. To increase the reliability, it is necessary to understand the causes of outages and types of equipment failures. In order to evaluate reliability of a system, few parameters are required, which are;

1.1 Mean Failure Rate

The mean failure rate λ of a given set data is the number of failure occurring per unit time. Mathematically, it is expressed as

$$\lambda = \frac{\sum f}{\sum T} \tag{1}$$

where $\sum f$ is the total number of failure and $\sum T$ is the cumulative operating period.

Since components of a failure could be more than one, for instance, in this study different types of faults occurring on a distribution feeder are considered, equation 1 is modified as

$$\lambda = \lambda_1 + \lambda_2 + \cdots \lambda_n \tag{2}$$

where λ_1, λ_2, λ_3,…, λ_n are failure rates due to different types of faults contributing to the overall failure rate λ.

1.2 Reliability

The reliability function $R(t)$ is the probability that no failures occur within time period 0 to time period t [13]. It is given by

$$R(t) = \exp(-\lambda t) \tag{3}$$

where t is time period (in days, months or years) for which the reliability is desired and λ is the failure rate per time unit.

1.3 Statistical Analysis

Statistical analysis is needed in this study for the purpose of checking whether there is any correlation between predicted total fault values obtained from model (the trend equation) and

actual total fault values for the data collected. In order to do this, linear correlation coefficient is used along with other measures of central tendency (mean, median and mode) and dispersion (standard deviation). Generally, for a pair of data set $X = x_1, x_2, \cdots x_n$ and $Y = y_1, y_2, \cdots y_n$, linear coefficient of correlation is given by

$$r = \frac{\sum xy}{\sqrt{(\sum x^2)(\sum y^2)}} \quad (4)$$

where x is the independent variable which representing the period of sixty (60 month) and y is dependent variable which stands for fault value of the period under consideration.

2.4 Regression Analysis

Regression or trend analysis is the study of the behaviour of a time series or a process in the past and its mathematical modelling so that future behaviour can be extrapolated from it. Two general approaches usually followed in trend analysis are [14]:

- The fitting of continuous mathematical functions through actual data to achieve the least overall error, known as regression analysis.
- The fitting of a sequence on discontinuous lines or curves to the data.

The second is usually employed for short-term forecasting. A time-varying event such as power system load can be broken down into the following four major components [14]:

- Basic trend.
- Seasonal variation (Monthly or yearly variation of load).
- Cyclic variation which influences of periods longer than the above and causes the load pattern to be repeated for two or three years (or even longer cycles).
- Random variations which occur on account of the day-to- day changes and in the case of power systems are usually dependent on the time of the week e.g. weekend, week day, weather etc.

The last three variations have a long-term mean of zero. Generally, in forecasting, either a continual variation process model or a model that is based only on certain points at regular intervals of the process is used. In either case, the process is modelled as time series [14].

The principle of regression theory is that any function $y = f(t)$ can be fitted to a set of points (x_1, y_1), (x_2, y_2) so as to minimize the sum of errors= squared at each point, that is:

$$\sum_{i}^{n} \{y_i - f(x_i)\}^2 = minimum \quad (5)$$

2.5 Collection of Fault Data

Monthly information and data on the various types of faults associated with the selected Eleweeran and Poly Road feeders are collected from IBEDC, Abeokuta Business Unit for period of five years (2014 – 2018) through personal contact with service personnel and maintenance staffs of the Business Unit.

Appendices I and II show monthly breakdown of faults recorded on Eleweeran 11 kV feeder and Poly Road feeder for the years 2014 – 2018 respectively. Tables 1 and 2, show the monthly total faults on Eleweeran and Poly Road 11 kV feeders, respectively for the five years period under consideration in this study. Table 3 shows the individual fault total over the five years period while Table 4 presents total yearly faults for the two feeders.

Table 1. *Monthly Total Faults on Eleweeran 11kV Feeder*

Month	2014	2015	2016	2017	2018
January	33	34	22	13	17
February	33	41	26	22	27
March	43	55	49	37	42
April	38	58	44	39	43
May	37	57	47	47	45
June	35	57	47	45	50
July	41	55	48	44	44
August	30	31	26	24	30
September	38	57	38	34	41
October	40	56	44	44	43
November	33	38	24	27	40
December	29	26	22	17	29
Total	**430**	**565**	**437**	**393**	**451**

Table 2. *Monthly Total Faults on Poly Road 11kV Feeder*

Month	2014	2015	2016	2017	2018
January	12	11	12	17	11
February	15	14	14	16	14
March	22	24	26	26	25
April	21	15	26	21	16
May	24	24	31	21	20
June	21	24	27	24	19
July	17	18	19	24	15
August	16	21	18	20	14
September	16	19	17	18	15
October	12	14	13	15	13

November	9	12	13	11	11
December	9	8	10	6	7
Total	**194**	**204**	**226**	**219**	**180**

Table 3. *Individual fault total for Eleweeran and Poly Road 11 kV Feeders from 2014 – 2018*

Fault Type	Eleweeran 11 kV feeder	Poly Road 11 kV feeder
Over-current	908	322
Earth	923	298
Instantaneous earth	115	178
Transient	335	225

Table 4. *Total yearly fault for Eleweeran and Poly Road 11 kV Feeders from 2014 – 2018*

Year	Eleweeran 11 kV feeder	Poly Road 11 kV feeder
2014	430	194
2015	565	204
2016	437	226
2017	393	219
2018	451	180

2.6. Trend Analysis of the Fault Data

In order to analyse the fault data to observe the trend and obtain predicted values, two approaches adopted are time series modellers and modelling of the pattern. The former gives the distribution of fault data against time (month) while the latter returns model equation to describe the data. MATLAB software is used to accomplish these tasks [5].

To aid further analysis of fault data on Eleweeran and Poly Road 11 kV feeders, trend curves generated from Tables 1 and 2, for Eleweeran and Poly Road 11 kV feeders, respectively are fitted with regression curves using MATLAB software built-in tool.

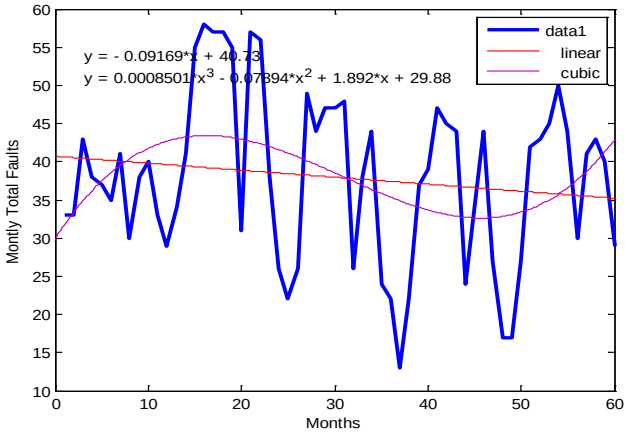

Figure 1. *Total fault from January 2014 to December 2018 (60 months) for Eleweeran 11 kV feeder with both Linear and Polynomial (Cubic) Curves fitting*

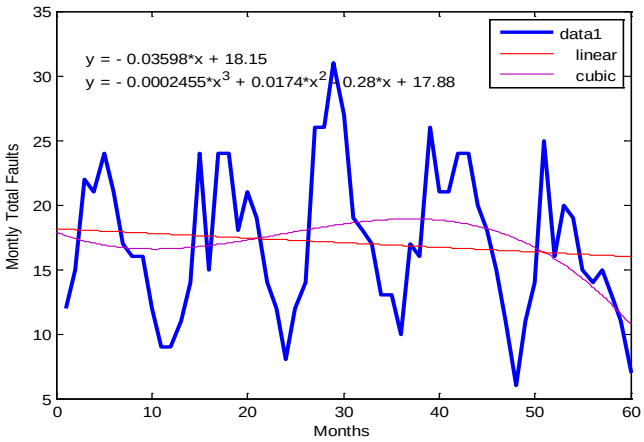

Figure 2. *Total fault from January 2014 to December 2018 (60 months) for Poly Road 11 kV feeder with both Linear and Polynomial (Cubic) Curves fitting*

Based on Figures 1 and 2, in terms of time period t (month), the following curve fits are obtained for Eleweeran 11 kV feeder, where LT is the linear predicted total fault and CT is the cubic predicted total fault.

$$LT_{eleweeran} = -0.09169t + 40.73 \quad (6)$$

$$CT_{eleweeran} = 0.0008501t^3 - 0.0789t^2 + 1.892t + 29.88 \quad (7)$$

$$LT_{polyroad} = -0.03598t + 18.15 \quad (8)$$

$$CT_{polyroad} = -0.0002455t^3 + 0.0174t^2 - 0.28t + 17.88 \quad (9)$$

3. Results and discussions

Having obtained trend equations for each of the two feeders under study, fault values are predicted from January 2014 to December 2018 from equations 6 - 9. The seasonal deviations (errors) between the predicted fault values and the actual fault values are calculated. These are presented in Tables 5 and 6, respectively, for Eleweeran and Poly Road 11 kV feeders.

Table 5. *Predicted Fault Values for Eleweeran 11 kV Feeder from January 2014 to December 2018 using trend equations*

Months (x)	Actual Total Monthly Faults (TT)	Linear Predicted Total Faults (LT)	LT-TT (nearest whole number)	Cubic Predicted Total Faults (CT)	CT-TT (nearest whole number)
1	33	40.6383	8	31.6939	-1
2	33	40.5466	8	33.355	0
3	43	40.4549	-3	34.8685	-8
4	38	40.3632	2	36.2394	-2
5	37	40.2715	3	37.4728	0
6	35	40.1799	5	38.5738	4
7	41	40.0882	-1	39.5475	-1
8	30	39.9965	10	40.3991	10
9	38	39.9048	2	41.1336	3
10	40	39.8131	0	41.7561	2
11	33	39.7214	7	42.2717	9
12	29	39.6297	11	42.6856	14
13	34	39.538	6	43.0028	9
14	41	39.4463	-2	43.2284	2
15	55	39.3546	-16	43.3676	-12
16	58	39.263	-19	43.4254	-15
17	57	39.1713	-18	43.4069	-14
18	57	39.0796	-18	43.3172	-14
19	55	38.9879	-16	43.1615	-12
20	31	38.8962	8	42.9448	12
21	57	38.8045	-18	42.6722	-14
22	56	38.7128	-17	42.3489	-14
23	38	38.6211	1	41.9799	4
24	26	38.5294	13	41.5703	16
25	22	38.4377	16	41.1253	19
26	26	38.3461	12	40.6499	15
27	49	38.2544	-11	40.1493	-9
28	44	38.1627	-6	39.6284	-4
29	47	38.071	-9	39.0925	-8
30	47	37.9793	-9	38.5467	-8
31	48	37.8876	-10	37.996	-10
32	26	37.7959	12	37.4455	11
33	38	37.7042	0	36.9004	-1
34	44	37.6125	-6	36.3657	-8
35	24	37.5208	14	35.8465	12
36	22	37.4292	15	35.348	13
37	13	37.3375	24	34.8753	22

38	22	37.2458	15	34.4333	12
39	37	37.1541	0	34.0273	-3
40	39	37.0624	-2	33.6624	-5
41	47	36.9707	-10	33.3436	-13
42	45	36.879	-8	33.076	-12
43	44	36.7873	-7	32.8648	-11
44	24	36.6956	13	32.7151	9
45	34	36.6039	3	32.6319	-1
46	44	36.5123	-7	32.6203	-11
47	27	36.4206	9	32.6855	6
48	17	36.3289	19	32.8325	16
49	17	36.2372	19	33.0665	16
50	27	36.1455	9	33.3925	6
51	42	36.0538	-6	33.8157	-8
52	43	35.9621	-7	34.3411	-9
53	45	35.8704	-9	34.9739	-10
54	50	35.7787	-14	35.7191	-14
55	44	35.687	-8	36.5819	-7
56	30	35.5954	6	37.5673	8
57	41	35.5037	-5	38.6805	-2
58	43	35.412	-8	39.9266	-3
59	40	35.3203	-5	41.3105	1
60	29	35.2286	6	42.8376	14

Table 6. *Poly Road: Predicted Fault Values for Poly Road 11 kV Feeder from January 2014 to December 2018 using trend equations*

Months (x)	**Actual Total Monthly Faults (TT)**	**Linear Predicted Total Faults (LT)**	**LT-TT (nearest whole number)**	**Cubic Predicted Total Faults (CT)**	**CT-TT (nearest whole number)**
1	12	18.114	6	17.6172	6
2	15	18.078	3	17.3876	2
3	22	18.0421	-4	17.19	-4
4	21	18.0061	-3	17.0227	-4
5	24	17.9701	-6	16.8843	-7
6	21	17.9341	-3	16.7734	-4
7	17	17.8981	1	16.6884	0
8	16	17.8622	2	16.6279	1
9	16	17.8262	2	16.5904	1
10	12	17.7902	6	16.5745	5
11	9	17.7542	9	16.5786	8
12	9	17.7182	9	16.6014	8

13	11	17.6823	7	16.6412	6
14	14	17.6463	4	16.6967	3
15	24	17.6103	-6	16.7664	-7
16	15	17.5743	3	16.8488	2
17	24	17.5383	-6	16.9425	-7
18	24	17.5024	-6	17.0458	-7
19	18	17.4664	-1	17.1575	-1
20	21	17.4304	-4	17.276	-4
21	19	17.3944	-2	17.3998	-2
22	14	17.3584	3	17.5275	4
23	12	17.3225	5	17.6576	4
24	8	17.2865	9	17.7886	10
25	12	17.2505	5	17.9191	6
26	14	17.2145	3	18.0475	4
27	26	17.1785	-9	18.1724	-8
28	26	17.1426	-9	18.2924	-8
29	31	17.1066	-14	18.4059	-13
30	27	17.0706	-10	18.5115	-8
31	19	17.0346	-2	18.6077	0
32	18	16.9986	-1	18.6931	1
33	17	16.9627	0	18.7661	2
34	13	16.9267	4	18.8253	6
35	13	16.8907	4	18.8692	6
36	10	16.8547	7	18.8964	9
37	17	16.8187	0	18.9053	2
38	16	16.7828	1	18.8945	3
39	26	16.7468	-9	18.8626	-7
40	21	16.7108	-4	18.808	-2
41	21	16.6748	-4	18.7293	-2
42	24	16.6388	-7	18.625	-5
43	24	16.6029	-7	18.4936	-6
44	20	16.5669	-3	18.3337	-2
45	18	16.5309	-1	18.1438	0
46	15	16.4949	1	17.9224	3
47	11	16.4589	5	17.6681	7
48	6	16.423	10	17.3793	11
49	11	16.387	5	17.0546	6
50	14	16.351	2	16.6925	3
51	25	16.315	-9	16.2916	-9
52	16	16.279	0	15.8503	0
53	20	16.2431	-4	15.3673	-5

54	19	16.2071	-3	14.841	-4
55	15	16.1711	1	14.2699	-1
56	14	16.1351	2	13.6527	0
57	15	16.0991	1	12.9877	-2
58	13	16.0632	3	12.2736	-1
59	11	16.0272	5	11.5089	1
60	7	15.9912	9	10.692	4

Consequently, the linear predictor models are used to generate predicted fault data on each of the two feeders under investigations. Presented in Table 7 are predicted total yearly faults on Eleweeran and Poly Road 11 kV feeders respectively using linear predictor model.

Table 7. *Total yearly predicted faults for Eleweeran and Poly Road 11 kV Feeders from 2014 – 2018 using Linear Predictors*

Year	Eleweeran 11 kV feeder	Poly Road 11 kV feeder
2014	482	215
2015	468	210
2016	455	205
2017	442	199
2018	429	194

It is clear from Table 7 above that predicted total yearly faults using linear predictor exhibit a downward linear trend for the two feeders under study, with the highest values recorded in 2014 for both feeders.

Next, monthly total faults are forecast for additional five years beginning from January 2019 to December 2023 (another 60 months) using linear predictor models for each of Eleweeran and Poly Road 11 kV feeders. Results are presented in Tables 8 and 9, for Eleweeran and Poly Road feeders, respectively. In addition, total yearly faults forecast for 2019 – 2023 are equally computed for the two feeders using linear predictor with results shown in Table 10.

Table 8. *Forecast fault values for Eleweeran 11 kV feeder from January 2019 to December 2023 (Nearest whole number) using Linear Predictor*

Month	Year				
	2019	**2020**	**2021**	**2022**	**2023**
January	35	34	33	32	31
February	35	34	33	32	31
March	35	34	33	32	31
April	35	34	33	32	30
May	35	34	33	31	30
June	35	34	32	31	30
July	35	33	32	31	30
August	34	33	32	31	30
September	34	33	32	31	30
October	34	33	32	31	30
November	34	33	32	31	30
December	34	33	32	31	30

Table 9. *Forecast fault values for Poly Road 11 kV feeder from January 2019 to December 2023 (Nearest whole number) using Linear Predictor*

Month	Year				
	2019	**2020**	**2021**	**2022**	**2023**
January	16	16	15	15	14
February	16	15	15	15	14
March	16	15	15	15	14
April	16	15	15	15	14
May	16	15	15	15	14
June	16	15	15	14	14
July	16	15	15	14	14
August	16	15	15	14	14
September	16	15	15	14	14
October	16	15	15	14	14
November	16	15	15	14	14
December	16	15	15	14	14

Just like what obtains in predicted total yearly faults via the use of linear predictor, values of forecast total monthly faults decrease marginally with increasing number of months. In fact, roughly a difference of a unit is noticed between forecast values of a particular year and preceding year for Eleweeran feeder while at Poly Road feeder, forecast values vary between 16 and 14 for the entire sixty months advance. Summation of entries in Tables 8 and 9 yield total yearly forecast data for the two feeders for year 2019 – 2023 as shown in Table10.

Table 10. *Total yearly forecast faults for Eleweeran and Poly Road 11 kV Feeders from 2019-2023*

Year	Eleweeran 11 kV feeder	Poly Road 11 kV feeder
2019	415	192
2020	402	181
2021	389	180
2022	376	173
2023	363	168

Again, there exists progressive decline in the number of total yearly forecast faults for the two feeders as shown in Table 10. Results of data statistics carried out on actual fault data as well as predicted faults using model equations for the two feeders is presented in Table 11. This is done to verify the statistical significance of the deviation (difference) in value between the actual monthly total faults and the predicted faults from January 2014 and December 2018 for Eleweeran 11 kV feeder and Poly Road 11 kV feeder.

Table 11. *Statistics of Faults Data from Eleweeran 11kV and Poly Road 11 kV Feeders*

Items	Poly Road Feeder		Eleweeran Feeder	
	Actual Fault Data	Predicted Fault Data (Linear Predictor)	Actual Fault Data	Predicted Fault Data (Linear Predictor)
Minimum	6	15.99	13	35.23
Maximum	31	18.11	58	40.64
Mean	17.05	17.05	37.93	37.93
Median	16	17.05	38.5	37.93
Mode	24	15.99	44	35.23
Standard Deviation	5.637	0.6284	11.05	1.601
Range	25	2.123	45	5.41
Linear Coefficient of Correlation	0.1115		0.1450	

In order to determine level of performance (reliability) of both Eleweeran and Poly Road 11 kV feeders, reliability index of each of the two feeders is computed using equation 2. The failure rate and reliability values for each year under consideration (2014 to 2018) for both feeders are evaluated. Also, the predicted failure rate and reliability values from 2014 to 2018 and the forecast failure rate and reliability values from 2019 to 2023 are determined.

Using values of total yearly fault data presented in Table 4 along with expressions stated in (1) – (4), the actual failure rate and reliability values for the two feeders readily emerge as presented in Tables 12, 13 and 14.

Table 12. *Failure rate and reliability figures for Eleweeran and Poly Road 11 kV Feeders from 2014-2018 based on actual fault data*

	Year				
Parameters	**2014**	**2015**	**2016**	**2017**	**2018**
Eleweeran 11 kV Feeder					
Failure rate/day	1.1781	1.5479	1.1973	1.0767	1.2356
% Reliability/year	0.3079	0.2127	0.3020	0.3407	0.2907
Poly Road 11 kV Feeder					
Failure rate/day	0.5315	0.5589	0.6192	0.6000	0.4932
% Reliability/year	0.5877	0.5718	0.5384	0.5488	0.6107

Table 13. *Failure rate and reliability figures for Eleweeran and Poly Road 11 kV Feeders from 2014-2018 based on predicted total yearly faults using linear predictor model*

	Year				
Parameters	**2014**	**2015**	**2016**	**2017**	**2018**
Eleweeran 11 kV Feeder					
Failure rate/day	1.3205	1.2822	1.2466	1.2110	1.1753
% Reliability/year	0.2670	0.2774	0.2875	0.2979	0.3087
Poly Road 11 kV Feeder					
Failure rate/day	0.5890	0.5753	0.5616	0.5452	0.5315
% Reliability/year	0.5549	0.5625	0.5703	0.5797	0.5877

Table 14. *Failure rate and reliability figures for Eleweeran and Poly Road 11 kV Feeders from 2019-2023 based on forecast total yearly faults using linear predictor model*

	Year				
Parameters	**2019**	**2020**	**2021**	**2022**	**2023**
Eleweeran 11 kV Feeder					
Failure rate/day	1.1370	1.1014	1.0658	1.0301	0.9945
% Reliability/year	0.3208	0.3324	0.3445	0.3570	0.3699
Poly Road 11 kV Feeder					
Failure rate/day	0.5260	0.4959	0.4932	0.4740	0.4603
% Reliability/year	0.5909	0.6090	0.6107	0.6225	0.6311

Result presented in Tables 12-14 revealed that for the actual fault data between years 2014 and 2018, Eleweeran feeder recorded its highest failure rate 0f 1.55 per day with corresponding reliability figure of 0.21% in 2015 while the highest reliability figure was obtained in 2017 as 0.34% with failure per day of 1.08. For Poly road feeder, 2018 was the best year with failure per day of 0.49, reliability figure of

0.61% while the worst year was 2016 having 0.62 failures per day and reliability figure of 0.54%.

For predicted fault data from Table 13, and forecast data from Table 14, both failure rate and reliability figure vary linearly with increasing year. For both feeders, the highest failure rate occurred in 2014 for predicted data while the best year in terms of reliability index was 2018. In the case of forecast data, low failure rate and best reliability figure will be recorded in 2023 while the year 2019 is least in terms of reliability index.

The study revealed that over-current fault, earth fault, transient fault and instantaneous fault were the most common faults associated with both feeders. While earth fault is the highest at Eleweeran feeder, over-current fault is the most common fault at Poly Road feeder. At both feeders, instantaneous earth fault is the least occurring fault. The trend plots using MATLAB software (version 2016) revealed that the individual faults and the monthly total faults trends for both feeders were non-linear.

In addition, with the trend equation, fault values were forecast for additional five years (additional 60 months) for both feeders with average values of 33 and 15 total faults per month respectively for Eleweeran and Poly Road feeders. The reliability analysis carried out revealed that for both feeders predicted total faults between 2014 and 2018 and forecast total faults from 2019 to 2023 followed the same trend with failure rate decreasing while reliability was increasing.

4. Conclusion

Results obtained from this study provide insight into patterns of faults occurring on Eleweeran and Poly Road 11 kV feeders in Abeokuta Business Unit of IBEDC. However, the followings are suggestions for future extensions of the investigation carried out in the present effort. Although, linear predictor is used to obtain forecast values in this study, it is recommended that other approaches such as Auto-Regressive Moving Average (ARMA) model can be used to enhance the accuracy of the model equation. In addition, the study can be further carried out to show the trend of individual fault occurrence which will help the distribution company to have a better plans towards mitigation the occurrence of faults and maintenance strategy so as to improve customer satisfaction.

Acknowledgement

The authors of this work sincerely appreciate the Ibadan Electricity Distribution Company (IBEDC), Abeokuta Regional Office and the National Population Commission for the data provided towards the success of this project.

References

[1]. Jorge S. “Analysis of Power Systems under Fault Conditions,” M.Sc. Dissertation, Electrical and Electronic Engineering, California State University, Sacramento, (2011).

[2]. Vijaysimha N., Chengaiah C. H. “Evaluation of Fault Analysis in Transmission Lines using Relay Settings,” Journal of Theoretical and Applied Information Technology, (2010), 126-134.

[3]. Tempa D. “Reliability Assessment of Distribution Systems - Including a case study on Wangdue Distribution System in Bhutan,” M.Sc. Dissertation, Department of Electrical Power Engineering, Norwegian University of Science and Technology, Oslo, (2009).

[4]. Nasser T. Power Systems Modelling and Fault Analysis, 2nd ed., Academic Press, Elsevier, (2019).

[5]. Charles J.K., Seung-Jae L., Sang-Hee K. “Evaluation of Feeder Monitoring Parameters for Incipient Fault Detection using Laplace Trend Statistics,” IEEE Transactions on Industry Applications, 40(6), (2004), 1-7.

[6]. Filomena A. D., Resener M., Salim R. H., Bretas A. S. “Distribution System Faults Analysis Considering Fault Resistance Estimation,” Electrical Power and Energy Systems, 33, (2011), 1326-1335.

[7]. Quiroga O. A., Melendez J., Herraiz S., Sanchez J. “Sequence Pattern Discovery of Events Caused by Ground Fault Trips in Power Distribution Systems,” in 18th Mediterranean Conference on Control and Automation, MED'10, Marrakech, (2010).

[8]. Shalangwa D. A., Shinggu D. Y., Jonathan T. “An Analysis of Electric Power Faults in Mubi Undertaking Station, Adamawa State, Nigeria,” Pacific Journal of Science and Technology, 10(2), (2009), 508-513.

[9]. Zhao Y., Hu X., Sun Z. “The Effect of Active Failure on the Power System Reliability Evaluation,” in 3rd International Conference on Mechanical Engineering and Intelligent Systems, (2015).

[10]. Shalash N. A., Ahmad A. Z., Jaber A. S. “Multi-Agent Approach for Reliability Assessment and Improvement of Power System Protection,” in The IRES International Conference, Moscow, (2017).

[11]. Volkanovski A., Cepin M., Mavko B. “Application of the Fault Tree Analysis for Assessment of Power System

Reliability," Reliability Engineering and System Safety, 94, (2009), 1116-1127.

[12]. Adelabu A. J., Haruna Y. S., Aliyu U. O. "Relaibility Assessment of Power Equipment in a Distribution Substation Using Fault Tree Analysis," Global Scientific Journals, 6(2), (2018), 249-259.

[13]. Hendi R. B., Seyed-Sheneva S., Gandomkar M. "Electrical Distribution System Reliability Improvement by Optical Placement of Fault Indicator using Immune Algorithm," International Journal of Engineering Research and Application, 2(2), (2012), 1383-1390.

[14]. Pabla A. S. Electric Power Distribution, 6th ed., New Delhi: Tata McGraw-Hill EducationPvt. Ltd., (2011).

APPENDIX I: FAULT DATA FOR 11kV INJECTION SUB-STATION, POLICE HQ, ELEWEERAN

2014					
Month	**Over Current**	**Earth Fault**	**Instantaneous Fault**	**Transient Fault**	**Total Fault**
Jan	20	10	1	2	33
Feb	21	10	1	1	33
Mar	15	18	4	6	43
Apr	10	18	3	8	38
May	10	17	2	8	37
Jun	9	18	1	7	35
Jul	15	18	2	6	41
Aug	8	19	1	2	30
Sept	10	22	2	4	38
Oct	15	18	2	5	40
Nov	22	8	1	2	33
Dec	20	8	0	1	29
Total	**175**	**184**	**20**	**52**	**430**

2015					
Month	**Over Current**	**Earth Fault**	**Instantaneous Fault**	**Transient Fault**	**Total Fault**
Jan	22	5	2	5	34
Feb	20	10	1	10	41
Mar	18	20	5	12	55
Apr	18	18	7	15	58
May	17	20	5	15	57
Jun	17	20	6	14	57
Jul	15	22	4	14	55
Aug	5	18	1	7	31
Sept	20	20	6	11	57
Oct	18	18	5	15	56
Nov	14	15	1	8	38
Dec	10	11	1	4	26
Total	**194**	**197**	**44**	**130**	**565**

2016					
Month	**Over Current**	**Earth Fault**	**Instantaneous Fault**	**Transient Fault**	**Total Fault**
Jan	10	8	2	2	22
Feb	12	12	1	1	26
Mar	21	18	4	6	49
Apr	22	16	2	4	44
May	22	18	2	5	47
Jun	20	20	1	6	47
Jul	18	20	3	7	48
Aug	6	17	1	2	26
Sept	15	18	2	3	38
Oct	18	20	2	4	44
Nov	10	12	1	1	24
Dec	8	11	1	2	22
Total	**182**	**190**	**22**	**43**	**437**

2017					
Month	**Over Current**	**Earth Fault**	**Instantaneous Fault**	**Transient Fault**	**Total Fault**
Jan	4	5	2	2	13
Feb	8	8	1	5	22
Mar	15	14	2	6	37
Apr	15	18	0	6	39
May	18	18	1	10	47
Jun	17	20	0	8	45
Jul	17	20	1	6	44
Aug	9	13	0	2	24
Sept	15	15	2	2	34
Oct	18	20	2	4	44
Nov	12	13	1	1	27
Dec	9	7	0	1	17
Total	**157**	**171**	**12**	**53**	**393**

2018					
Month	**Over Current**	**Earth Fault**	**Instantaneous Fault**	**Transient Fault**	**Total Fault**
Jan	10	5	0	2	17
Feb	12	10	0	5	27
Mar	17	18	1	6	42
Apr	20	18	2	3	43
May	20	20	1	4	45
Jun	19	20	4	7	50
Jul	20	17	1	6	44
Aug	13	11	3	3	30
Sept	18	15	2	6	41
Oct	18	18	2	5	43
Nov	17	19	1	3	40
Dec	16	10	0	3	29
Total	**200**	**181**	**17**	**57**	**451**

APPENDIX II: FAULT DATA FOR 11kV INJECTION SUB- STATION, POLY ROAD, ABEOKUTA

2014					
Month	**Over Current**	**Earth Fault**	**Instantaneous Fault**	**Transient Fault**	**Total Fault**
Jan	10	1	0	1	12
Feb	10	3	1	1	15
Mar	6	11	2	3	22
Apr	6	8	3	4	21
May	5	8	6	5	24
Jun	4	7	4	6	21
Jul	3	5	3	6	17
Aug	1	6	3	6	16
Sept	2	6	6	2	16
Oct	5	3	1	3	12
Nov	9	0	0	0	9
Dec	7	1	1	0	9
Total	**68**	**59**	**30**	**37**	**194**

2015					
Month	**Over Current**	**Earth Fault**	**Instantaneous Fault**	**Transient Fault**	**Total Fault**
Jan	8	2	1	0	11
Feb	9	2	1	2	14
Mar	7	9	3	5	24
Apr	4	7	1	3	15
May	4	7	7	6	24
Jun	5	6	5	8	24
Jul	1	5	5	7	18
Aug	3	5	6	7	21
Sept	4	6	7	2	19
Oct	4	2	4	4	14
Nov	8	2	2	0	12
Dec	6	1	1	0	8
Total	**63**	**54**	**43**	**44**	**204**

2016					
Month	**Over Current**	**Earth Fault**	**Instantaneous Fault**	**Transient Fault**	**Total Fault**
Jan	7	3	2	0	12
Feb	10	3	0	1	14
Mar	6	12	3	5	26
Apr	6	12	4	4	26
May	3	10	6	12	31
Jun	3	10	2	12	27
Jul	2	5	5	7	19
Aug	1	4	5	8	18
Sept	3	5	7	2	17
Oct	6	2	3	2	13
Nov	11	1	1	0	13
Dec	7	1	1	1	10
Total	**65**	**68**	**39**	**54**	**226**

2017					
Month	**Over Current**	**Earth Fault**	**Instantaneous Fault**	**Transient Fault**	**Total Fault**
Jan	12	4	0	1	17
Feb	11	3	0	2	16
Mar	8	10	3	5	26
Apr	4	8	4	5	21
May	3	6	4	8	21
Jun	3	7	4	10	24
Jul	1	8	5	10	24
Aug	1	8	5	6	20
Sept	2	6	7	3	18
Oct	4	5	3	3	15
Nov	9	1	1	0	11
Dec	5	0	1	0	6
Total	**63**	**66**	**37**	**53**	**219**

2018					
Month	**Over Current**	**Earth Fault**	**Instantaneous Fault**	**Transient Fault**	**Total Fault**
Jan	8	2	1	0	11
Feb	10	3	0	1	14
Mar	7	12	2	4	25
Apr	5	6	2	3	16
May	4	6	5	5	20
Jun	4	5	3	7	19
Jul	2	3	4	6	15
Aug	0	4	4	6	14
Sept	2	5	6	2	15
Oct	5	3	2	3	13
Nov	10	1	0	0	11
Dec	6	1	0	0	7
Total	**63**	**51**	**29**	**37**	**180**

MANAS Journal of Engineering
ISSN 1694-7398 | e-ISSN 1694-7398

Volume 8 (Issue 1) (2020) Pages 49-54

Real time traffic signal timing approach based on artificial neural network

Ali Tahir Karaşahin[1,*], Abdullah Erdal Tümer[2,3]

[1]Karabuk University, Department of Mechatronics Engineering, Karabuk, Turkey, tahirkarasahin@karabuk.edu.tr, ORCID: 0000-0002-7440-1312
[2]Necmettin Erbakan University, Department of Computer Engineering, Konya, Turkey, tumer@erbakan.edu.tr, ORCID: 0000-0001-7747-9441
[3]Kyrgyz-Turkish Manas University, Higher School of Vocational Education, Bishkek, Kyrgzstan

ABSTRACT

As the population increases, is more and more increasing the number of vehicles in cities. The increasing number of vehicle make traffic management complicated. Difficult traffic management leads to more fuel consumption, CO_2 and other harmful emissions. Therefore, real-time optimization of traffic lights (signaling) used in traffic management can make traffic management more efficient. In this study, green light time is optimized by estimating the number of vehicles in an intersection with signal lights in Konya city center through artificial neural network. The results are evaluated with different performance criteria and it has been shown that the developed estimation model can be successfully used to optimize the green light durations.

ARTICLE INFO

Research article

Received: 13.04.2020
Accepted: 27.05.2020

Keywords:
Dynamic traffic control, artificial neural network, traffic signalization, optimization

[*]Corresponding author

1. Introduction

Research on the application of information and communication technologies to different fields of study has increased. For example, intelligent transportation applications have been developed for traffic congestion, which is one of the fastest urbanization problems. Traffic congestion causes time loss, increased fuel consumption and emissions of harmful such as CO_2. In addition, it causes distress and discomfort to drivers. Many methods for reducing traffic congestion have been identified with increasing urban populations. Increasing traffic signal lights, intersections and road capacities are some of these methods. Green time periods at intersections are determined by vehicle counts. This method is also called constant time management. Many efforts have been made to improve the efficiency of existing traffic management. Some of the smart city applications are aimed at the technological solution of the traffic density at the intersections. For this the duration of traffic signal lights needs to be optimized.

Besides traditional traffic signal lights management techniques, there are also advanced traffic control techniques. A sample scenario studies have been carry out for traffic management with JACK agent based software. In the scenario solved with JACK, the aim is to separate the vehicles from the intersection as soon as possible. Thanks to the proposed traffic management, traffic accidents and congestion will be reduced and it has been indicating traffic flow will accelerate [6].

There are different studies in the literature to improve the average delay time and in signalized intersections. In [12], artificial neural network (ANN) techniques have been used to improve the average delay time. As a result of the study, it has been shown that the artificial neural network model can be used as a prediction model in isolated signalized intersections. Also, the developing ANN model for estimating average vehicle delays at isolated signalized intersections was better than other analytical formulas.

In another study [15,17], it has been indicated that the most suitable solution for the traffic problem was to use the existing capacity efficiently. Therefore, artificial intelligence techniques should be used an operatively in problem solving. In addition to traffic control social, economic, and ecological importance benefits of artificial intelligence techniques are emphasized.
In the artificial neural network works carried out in the field of transport engineering, transportation planning, design,

maintenance and repair of the road superstructure, operation of transportation systems, estimation of transportation parameters and traffic engineering applications are divided into 5 groups [5]. Artificial neural network is thought to produce faster and more reliable solutions to problems which cannot be expressed mathematically in transportation engineering [1,11].

The rapid increase in the number of vehicles in traffic as a reflection of increasing population and economic developments has brought with them other problems [14]. As a result of the increase the number of vehicles and in traffic movements, traffic accidents both in the world and in our country have also increased [13]. Traffic accident models in our country have been researched and it has been pointed out that needs to be done in this regard [9].

In [2], IOT based has been indicated dynamic traffic signal lights control. IR sensors and Arduino controller has been used for efficient traffic management. With the help of sensors, the vehicles in the intersections were detected and green time duration was determined according to the traffic density.

In [4], the estimated number of stops at intersections was modeled with ANNs. Intersection approach volumes, cycle length and left return strip presence, input, average delay and number of stops per vehicle have been indicated as output parameters. The aim of this study is to optimize the timing of the traffic signal lights taking into account the output parameters.

There are other studies focusing on reducing traffic congestion by optimizing the traffic sign distribution [3,10,16,18-21]. It is carried out in studies that try to solve the traffic congestion problem through electric and autonomous vehicles and related vehicles that come to the agenda. There is also another point of view that, with autonomous vehicles, existing solutions will be offered easier solutions [7].

Similarly, Dynamic Intersection Control System (DICS) has been used in Konya since 2013. The system produces green time according to traffic density. The applied green time duration is based on the density data from the vehicle counting cameras placed at the intersection. The DICS is based on two main objectives. One of them is to maximize the number of vehicles passing through the intersection in unit time, and the second is to minimize the average waiting time. For this purpose, the system installed at signalized intersections produces dynamic green time with intelligent traffic camera capable of determining vehicle counting and density for all directions connected to the intersection. In Fig. 1 shows the DICS.

Figure 1. *Implementation of DICS.*

Another equipment of the DICS is vehicle counting cameras. Vehicle counting cameras is produce instant traffic data such as number of vehicles, occupancy rate, tail length and density detection. The vehicle counting camera determines the density of vehicles by means of a drawing area (red line) to generate instant traffic data. Another line (green line) also determines the number of vehicles. However, the accuracy of the number of vehicles ranged from 70% to 90%. In Fig.2 shows the vehicle counting camera drawing area.

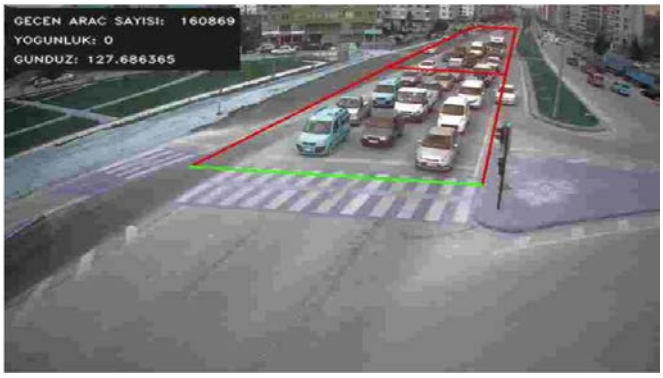

Figure 2. *Vehicle counting camera drawing area.*

Thanks to the system in 77 different intersections in Konya, 1 million liters of fuel savings and 1,700 tons of carbon emissions were reduced.

This study was carried out with the data obtained from Konya Metropolitan Municipality Transport Traffic Signalization Department. Vehicle count values at the determined intersection were estimated at a higher rate.

2. Material and methods

To optimize the green time, the vehicles were first counted manually. Used the input parameters in Table 1, the vehicle numbers were estimated using artificial neural networks. Artificial neural network (ANN) is a system derived from our

biological nervous system. The purpose of ANN is to make calculation between input and output values. There are two basic operations in ANN. One of them is the training process. The other basic process is the test. If we want the ANN to establish a connection between the input and the output, we must first pass the method through a well-defined training data set. Our training data set should include the outputs we expect from the ANN to respond. There must be data on all possible conditions in the training data set. The stronger our training data set, the stronger the output of the ANN will be. ANN consists of three layers and the neurons located in these layers, including the entrance, exit and hidden layer. A basic ANN model is shown in Fig. 3.

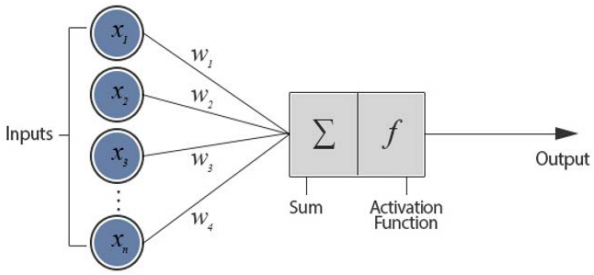

Figure 3. *Artificial neural network model [8].*

The ANN model starts the training and testing process with input values from the outside world.

Each input value collected cannot be expected to have the same effect. For this reason, weights for each input value are available. Input values collected from the outside world are pre-treated with weight ratios. Then it is produced as ANN output with collection and activation function.

2.1. Dynamic Intersection Planning

In the center of Konya, the dynamic intersection system is implemented at 77 intersections. There are vehicle counting cameras for every direction connected to the intersection. It has been consisting of a central software that collects data from all cameras. A dynamic intersection example is shown in Fig. 4.

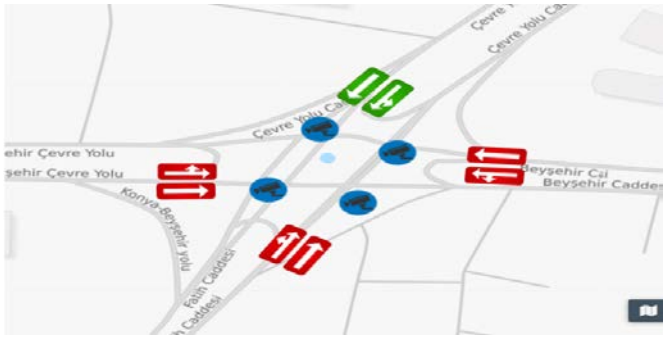

Figure 4. *Dynamic intersection*

Images from cameras are processed in real-time on embedded platforms that are special for image processing. As a result of image processing, instant traffic data such as vehicle speed, number of vehicles, ratio of occupation, queue length are produced. With produce this information, different signal planning is made for each intersection. For this study, 4 plans are employed at the selected intersection. The plans were obtained by taking expert opinions. While preparing the plans, the vehicles were counted manually. Different plans have been produced for different time intervals for each intersection according to traffic densities. An exemplary plan for 07:00 - 09:00 is presented in table 2. This plan will activate the green time duration for between minimum 15 seconds and maximum 35 seconds, depending on the traffic density in the city center direction between 07:00 and 09:00. Even if there is no vehicle flow in the city center direction, the green time will be on for 15 seconds. Likewise, even if the vehicle density continues for a long duration, it cannot go beyond the maximum time. The green time has been applied in the sequence indicated in the signal plan. The system is applying between minimum and maximum green time according to traffic density.

Table 1. *Traffic Signal Timing Plan*

Time	07:00 – 09:00	
Direction	***Min (sec.)***	***Max (sec)***
to city center	15	35
to aziz street	15	22
to uniesity	20	50
to hospital	25	65

2.1. Data Set

The data used in the ANN model was obtained by Konya Metropolitan Municipality Transport Traffic Signalization Department. There are also data from the average vehicle speed determination sensor located throughout Konya. In the ANN model, Beyşehir Intersection Medical School direction was studied. Beyşehir intersection, the green time duration applied to the specified direction, the number of vehicles passing and the average speed data for the specified route were obtained. The data set description used in the ANN model is shown in Table 1. ANN training and tests were carried out with 603 data sets. 442 data for ANN training and 161 data for the test were used.

Table 2. *Data set ranges and their statistics*

Parameters	Data Description		
Input	***Ranges***	***Std. Dev.***	***Unit***
Green Time Duration	15-65	28±11.18	sec
Number of plans	1-4		pcs
Vehicle speed	19-45	34±6.16	km/h
Output			
Number of vehicle	1-67	20±11.94	pcs

The normalization equation applied to the ANN input values is shown in Formula 2.

$$x' = 0.8 + \frac{x_i - x_{\min}}{x_{\max} - x_{\min}} + 0.1$$

In the formula; x' refers to the normalized value, x_i input value, the smallest number in the x_{min} input set, the largest number in the x_{max} input set.

For estimation, the MATLAB program was used in the Neural Network Tool. The properties of the artificial neural network are as follows:

- Input values; Green time, applied signal plan, average of vehicle speed
- Output values: vehicle count
- Network type: feed forward backpropagation
- Traning function: Trainlm
- Learning function: Learngdm
- Performance function: MSE(Mean Square Error)
- Hidden layer count: 4
- Input layer transfer function: Tansig
- Output layer transfer function: Tansig
- Number of epocs: 500

The performance and accuracy of the generated network were evaluated by using [6,12,17] Mean Squared Error (MSE), Root Mean Square Error (RMSE) and correlation coefficient (R2) used in many studies.

3. Results

The ANN model, which is trained and tested with the MATLAB NNtool, is shown in Fig. 5.

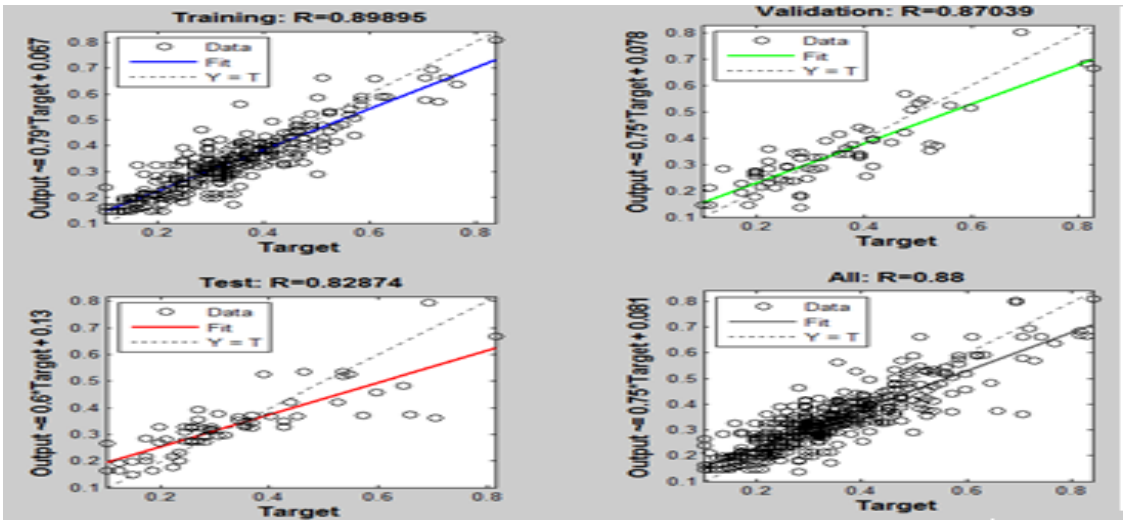

Figure 5. *ANN learning result*

ANN test results and performance evaluation criteria developed for use in DICS are given in Table 3.

Table 3. *ANN performance and test result*

correlation coefficient (r)	0.889
coefficient of determination (r^2)	0.791
mean squared error (MSE)	0.007
root mean square error (RMSE)	0.084

A graphical representation of the output values estimated and real data by ANN is shown in Fig. 6. It has been shown that the number of vehicles can be determined by 79% accuracy rate with the developed architecture. It is possible to get more successful accuracy rates by trying different architectures.

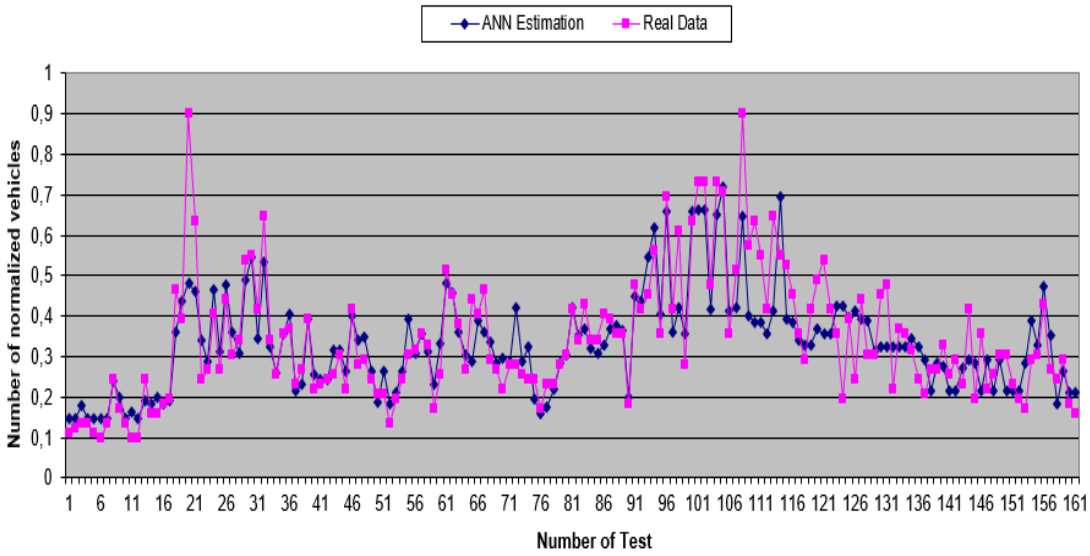

Figure 6. *Artificial Neural Network Model Comparison with Real Data*

According to current dynamic intersection system expert opinion, the signal works according to density and counting results determined by vehicle counting cameras at plan time and green time interval. Green time duration is determined by the density of the vehicle. The vehicle count results are used effectively in traffic planning studies. While the success of the vehicle counting camera at this intersection was around 70%, vehicle count accuracy was increased to 79% with artificial neural networks. Increasing vehicle count accuracy will have a direct impact on the decisions to be made in traffic planning studies. The estimation of the vehicle count in this study produces 9% more successful results.

In the dynamic intersection control system, a study was carried out for vehicle counting which is decisive in deciding green time duration. The data were trained and tested. Developed ANN model; The MSE performance function value was 0.007083 and the maximum correlation coefficient was R: 0.89895. Estimation results showed 9% better performance than vehicle counting camera. It has been demonstrated that with the implementation of vehicle estimation with ANN, more economic system can be realized with less personnel. This state will reduce serious fuel savings and the spread of harmful gas emissions.

4. Discussion

Dynamic Intersection Control System can be developed so that a separate signal plan for each week of the year and every day of the week is recommended. Another optimization study is to determine the minimum, average and maximum green times for each direction in the intersection. Determination of the green time duration interval with artificial intelligence algorithms will be an original application. Thus, more economical planning can be done with less personnel in less time, without the counting of manual vehicles. Traffic accidents, meteorological adversities, sports activities and fairs are created traffic density. Thanks to the new systems to be proposed in this style, the problem of preparing separate signal plan will have eliminated.

Acknowledgment

Ali Tahir and Abdullah Erdal thank the Konya Metropolitan Municipality Transport Traffic Signalization Department, which share the data of the Beyşehir intersection which operates with the DICS via the Traffic Control Center (TCC) software tool.

References

[1]. Altun İ., Dündar S., Yöntem K. “Yapay Sinir Ağlari İle Trafik Akim Kontrolü”. Deprem Sempozyumu, Kocaeli, (2005), 1335-1344.

[2]. Babu K.R.M., IOT for ITS: An IOT Based Dynamic Traffic Signal Control. (Ed.),^(Eds.). 2018 International Conference on Inventive Research in Computing Applications (ICIRCA), (2018).

[3]. Day C.M., Li H., Richardson L.M., Howard J., Platte T., Sturdevant J.R., Bullock D.M. “Detector-free optimization of traffic signal offsets with connected vehicle data”. Transportation Research Record, 2620(1), (2017), 54-68.

[4]. Dogan E., Payidar Akgungor A., Arslan T. Estimation of delay and vehicle stops at signalized intersections

using artificial neural network. Engineering Review: Međunarodni časopis namijenjen publiciranju originalnih istraživanja s aspekta analize konstrukcija, materijala i novih tehnologija u području strojarstva, brodogradnje, temeljnih tehničkih znanosti, elektrotehnike, računarstva i građevinarstva, 36(2), (2016). 157-165.

[5]. Dougherty M. "A review of neural networks applied to transport". Transportation Research Part C: Emerging Technologies, 3(4), (1995), 247-260.

[6]. Ergün S., Aydoğan T. "Kavşak Sinyalizasyon Sisteminin JACK Etmen Geliştirme Platformunun Kullanılarak Oluşturulması". Bilişim Teknolojileri Dergisi, 6(1), (2013), 816.

[7]. Guler S.I., Menendez M., Meier L. "Using connected vehicle technology to improve the efficiency of intersections". Transportation Research Part C: Emerging Technologies, 46, (2014), 121-131.

[8]. Jacobson L. Introduction to Artificial Neural Networks. The Project Spot, 5. (2013).

[9]. Kiyildi R.K. (2017, September). Türkiye için Yapay Sinir Ağları Yöntemi ile Trafik Kazası Tahmini Araştırması. In 5th International Symposium on Innovative Technologies in Engineering and Science 29-30 September 2017 (ISITES2017 Baku-Azerbaijan).

[10]. Li L., Wen D. "Parallel systems for traffic control: A rethinking". IEEE Transactions on Intelligent Transportation Systems, 17(4), (2015), 1179-1182.

[11]. Liu H.X., Wu X., Ma W., Hu H. "Real-time queue length estimation for congested signalized intersections". Transportation Research Part C: Emerging Technologies, 17(4), (2009), 412-427.

[12]. Murat Y.Ş., Başkan Ö. "İzole Sinyalize Kavşaklardaki Ortalama Taşit Gecikmelerinin Yapay Sinir Ağlari İle Modellenmesi". Pamukkale Üniversitesi Mühendislik Bilimleri Dergisi, 12, (2006), 214-227.

[13]. Nason N. TRAFFIC SAFETY FACTS 2005-A Compilation of Motor Vehicle Crash Data from the Fatality Analysis Reporting System and the General Estimates System, National Highway Traffic Safety Administration. National Center for Statistics and Analysis, US Department of Transportation, Washington, DC, 20590. (2005).

[14]. Rodegerdts L.A., Nevers B.L., Robinson B., Ringert J., Koonce P., Bansen J., Nguyen T., McGill J., Stewart D., Suggett J. "Signalized intersections: informational guide (Saito, M., & Fan, J. (1999). Multilayer artificial neural networks for level-of-service analysis of signalized intersections". Transportation Research Record, 1678(1), (2004), 216-224.

[15]. Talebpour A., Mahmassani H.S. "Influence of connected and autonomous vehicles on traffic flow stability and throughput". Transportation Research Part C: Emerging Technologies, 71, (2016), 143-163.

[16]. Tektaş M., Akbaş A., Topuz V. Yapay zeka tekniklerinin trafik kontrolünde kullanilmasi üzerine bir inceleme, (2002).

[17]. Timotheou S., Panayiotou C.G., Polycarpou M.M. "Distributed traffic signal control using the cell transmission model via the alternating direction method of multipliers". IEEE Transactions on Intelligent Transportation Systems, 16(2), (2014), 919-933.

[18]. Xie X.-F., Smith S.F., Lu L., Barlow G.J. Schedule-driven intersection control. Transportation Research Part C: Emerging Technologies, 24, (2012), 168-189.

[19]. Zhou Z., De Schutter B., Lin S., Xi Y. "Two-level hierarchical model-based predictive control for large-scale urban traffic networks". IEEE Transactions on Control Systems Technology, 25(2), (2016), 496-508.

[20]. Zhu F., Ukkusuri S.V. "A linear programming formulation for autonomous intersection control within a dynamic traffic assignment and connected vehicle environment". Transportation Research Part C: Emerging Technologies, 55, (2015), 363-378.

MANAS Journal of Engineering
ISSN 1694-7398 | e-ISSN 1694-7398

Volume 8 (Issue 1) (2020) Pages 55-58

Analysis of Turkish 6/49 lottery results

Alper Vahaplar[1], Murat Erşen Berberler[2,*]

[1]Dokuz Eylül University, Faculty of Science, Department of Statistics, İzmir, Türkiye, alper.vahaplar@deu.edu.tr, ORCID: 0000-0002-3566-3870

[2]Dokuz Eylül University, Faculty of Science, Department of Computer Science, İzmir, Türkiye, murat.berberler@deu.edu.tr, ORCID: 0000-0002-9227-2040

ABSTRACT

Turkish 6/49 Lottery is a chance game based on the selection of 6 of the 49 numbers by the draw machine, which has been of interest since the first day; such that statistics of this game, winning strategies, formulas etc., a number of popular books and newspaper articles have been published and some of the internet sites are now providing updated information to interested people; but a large part of these publications seem to be far from scientific point of view. In this study, all the draws in the past will be analyzed and the probability of being correctly guessed will be discussed by adhering to the theory of probability and statistical confidence tests.

ARTICLE INFO

Research article

Received: 31.03.2020
Accepted: 22.05.2020

Keywords:
6/49 lottery,
probability,
confidence tests,
randomness

*Corresponding author

1. Introduction

Turkish 6/49 Lottery or officially "Sayısal Loto 6/49" has been played since 1996, November 6th and as of the date this paper is written, the number of draws reached 1107. The winners of this lottery are evident on Saturday evenings, 49 balls with numbers from 1 to 49 printed on them, 6 of them are drawn with the help of the lottery machine in the presence of a notary. Among the 6 numbers determined as the draw result, the ones who know 6, 5, 4, or 3 correct win lottery prize. There are no restrictions on the order in which the 6 numbers can be left out of the machine, the numbers from the drawing result are announced in ascending order, and therefore the computation is expressed in terms of mathematical combination. Considering that 6 numbers out of 49 numbers can be selected as 13.983.816 different types, the probability of correctly estimating the complete of 6 numbers that give big prize is approximately 1 in 14 million. The probability of guessing exactly 5 is obtained as $\frac{\binom{6}{5}\binom{43}{1}}{\binom{49}{6}} = \frac{258}{13983816}$, except that the case of 6 numbers are all correctly estimated. In a similar way, the likelihood of knowing exactly 4 with the exception of the cases of 6 and 5 are all correctly estimated is $\frac{\binom{6}{4}\binom{43}{2}}{\binom{49}{6}} = \frac{13545}{13983816}$, the probability of knowing exactly 3 is obtained by excluding the cases of 6, 5, and 4 are all correctly estimated is $\frac{\binom{6}{3}\binom{43}{3}}{\binom{49}{6}} = \frac{246820}{13983816}$. In accordance with all this information, in the following section, the weekly draws of Turkish 6/49 Lottery will be analyzed by statistical methods and the results will be interpreted.

2. Method

The χ^2 goodness of fit test is one of the standard statistical tests used to verify whether two sets of data contain samples drawn from the same probability distribution. The chi-square statistic is a measure of how much the observed cell counts in a two-way table diverge from the expected cell counts [6]. This non-parametric test can be used even to test the hypothesis of no association between two or more groups or criteria and to test how likely the observed distribution of the data fits with the distribution expected [5]. The assumptions of χ^2 goodness of fit test are listed as:

- The data must be randomly drawn from the population,
- There must be at least 5 expected frequencies in each group of categorical variable.
- The variables under consideration must be mutually exclusive.

In order to test the equiprobability of N individual numbers (which are 1 – 49 for Turkish 6/49 Lottery), frequencies are obtained. The expected probability for each can be considered as 1/N assuming the probability distribution is uniform. The goodness of fit test calculates a test statistic using observed frequencies and expected frequencies. For *n* draws of *k/N* type lottery, the expected count for any number *i* will be $E_i = \frac{nk}{N}$ [3].

$$\chi^2 = \sum_{i=1}^{N} \frac{(\boldsymbol{O_i} - \boldsymbol{E_i})^2}{\boldsymbol{E_i}} \quad (1)$$

The null hypothesis of χ^2 is that observed values are equal to the expected values:
$H_0 : O_i = E_i$ (Observed and Expected data are the samples of the same distribution)

$H_a : O_i \neq E_i$

The test outputs χ2 value and a p-value to compare to the desired significance level (α). If p<α, then H0 is rejected and accepted otherwise.

In this study, 1107 draws of Turkish 6/49 Lottery was concerned. For 1107 draws, the frequency table of 49 numbers and p-value of χ2 test is as follows:

Table 1. *Frequencies of 49 lotto numbers over 1107 draws*

i	O_i	***i***	O_i	***i***	O_i	***i***	***Oi***	***i***	O_i
1	149	11	136	21	151	*31*	*122*	41	143
2	138	12	141	22	144	*32*	*144*	42	130
3	137	13	136	23	130	*33*	*120*	43	104
4	127	14	141	24	128	*34*	*131*	44	130
5	137	15	133	25	133	*35*	*129*	45	123
6	122	16	150	26	148	*36*	*149*	46	134
7	133	17	144	27	137	*37*	*115*	47	143
8	138	18	156	28	127	*38*	*158*	48	125
9	142	19	133	29	128	*39*	*137*	49	134
10	129	20	136	30	137	*40*	*150*		

p-value = 0,809578063, χ^2 = 39.322 and df = 48

If the level of significance (α) is accepted as 0.05, the test result can be interpreted as there is no sufficient evidence to reject the claim in the null hypothesis. In other words, from this perspective, 1107 draws of Turkish 6/49 Lottery seem to be fair.

The same analysis is applied to packages of 25, 50 and 100 consecutive draws in total of 1100 draws. The overall is again proved to be fair but for some sequences of draws seemed suspicious in terms of p-values being less than α=0.05.

Table 2. *p-values in short sequences of draws.*

Draws	**p-value**	**Draws**	**p-value**
351 - 375	0,010509424	401 - 500	0,938341051
351 - 400	0,044315743	501 - 600	0,805498036
651 - 700	0,00499506	601 - 700	0,07817169
1 - 100	0,360785414	701 - 800	0,86715685
101 - 200	0,448803486	801 - 900	0,871352253
201 - 300	0,528784303	901 - 1000	0,84498258
301 - 400	0,378982582	1001 - 1100	0,99491968

This situation can be interpreted as a result of randomness in small samples. As sample sizes are enlarged, p-values are determined to increase.

The total number of possible combinations of k numbers chosen from a set of N numbers is given by the combinatorial coefficient

$$\binom{N}{k} = \frac{N!}{k!\,(N-k)!} \quad (2)$$

where N = 49 and k = 6 for Turkish 6/49 Lottery. The players get a reward in cases of truly guessing 3, 4, 5 or all of the 6 numbers drawn. The asymptotic distribution of χ^2 statistics is neither uniform nor chi-square because the numbers are drawn *without replacement*. When one of 49 numbers is selected, there is no chance for the same number to be selected again in the same draw [3],[7].

Let X be the random variable defined as number of matches out of k randomly drawn numbers among N numbers with equiprobability. In this case, the distribution of X is said to be hypergeometric. The probability of matching *i* numbers of *k* numbers drawn in N numbers is [1],[4].

$$P[X = i] = \frac{\binom{k}{i}\binom{N-k}{k-i}}{\binom{N}{k}} \quad (3)$$

Let Y be the random variable denoting the sorted outcome vector of a draw .Y = [$Y_{(1)}$, $Y_{(2)}$, …$Y_{(k)}$] where $Y_{(i)}$ is the random variable corresponding to the i^{th} element in the sorted outcome. Recall that $Y_{(1)} < Y_{(2)} < \ldots < Y_{(k)}$.Under these assumptions, the probability of i^{th} number in the sorted outcome vector having the value of *r* is derived from Equation (3) as:

$$P\left[Y_{(i)} = r\right] = \frac{\binom{r-1}{i-1}\binom{N-r}{k-i}}{\binom{N}{k}} \quad (4)$$

It is clear that if $Y_{(i)} = r$, then only $i - 1$ numbers fall between 1 and $r - 1$, and $k - i$ numbers fall between $r + 1$ and N. Using Eq. (4) to determine the expected value of Y(i) in terms of E[x]=∑x.p(x) [1]:

$$E[Y_{(i)}] = \frac{\sum_{r=i}^{N-k+i} r\binom{r-1}{i-1}\binom{N-r}{k-i}}{\binom{N}{k}} = \frac{(N+1)i}{(k+1)} \qquad (5)$$

So the expected values of Turkish 6/49 lottery are determined as

μ = [50/7, 100/7, 150/7, 200/7, 250/7, 300/7]

μ = [7.142857143, 14.28571429, 21.42857143, 28.57142857, 35.71428571, 42.85714286]

which are very close to the average value of 1107 draws

Y = [7.044263776, 14.08852755, 21.15898826, 28.35772358, 35.4263776, 42.64046974]

A t-test is applied to the expected values and the previous results using H_0 = the difference in means is equal to 0. The results are as follows:

t = 0.027775, df = 9.9999, p-value = 0.9784
alternative hypothesis: true difference in means is not e
qual to 0
95 percent confidence interval: -16.94890 17.37678
sample estimates:
mean of x mean of y
25.00000 24.78606

Commenting on p-value result of the test (0.9874), Turkish 6/49 lottery is said to be fair in perspective of hypergeometric distributed random variables.

Another study on fairness or equiprobability on lottery games results belongs to Drakakis et. al. [2]. This study focuses on the minimal distance of consecutive result of a draw. Let $Y_{(1)}$, $Y_{(2)}$, …$Y_{(k)}$ be numbers within range 1…N. The minimal distance d is defined as

$$d = \min_{1 \le i \le j \le k} |Y_{(j)} - Y_{(i)}| \qquad (6)$$

As an example, if the sorted outcome vector Y has numbers (4, 17, 19, 23, 30, 44) drawn, then d = 19 – 17 = 2 for this individual sample. Assuming the numbers are randomly chosen and the outcome vector Y is uniformly distributed within the sample space of $\binom{N}{k}$ k-tuples, the probability distribution of random variable d is

$$P(d \le r) = 1 - \frac{\binom{N-(r-1)(k-1)}{k}}{\binom{N}{k}} \qquad (7)$$

At this stage, the minimal distance frequencies of previous 1107 draws are computed and compared with the expected values using χ^2 goodness of fit test.

Table 3. *Observed and expected values of distances and their probabilities*

d	Observed	Expected	P(d<r)
1	548	548,1847	0,000000
2	295	300,5365	0,495198
3	148	151,8123	0,271487
4	72	68,86258	0,137139
5	36	26,94897	0,062207
6	7	8,507166	0,024344
7	1	1,910123	0,007685
8	0	0,231077	0,001726

The p-value of χ^2 goodness of fit test is calculated as 0.6658057 which gives no doubt about the randomness / fairness or equiprobability of Turkish 6/49 Lottery for the previous 1107 draws.

3. Summary and conclusion

Based on the literature Turkish 6/49 Lottery Game results are investigated in terms of fairness and randomness using different methods. The previous data of 1107 games of lottery has been analyzed and inspected to be fair. In the first part of the study basic χ^2 goodness of fit test is introduced and the application on Turkish data set is presented. For the overall analysis of the lottery results gave no evidence on being unfairness as of test result. But in particular investigation of consecutive weeks, small p-values like 0.00499 which constitutes strong statistical evidence to conclude that the observed data are statistically different from the expected values. As a further research, those specific results in the determined weeks can be analyzed in different tests or methods.

As an alternative research of randomness, the sorted outcomes of the results for each week are considered to be a random variable in hypergeometric distribution. The expected values and the observed results are tested. According to the results, H_0 is failed to reject, meaning no conclusions can be made on "observed values are statistically different from the expected values".

Lastly, the minimum distance metric in the 6-tuples of outcomes were used for testing the empirical and observed values. Applying χ^2 goodness of fit test again resulted as there is no evidence for rejecting the null hypothesis that both data samples are drawn from the same distribution.

The statistical computations and hypothesis tests are performed in R Version 3.4.3 using R-Studio Version 1.1.419. (https://www.R-project.org/)

4. Further research

Using the historical data of Turkish 6/49 lottery, some predictions can be made for the future Sample size of 1107 may be insufficient to conclude on some hypothesis. So the test explained above can be repeated for large samples or on other similar game results.

As the sample size increases, some prediction algorithms can be studied to guess the numbers in 6-tuples.

References

[1] Coronel-Brizio H.F., Hernández-Montoya A.R., Rapallo F., Scalas E., "Statistical auditing and randomness test of lotto k/N-type games", Physica A: Statistical Mechanics and its Applications, 387(25), (2008), 6385-6390.

[2] Drakakis K., "A note on the appearance of consecutive numbers amongst the set of winning numbers in Lottery", Facta Universitatis: Mathematics and Informatics, 22(1), (2007), 1–10.

[3] Genest C., Lockhart R.A. and Stephens, M.A., "Chi-square and the lottery", Journal of the Royal Statistical Society, Series D, 51, (2002), 243—257.

[4] Neufeld E., Goodwin S., "The 6-49 lottery paradox", Computational Intelligence, 14(3), (1998), 273-286.

[5] Rana R, Singhal R., "Chi-square test and its application in hypothesis testing", Journal of the Practice of Cardiovascular Sciences, 1, (2015), 69-71.

[6] Moore, David S., George P. McCabe, and Bruce A. Craig. "Introduction to the Practice of Statistics", New York: W.H. Freeman, (2009).

[7] Harry Joe, "Tests of uniformity for sets of lotto numbers", Statistics & Probability Letters, 16(3), (1993), 181-188.

MANAS Journal of Engineering
ISSN 1694-7398 | e-ISSN 1694-7398

Volume 8 (Issue 1) (2020) Pages 59-67

A new approach on the stability of fractional singular systems with time-varying delay

Yener Altun

Yuzuncu Yil University, Ercis Management Faculty, Department of Business Administration, Van, Turkey, yeneraltun@yyu.edu.tr, ORCID: 0000-0003-1073-5513

ABSTRACT

In this research article, we discussed the asymptotic stability of fractional singular systems with Riemann–Liouville (RL) derivative and constructed some sufficient conditions. The proposed stability criteria are based upon the linear matrix inequalities (LMIs) approach, which can be easily checked using meaningful Lyapunov-Krasovskii functionals. Finally, we presented two simple numerical examples with their simulations to demonstrate the effectiveness and benefits of the proposed method. The theoretical results obtained in this research contribute to existing ones in the literature.

ARTICLE INFO

Research article

Received: 31.03.2020
Accepted: 22.05.2020

Keywords:
Fractional singular system,
RL derivate,
LMI,
Lyapunov-Krasovskii functional,
asymptotic stability

1. Introduction

Singular systems, which are also referred implicit or descriptor systems are dynamic systems. The study of stability problem for dynamic systems with time delay or without has theoretical and practical significance. There are many books and articles made in this sense, for example: [1-27]. In this direction, there are many studies on the qualitative features of solutions of singular and non-singular systems with and without delay [26]. However, there are very few studies on the qualitative behaviors of fractional-order singular systems. During last years, studies on the stability analysis of fractional dynamic systems, including stability, chaos and bifurcation, have become a hot topic of investigation. Although fractional analysis has a long history, interest in common science and engineering practices is growing commonly [13,18]. The singular systems with time delays have already been applied in many areas such as electrical circuits, memorization, moving robots, locomotion, economic systems and many other systems, see References [6, 8–10]. Therefore, the stability problem for differential and RL fractional differential singular systems has attracted researchers.

Investigating the stability of fractional-order singular systems is more complex than the integer-order singular systems. Therefore, it is necessary and interesting to examine the stability of fractional-order singular systems playing important role in both theory and applications. When the related literature is searched in particular, various approaches towards the stability of fractional-order singular systems have attracted attention in recently [5, 15, 17, 20]. In this direction, the Lyapunov-Krasovskii functional method presents a very powerful approach for analyzing the qualitative properties of the fractional-order singular systems. However, the fractional derivative of the Lyapunov functionals is computationally quite difficult. That is the main reason why there are very few works for stability of delayed fractional-order singular systems.

On the basis of the above discusses, this research article deals with the asymptotically stability of fractional singular systems with RL fractional derivate. When compared to integer-order singular systems with delay, it is seen that the works related to the stability of delayed fractional-order singular systems are still in the process of benefiting. The goal of this research, difficulty and its contribution can be summarized as follows:

(i) According to nonsingular ones, it is not easy to meet the existence of solutions in the stability analysis of singular systems since the initial conditions may not be consistent. Also, it is not easy to calculate the fractional-order derivatives of Lyapunov functionals constructed for these systems. To overcome this challenge, we derived a meaningful Lyapunov functional including the terms fractional derivative and integral. The method employed in this article is advantageous in that integer-order derivatives of the Lyapunov functionals can directly calculate.

(ii) The basic goal of this research article is to search the asymptotically stability of fractional singular systems with RL derivate. As proof technique, this article includes the LMIs, Lyapunov functional method and some fundamental inequalities.

(iii) We consider that the theoretical results achieved in this research will contribute to the related literature and studies on the qualitative properties of fractional-order singular systems.

Notations: $\Re^n$ states the $n-$dimensional Euclidean space; $\|.\|$ states the Euclidean norm for vectors; X^T states the transpose of the matrix X; Y is negative-definite (or positive-definite) if $\langle Yx, x\rangle < 0$ or $\langle Yx, x\rangle > 0$) for all $x \neq 0$; $\|Z\| = \sqrt{\lambda_{\max}(Z^T Z)}$ states the spectral norm of matrix Z; $\lambda_{\max}(P)$ states the maximum of eigenvalues of the matrix P

2. Preliminaries

In the current this research motivated by above discussions, we consider the following fractional-order singular system with time-varying delay

$$E\,{}^{RL}_{t_0}D_t^q x(t) = Ax(t) + Bx(t-\tau(t)) + C\int_{t-\tau(t)}^{t} x(s)ds, \tag{1}$$

with the given initial condition

$${}^{RL}_{t_0}D_t^{q-1} x(t) = \vartheta(t), \quad t \in [-\tau, 0], \tag{2}$$

where $x(t) \in \Re^n$ is state vector; ${}^{RL}_{t_0}D_t^q x(.)$ states a q order RL derivative of $x(.)$ with $q \in (0,1)$; $A,\ B,\ C \in \Re^{n\times n}$ are known constant matrices with suitable dimensions; the matrix $E \in \Re^{n\times n}$ may be singular, that is rank $E = r \leq n$, differentiable function $\tau(t)$ is a variable delay for all $t \geq 0$,

$$0 \leq \tau(t) \leq \tau \quad \text{and} \quad \dot{\tau}(t) \leq \delta < 1. \tag{3}$$

Before giving our main result, the following property, fundamental definitions and lemmas are presented.

Definition 1. ([5]) The RL fractional integral and RL fractional derivative are defined as, respectively

$${}_{t_0}D_t^{-q} x(t) = \frac{1}{\Gamma(q)}\int_{t_0}^{t}(t-s)^{q-1}x(s)ds, \qquad (q>0),$$

$${}_{t_0}D_t^{q} x(t) = \frac{1}{\Gamma(n-q)}\frac{d^n}{dt^n}\int_{t_0}^{t}\frac{x(s)}{(t-s)^{q+1-n}}ds, \qquad (n-1 \leq q < n),$$

where Γ is a Gamma function.

Property 1. ([5]) For $x(t) \in \Re^n$, if $p > q > 0$, then the following relation holds

$$ {}_{t_0}^{RL}D_t^q\left({}_{t_0}D_t^{-p}x(t)\right)={}_{t_0}^{RL}D_t^{q-p}x(t). $$

Definition 2. ([18])

(i) System (1) or the pair (E,A) is said to be regular if $\det(s^qE-A)$ is not identically zero.

(ii) The pair (E,A) is said to be impulse free if $\deg(\det(s^qE-A))=rank(E)$.

Lemma 1. ([18]) For a vector of differentiable function $x(t)\in\Re^n$ and constant matrix $W=W^T(\geq 0)\in\Re^{n\times n}$, then

$$ \frac{1}{2}{}_{t_0}^{RL}D_t^q\left\{x^T(t)Wx(t)\right\}\leq x^T(t)W{}_{t_0}^{RL}D_t^q\left\{x(t)\right\},\qquad q\in(0,1), $$

for all $t\geq 0$.

Lemma 2. ([1]) For any symmetric positive definite matrix $\Sigma\in D^{n\times n}$, scalar $\lambda>0$ and vector function $\tilde{g}:[0,\lambda]\to\Re^n$, such that the integrations given in the following are well defined, then

$$ \lambda\int_0^{\lambda}\tilde{g}^T(s)\Sigma\tilde{g}(s)ds\geq\left[\int_0^{\lambda}\tilde{g}(s)ds\right]^T\Sigma\left[\int_0^{\lambda}\tilde{g}(s)ds\right]. $$

3. Stability

In this section, we provide a few novel sufficient conditions for the stability of delayed fractional singular systems by constructing meaningful Lyapunov functional including fractional integral and derivative terms.

Theorem 1. If there exist a matrix P and matrices $Q=Q^T>0,\ R=R^T>0,\ S=S^T>0$ and $U=U^T>0$ such that $E^TP=P^TE\geq 0$ and

$$ \Xi=\begin{bmatrix}\Xi_{11} & \Xi_{12} & \Xi_{13}\\ \Xi_{12}^T & \Xi_{22} & \Xi_{23}\\ \Xi_{13}^T & \Xi_{23}^T & \Xi_{33}\end{bmatrix}<0, \tag{4} $$

where

$$ \begin{aligned}
\Xi_{11}&=P^TA+A^TP+Q+\tau^2S+A^T\left(E^TRE+\tau^2E^TUE\right)A,\\
\Xi_{12}&=P^TB+A^T\left(E^TRE+\tau^2E^TUE\right)B,\\
\Xi_{13}&=P^TC+A^T\left(E^TRE+\tau^2E^TUE\right)C,\\
\Xi_{22}&=B^T\left(E^TRE+\tau^2E^TUE\right)B-(1-\delta)Q,\\
\Xi_{23}&=B^T\left(E^TRE+\tau^2E^TUE\right)C,\\
\Xi_{33}&=-S+C^T\left(E^TRE+\tau^2E^TUE\right)C.
\end{aligned} $$

Then the trivial solution of fractional singular system (1) with (2) is asymptotically stable.

Proof. For this theorem, we define the following Lyapunov-Krasovskii functional including the fractional derivative and integral terms

$$V(t) = \sum_{j=1}^{3} V_j(t), \tag{5}$$

$$V_1(t) = {}_{t_0}^{RL}D_t^{q-1}\left(x^T(t)P^T Ex(t)\right),$$

$$V_2(t) = \int_{t-\tau(t)}^{t} x^T(s)Qx(s)ds + \int_{-\tau(t)}^{0} ({}_{t_0}^{RL}D_t^q x(t+s))^T E^T RE({}_{t_0}^{RL}D_t^q x(t+s))ds,$$

$$V_3(t) = \tau\int_{-\tau}^{0}\int_{t+\beta}^{t} x^T(s)Sx(s)dsd\beta + \tau\int_{-\tau}^{0}\int_{t+\beta}^{t} ({}_{t_0}^{RL}D_s^q x(s))^T E^T UE({}_{t_0}^{RL}D_s^q x(s))dsd\beta.$$

From Definition 1, we know that $V_1(t), V_2(t)$ and $V_3(t)$ are positive definite functionals. By Property 1 and Lemma 1, computing the differential of $V(t)$ along the solutions of fractional singular system in (1)

$$\dot{V}(t) = \sum_{j=1}^{3} \dot{V}_j(t)$$

for

$$\begin{aligned}
\dot{V}_1(t) &= {}_{t_0}^{RL}D_t^q(x^T(t)P^T Ex(t)) \le 2x^T(t)P^T E\,{}_{t_0}D_t^q(x(t)) \\
&= 2x^T(t)P^T[Ax(t) + Bx(t-\tau(t)) + C\int_{t-\tau(t)}^{t} x(s)ds] \\
&= x^T(t)(P^TA + A^TP)x(t) + 2x^T(t)P^TBx(t-\tau(t)) \\
&\quad + 2x^T(t)P^TC\int_{t-\tau(t)}^{t} x(s)ds.
\end{aligned} \tag{6}$$

By (3), computing the differential of $V_2(t)$, we obtained

$$\begin{aligned}
\dot{V}_2(t) &= x^T(t)Qx(t) - (1-\dot{\tau}(t))x^T(t-\tau(t))Qx(t-\tau(t)) \\
&\quad +({}_{t_0}^{RL}D_t^q x(t))^T E^T RE({}_{t_0}^{RL}D_t^q x(t)) \\
&\quad -(1-\dot{\tau}(t))({}_{t_0}^{RL}D_t^q x(t-\tau(t)))^T E^T RE({}_{t_0}^{RL}D_t^q x(t-\tau(t))) \\
&\le x^T(t)Qx(t) - (1-\delta)x^T(t-\tau(t))Qx(t-\tau(t)) \\
&\quad +({}_{t_0}^{RL}D_t^q x(t))^T E^T RE({}_{t_0}^{RL}D_t^q x(t)) \\
&\quad -(1-\delta)({}_{t_0}^{RL}D_t^q x(t-\tau(t)))^T E^T RE({}_{t_0}^{RL}D_t^q x(t-\tau(t))) \\
&\le x^T(t)Qx(t) - (1-\delta)x^T(t-\tau(t))Qx(t-\tau(t)) \\
&\quad +({}_{t_0}^{RL}D_t^q x(t))^T E^T RE({}_{t_0}^{RL}D_t^q x(t)).
\end{aligned} \tag{7}$$

By Lemma 2, computing the differential of $V_3(t)$, we have

$$\begin{aligned}\dot{V}_3(t) &= \tau^2 x^T(t)Sx(t) - \tau\int_{t-\tau}^{t} x^T(s)Sx(s)ds \\ &\quad + \tau^2({}^{RL}_{t_0}D_t^q x(t))^T E^T UE({}^{RL}_{t_0}D_t^q x(t)) \\ &\quad - \tau\int_{t-\tau}^{t}({}^{RL}_{t_0}D_s^q x(s))^T E^T UE({}^{RL}_{t_0}D_s^q x(s))ds \\ &\le \tau^2 x^T(t)Sx(t) - \tau\int_{t-\tau}^{t} x^T(s)Sx(s)ds \\ &\quad + \tau^2({}^{RL}_{t_0}D_t^q x(t))^T E^T UE({}^{RL}_{t_0}D_t^q x(t)).\end{aligned} \tag{8}$$

For any $s \in [t-\tau, t]$,

$$-\tau\int_{t-\tau}^{t} x^T(s)Sx(s)ds \le -\tau\int_{t-\tau(t)}^{t} x^T(s)Sx(s)ds \le -\left(\int_{t-\tau(t)}^{t} x(s)ds\right)^T S\left(\int_{t-\tau(t)}^{t} x(s)ds\right). \tag{9}$$

According to (7) and (8), we have

$$\begin{aligned}&({}^{RL}_{t_0}D_t^q x(t))^T E^T RE({}^{RL}_{t_0}D_t^q x(t)) + \tau^2({}^{RL}_{t_0}D_t^q x(t))^T E^T UE({}^{RL}_{t_0}D_t^q x(t)) \\ &= [Ax(t) + Bx(t-\tau(t)) + C\int_{t-\tau(t)}^{t} x(s)ds]^T \left(E^T RE + \tau^2 E^T UE\right) \\ &\quad \times [Ax(t) + Bx(t-\tau(t)) + C\int_{t-\tau(t)}^{t} x(s)ds] \\ &= x^T(t)A^T\left(E^T RE + \tau^2 E^T UE\right)Ax(t) \\ &\quad + x^T(t)A^T\left(E^T RE + \tau^2 E^T UE\right)Bx(t-\tau(t)) \\ &\quad + x^T(t)A^T\left(E^T RE + \tau^2 E^T UE\right)C\int_{t-\tau(t)}^{t} x(s)ds \\ &\quad + x^T(t-\tau(t))B^T\left(E^T RE + \tau^2 E^T UE\right)Ax(t) \\ &\quad + x^T(t-\tau(t))B^T\left(E^T RE + \tau^2 E^T UE\right)Bx(t-\tau(t)) \\ &\quad + x^T(t-\tau(t))B^T\left(E^T RE + \tau^2 E^T UE\right)C\int_{t-\tau(t)}^{t} x(s)ds \\ &\quad + (\int_{t-\tau(t)}^{t} x(s)ds)^T C^T\left(E^T RE + \tau^2 E^T UE\right)Ax(t) \\ &\quad + (\int_{t-\tau(t)}^{t} x(s)ds)^T C^T\left(E^T RE + \tau^2 E^T UE\right)Bx(t-\tau(t)) \\ &\quad + (\int_{t-\tau(t)}^{t} x(s)ds)^T C^T\left(E^T RE + \tau^2 E^T UE\right)C\int_{t-\tau(t)}^{t} x(s)ds.\end{aligned} \tag{10}$$

From (6)-(10), we can conclude that

$$\dot{V}(t) \le \mu^T(t)\Xi\mu(t),$$

where $\mu^T = \left[x^T(t) \quad x^T(t-\tau(t)) \quad \left(\int_{t-\tau(t)}^{t} x(s)ds\right)^T \right]$ and Ξ is defined (4). If $\Xi < 0, \dot{V}(t)$ is negative definite for $\mu(t) \neq 0.$ Therefore, the fractional singular system defined in (1) is asymptotically stable.

4. Illustrative examples with numeric simulations

To show the usefulness of the employed method, we present the following examples with simulation results.

Example 1 For $n = 2,$ as a special state of (1), we take into account the following singular system with a constant delay and RL derivate

$$E\,{}_{t_0}^{RL}D_t^q x(t) = Ax(t) + Bx(t-\tau(t)) + C\int_{t-\tau}^{t} x(s)ds, \qquad t \ge 0, \tag{11}$$

where $0 < q \le 1,\ \tau = 0.4,$

$$E = \begin{bmatrix} 1 & 0 \\ 0 & 0 \end{bmatrix}, A = \begin{bmatrix} -6.2 & 1.6 \\ 1.6 & -7.6 \end{bmatrix},\ B = \begin{bmatrix} 0.6 & -1.2 \\ -1.1 & 1.3 \end{bmatrix},\ C = \begin{bmatrix} 0.8 & 0.2 \\ 0.3 & 0.4 \end{bmatrix}.$$

Let us choose

$$P = \begin{bmatrix} 3.6 & 0 \\ 0 & 2.8 \end{bmatrix},\ Q = \begin{bmatrix} 1.8 & 0.12 \\ 0.12 & 1.5 \end{bmatrix}, R = \begin{bmatrix} 0.16 & 0 \\ 0 & 0.16 \end{bmatrix},$$

$$S = \begin{bmatrix} 12 & 0.1 \\ 0.1 & 8 \end{bmatrix} \text{ and } U = \begin{bmatrix} 0.4 & 0.1 \\ 0.1 & 0.4 \end{bmatrix}.$$

By MATLAB-Simulink, under the above assumptions, we can easily obtain that all the eigenvalues in LMI defined in (4) are $\lambda_{\max}(\Xi) \le -0.4621$. Thus, according to Theorem 1, this shows that the origin of system (11) is asymptotically stable.

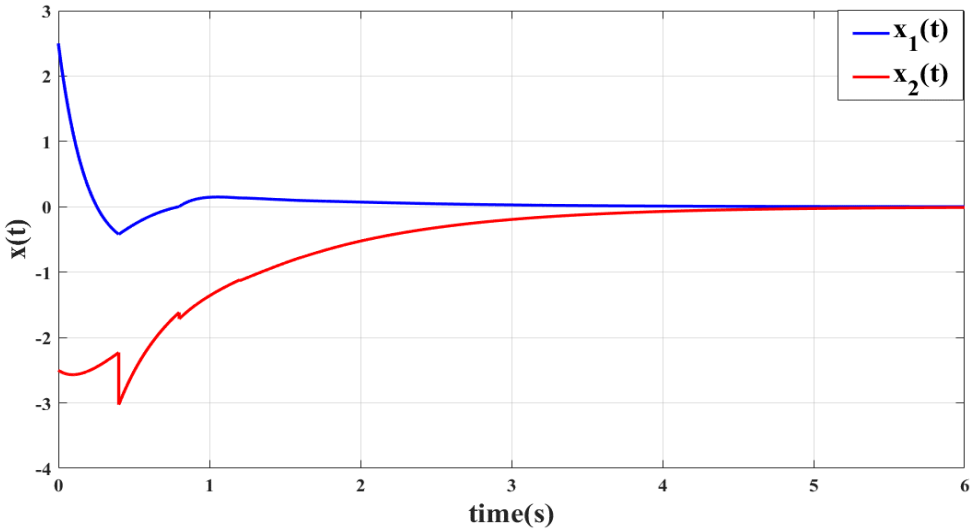

Figure 1. *The simulation of* $x(t)$ *in Example 1 for* $\tau = 0.4$.

Example 2 For $n = 2,$ as a special state of (1), we take into account the following singular system with time-varying delay and RL derivate

$$E\,{}_{t_0}^{RL}D_t^q x(t) = Ax(t) + Bx(t-\tau(t)) + C\int_{t-\tau(t)}^{t} x(s)ds, \qquad t \geq 0, \tag{12}$$

where $0 < q \leq 1,\ \tau(t) = 0.1 + 0.2\sin^2 t \leq 0.3 = \tau$,

$$E = \begin{bmatrix} 2 & 0 \\ 0 & 0 \end{bmatrix},\ A = \begin{bmatrix} -8.2 & 2.8 \\ 2.8 & -7.6 \end{bmatrix},\ B = \begin{bmatrix} 0.9 & -1.2 \\ -1.3 & 1.2 \end{bmatrix},\ C = \begin{bmatrix} 0.7 & 0.1 \\ 0.2 & 0.6 \end{bmatrix}.$$

Since $\dot{\tau}(t) = 0.2\sin 2t \leq \delta < 1,$ it can be selected $\delta = 0.2$. Let us choose

$$P = \begin{bmatrix} 4 & 0 \\ 0 & 3 \end{bmatrix},\ Q = \begin{bmatrix} 1.8 & 0.14 \\ 0.14 & 1.6 \end{bmatrix},\ R = \begin{bmatrix} 0.08 & 0 \\ 0 & 0.08 \end{bmatrix},$$

$$S = \begin{bmatrix} 16 & 0.1 \\ 0.1 & 10 \end{bmatrix} \text{ and } U = \begin{bmatrix} 0.2 & 0.1 \\ 0.1 & 0.2 \end{bmatrix}.$$

By MATLAB-Simulink, under the above assumptions, we can easily obtain that all the eigenvalues in LMI defined in (4) are $\lambda_{\max}(\Xi) \leq -0.0197$. Thus, according to Theorem 1, this shows that the origin of system (12) is asymptotically stable.

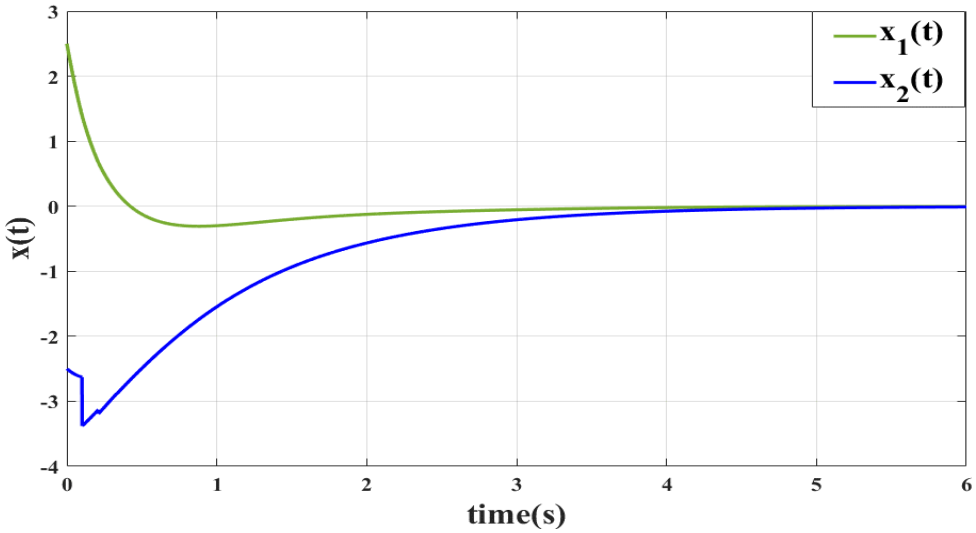

Figure 2. *The simulation of* $x(t)$ *in Example 2 for* $\tau(t) = 0.1 + 0.2\sin^2 t$.

When the theoretical results of the above *Example 1* and *Example 2* are examined, it is seen that the origin of addressed system in the examples is asymptotically stable under different initial conditions. Moreover, the theoretical results of this research article are supported by the simulations in Figure 1 and Figure2.

5. Discussion and conclusion

In this study, we have derived some new sufficient conditions concerning the asymptotically stability of singular systems with time-varying delay and RL derivate. Stability criteria have been derived by constructing meaningful a Lyapunov-Krasovskii functional and expressing in terms of LMI. Using MATLAB-Simulink, two examples with numerical simulation are given to illustrate the usefulness of the stability criteria of the addressed singular system. Consequently, the results obtained in this article provide contribution to the improvement and generalization of the classical integer-order delayed singular systems.

References

[1]. Altun Y., "Further results on the asymptotic stability of Riemann–Liouville fractional neutral systems with variable delays", Adv. Difference Equ., 437, (2019), 1-13.

[2]. Altun, Y. "Improved results on the stability analysis of linear neutral systems with delay decay approach", Math Meth Appl Sci., 43, (2020), 1467–1483.

[3]. Altun Y., "New Results on the Exponential Stability of Class Neural Networks with Time-Varying Lags", BEU Journal of Science, 8, (2019), 443-450.

[4]. Altun Y., Tunç C., "New Results on the Exponential Stability of Solutions of Periodic Nonlinear Neutral Differential Systems", Dynamic Systems and Applications, 28, (2019), 303-316.

[5]. Chartbupapan C., Bagdasar O., Mukdasai K., "A Novel Delay-Dependent Asymptotic Stability Conditions for Differential and Riemann-Liouville Fractional Differential Neutral Systems with Constant Delays and Nonlinear Perturbation", Mathematics, 8, (2020), 1-10.

[6]. Ding Y., Zhong S., Chen W., "A delay-range-dependent uniformly asymptotic stability criterion for a class of nonlinear singular systems", Nonlinear Anal. Real World Appl., 12, (2011), 1152–1162.

[7]. Duarte-Mermoud M.A., Aguila-Camacho N., Gallegos J.A., Castro-Linares R., "Using general quadratic Lyapunov functions to prove Lyapunov uniform stability for fractional order systems" Commun. Nonlinear Sci. Numer. Simul., 22, (2015), 650–659.

[8]. Feng Y., Zhu X., Zhang Q., "Delay-dependent stability criteria for singular time-delay systems", Acta Automat. Sin., 36, (2010), 433–437.

[9]. Feng Z., Lam J., Gao H., "α-dissipativity analysis of singular time-delay systems" Automatica, 47, (2011), 2548–2552.

[10]. Fridman E., Shaked U., "$H\infty$ control of linear state-delay descriptor systems: an LMI approach", Linear Algebra Appl., 351, (2002), 271–302.

[11]. Guabao L., "New results on stability analysis of singular time delay systems", International Journal of Systems Science, 48, (2017), 1395–1403.

[12]. Hale J., "Theory of Functional Differential Equations" in Springer-Verlag, New York, USA, 1977.

[13]. Kilbas A.A., Srivastava H.M., Trujillo J.J., "Theory and Application of Fractional Differential Equations" in Elsevier, New York, USA, (2006).

[14]. Liu S., Li X., Zhou X.F., Jiang W., "Lyapunov stability analysis of fractional nonlinear systems", Appl. Math. Lett., 51, (2016), 13–19.

[15]. Liu S., Wu X., Zhang Y.J., Yang R., "Asymptotical stability of Riemann–Liouville fractional neutral systems", Appl. Math. Lett., 69,(2017), 168–173.

[16]. Liu S., Wu X., Zhou X.F., Jiang W., "Asymptotical stability of Riemann-Liouville fractional nonlinear systems", Nonlinear Dynamics, 86, (2016), 65–71.

[17]. Liu S., Zhou X.F., Li X., Jiang W., "Stability of fractional nonlinear singular systems its applications in synchronization of complex dynamical networks" Nonlinear Dynam., 84, (2016), 2377–2385.

[18]. Liu S., Zhou X.F., Li X., Jiang W., "Asymptotical stability of Riemann–Liouville fractional singular systems with multiple time-varying delays", Appl. Math. Lett., 65, (2017), 32–39.

[19]. Liu Z.Y., Lin C., Chen B., "A neutral system approach to stability of singular time-delay systems", J. Franklin Inst., 351, (2014), 4939–4948.

[20]. Lu Y.F., Wu R.C., Qin Z.Q., "Asymptotic stability of nonlinear fractional neutral singular systems", J. Appl. Math. Comput., 45, (2014), 351–364.

[21]. Podlubny I., "Fractional Differential Equations" in Academic Press., New York, USA, 1999.

[22]. Qian D., Li C., Agarwal R.P., Wong P.J.Y., "Stability analysis of fractional differential system with Riemann–Liouville derivative", Math. Comput. Model., 52, (2010), 862–874.

[23]. Sabatier J., Moze M., Farges C., "LMI stability conditions for fractional order systems" Comput. Math. Appl., 59, (2010), 1594-1609.

[24]. Tunç C., Altun Y., "Asymptotic stability in neutral differential equations with multiple delays", J. Math. Anal., 7, (2016), 40–53.

[25]. Xu S., Van Dooren P., Stefan R., "Robust stability and stabilization for singular systems with state delay and parameter uncertainty", IEEE Trans. Autom. Control, 47, (2002), 1122–1128.

[26]. Yiğit A., Tunç C. "On the stability and admissibility of a singular differential system with constant delay", International Journal of Mathematics and Computer Science, 15, (2020), 641–660.

[27]. Zhou X. F., Hu L.G., Liu S., Jiang W., "Stability criterion for a class of nonlinear fractional differential systems", Appl. Math. Lett., 28, (2014), 25–29.

MANAS Journal of Engineering
ISSN 1694-7398 | e-ISSN 1694-7398

Volume 8 (Issue 1) (2020) Pages 68-76

Stability of the third order rational difference equation

Mehmet Emre Erdogan

Selcuk University, Department of Mathematics, 42250, Konya, Turkey, m_emre448@hotmail.com, ORCID: 0000-0002-7421-0815

ABSTRACT

In this paper, we examine the global stability and boundedness of the difference equation

$$x_{n+1}=\frac{\alpha x_n x_{n-1}+\beta x_n x_{n-2}}{\gamma x_{n-1}+\theta x_{n-2}}$$

where the initial conditions x_{-2}, x_{-1}, x_0 are non zero real numbers and α, β, γ and θ are positive constants such that

$$\alpha+\beta \leq \gamma+\theta.$$

Also, we discuss and illustrate the stability of the solutions of the considered equation via MATLAB at the end of study to support our results.

ARTICLE INFO

Research article

Received: 02.04.2020
Accepted: 22.06.2020

Keywords:
Asymptotic stability, difference equation, global behavior

AMS: 39A10, 39A21, 39A30

1. Introduction

Some mathematical models we construct to better understand and analyze daily life includes amounts that are bound to known values at equal intervals at certain times. These amounts are expressed through sequences as a function of time. These sequences can be expressed as difference equations for the assumptions in the models. Difference equations are used in some modeling such as population growth models, Finance and economic models, business models, consumer behavior models etc. As this topic is interesting for researchers, it will continue to increase researches by using difference equations in the following years. The problems in these studies will be aimed at finding the stability of nonlinear difference equations. Finding solutions and analyzing stability in these studies is a challenging task. Until now, many studies have been done on the stability of nonlinear difference equations. For example:

Yang et al. [1] investigated the global asymptotic stability of the difference equation

$$x_{n+1}=\frac{x_{n-1}x_{n-2}+x_{n-3}+a}{x_{n-1}+x_{n-2}x_{n-3}+a}.$$

Kulenovic, Ladas and Sizer et al. [2] studied the behavior of rational recursive sequence

$$x_{n+1}=\frac{\alpha x_n+\beta x_{n-1}}{\gamma x_n+\delta x_{n-1}}.$$

Elabbasy and colleagues et al. [3] investigated and study some special cases of the difference equation

$$x_{n+1}=\frac{a x_{n-l}x_{n-k}}{b x_{n-p}-c x_{n-q}}.$$

Abdul Khaliq and Elsayed et al. [4] studied behavior and obtained some special cases of the difference equation

$$x_{n+1}=\frac{\alpha x_n x_{n-l}}{\beta x_{n-m}+\gamma x_{n-l}}.$$

See also [5−14]. Our aim is examine the global behavior of the following third-order rational difference equation that will serve as the basis for such modeling

$$x_{n+1}=\frac{\alpha x_n x_{n-1}+\beta x_n x_{n-2}}{\gamma x_{n-1}+\theta x_{n-2}} \tag{0.1}$$

where the initial conditions x_{-2}, x_{-1}, x_0 are non zero real numbers and $\alpha, \beta, \gamma, \theta$ are positive constants such that

$$\alpha+\beta \le \gamma+\theta.$$

A computational examples given at the end of study and simulated solutions of some problems via MATLAB. We hope that the results of this study contribute to the development of the theory on the global stability of nonlinear rational differential equations.

Let us give some definitions and theorems that we need.

Definition 1.1. [15] A difference equation of order $(k+1)$ is an equation of the form

$$x_{n+1}=F(x_n, x_{n-1}, \ldots, x_{n-k}), \quad n=0,1,... \tag{0.2}$$

where F is a function that maps some set I^{k+1} into I. The set I is usually an interval of real numbers, or a union of intervals, or a discrete set such as the set of integers $\square = \ldots, -1, 0, 1, \ldots$.

A solution of (1.2) is a sequence $\{x_n\}_{n=-k}^{\infty}$ that satisfies (1.2) for all $n \ge 0$.

A solution of (1.2) that is constant for all $n \ge -k$ is called an equilibium solution of (1.2). If

$$x_n = \overline{x}, \quad \text{for all} \quad n \ge -k$$

is an equilibrium solution of (1.2), then $\overline{x}$ is called an **equilibrium point**, or simply an **equilibrium** of (1.2).

Definition 1.2. [15] Let $\overline{x}$ be an equilibrium point of (1.2).

i. An equilibrium point $\overline{x}$ of (1.2) is called **locally stable** if, for every $\delta > 0$, there exists $\delta > 0$ such that if $\{x_n\}_{n=-k}^{\infty}$ is a solution of (1.2) with

$$|x_{-k}-\overline{x}|+|x_{1-k}-\overline{x}|+\cdots+|x_0-\overline{x}|<\delta,$$

then

$$|x_n-\overline{x}|<\delta \text{ for all } n \ge 0.$$

ii. An equilibrium point $\overline{x}$ of (1.2) is called **locally asymptotically stable** if, it is locally stable, and if in addition there exists $\gamma > 0$ such that if $\{x_n\}_{n=-k}^{\infty}$ is a solution of (1.2) with

$$|x_{-k}-\overline{x}|+|x_{-k+1}-\overline{x}|+\cdots+|x_0-\overline{x}|<\gamma$$

then

$$\lim_{n\to\infty} x_n = \bar{x}.$$

iii. An equilibrium point $\bar{x}$ of (1.2) is called **global attractor** if, for every solution $\{x_n\}_{n=-k}^{\infty}$ of (1.2), we have

$$\lim_{n\to\infty} x_n = \bar{x}.$$

iv. An equilibrium point $\bar{x}$ of (1.2) is called **global asymptotically stable** if $\bar{x}$ is locally stable and $\bar{x}$ is also global attractor of (1.2).

v. An equilibrium $\bar{x}$ of (1.2) is called **unstable** if $\bar{x}$ is not locally stable.

Definition 1.3. [15] Suppose that the function F is continuously differentiable in some open neighborhood of an equilibrium point $\bar{x}$. Let

$$q_i = \frac{\partial F}{\partial u_i}(\bar{x},\bar{x},\ldots,\bar{x}), \text{ for } i = 0,1,\ldots,k$$

denote the partial derivative of $F(u_0,u_1,\ldots,u_k)$ with respect to u_i evaluated at the equilibrium point $\bar{x}$ of (1.2). Then the equation

$$y_{n+1} = q_0 y_n + q_1 y_{n-1} + \cdots + q_k y_{n-k}, n = 0,1,... \tag{0.3}$$

is called the linearized equation of (1.2) about the equilibrium point $\bar{x}$, and the equation

$$\lambda^{k+1} - q_0\lambda^k - \cdots - q_{k-1}\lambda - q_k = 0 \tag{0.4}$$

is called the characteristic equation of (1.2) about $\bar{x}$.

The following theorem state necessary and sufficient conditions to determine the local asymptotic stability of the equilibrium points of the (1.2).

Theorem 1.1. [15] Assume that a_3, a_2, a_1 and a_0 are real numbers. Then a necessary and sufficient condition for all roots of the equation

$$\lambda^3 + a_2\lambda^2 + a_1\lambda + a_0 = 0$$

to lie inside the unit disk is

$$|a_2 + a_0| < 1 + a_1, \quad |a_2 - 3a_0| < 3 - a_1, \quad \text{and} \quad a_0^2 + a_1 - a_0 a_2 < 1.$$

Theorem 1.2. [15] Let $[p,q]$ be an interval of real numbers and assume that $f:[p,q]^3 \to [p,q]$ is a continuous function satisfying the following properties:

a) $f(x,y,z)$ is non-decreasing in $y,z \in [p,q]$ for each $x \in [p,q]$, and non-increasing in $x \in [p,q]$ for each $y,z \in [p,q]$;

b) If $(m,M) \in [p,q]\times[p,q]$ is a solution of the system

$$M = f(m,M,M) \text{ and } m = f(M,m,m)$$

then $m = M$.

Then (1.2) has a unique equilibrium $\bar{x} \in [p,q]$ and every solution of (1.2) converges to $\bar{x}$.

2. Dynamics of (1.1)

In this section, we investigate the dynamics of (1.1) under the assumptions that all parameters in the equation are positive and the initial conditions are non-negative.

2.1. Local Stability of (1.1)

(1.1) has a unique equilibrium point and is given by the equation

$$\bar{x} = \frac{\alpha \bar{x}^2 + \beta \bar{x}^2}{\gamma \bar{x} + \theta \bar{x}},$$

so,

$$\bar{x}^2(\gamma + \theta) = \bar{x}^2(\alpha + \beta).$$

If $\alpha + \beta < \gamma + \theta$, $\bar{x}_1 = 0$ is the equilibrium point of (1.1),
if $\alpha + \beta = \gamma + \theta$ then $\bar{x}_2 \in$ □ is the equilibrium point of (1.1).

Let $f : (0,\infty)^3 \to (0,\infty)$ be a function defined by

$$f(u,v,t) = \frac{\alpha uv + \beta ut}{\gamma v + \theta t}. \tag{1.1}$$

So,

$$\frac{\partial f}{\partial u}(\bar{x},\bar{x},\bar{x}) = \frac{\alpha + \beta}{\gamma + \theta},$$
$$\frac{\partial f}{\partial v}(\bar{x},\bar{x},\bar{x}) = \frac{\alpha\theta - \beta\gamma}{(\gamma + \theta)^2},$$
$$\frac{\partial f}{\partial t}(\bar{x},\bar{x},\bar{x}) = \frac{\beta\gamma - \alpha\theta}{(\gamma + \theta)^2}.$$

The linearized equation of (1.1) is

$$y_{n+1} - \frac{\alpha + \beta}{\gamma + \theta} y_n - \frac{\alpha\theta - \beta\gamma}{(\gamma + \theta)^2} y_{n-1} - \frac{\beta\gamma - \alpha\theta}{(\gamma + \theta)^2} y_{n-2} = 0, \tag{1.2}$$

and the characteristic equation of (1.1) is

$$\lambda^3 - \frac{\alpha + \beta}{\gamma + \theta}\lambda^2 - \frac{\alpha\theta - \beta\gamma}{(\gamma + \theta)^2}\lambda - \frac{\beta\gamma - \alpha\theta}{(\gamma + \theta)^2} = 0. \tag{1.3}$$

Theorem 2.1. The equilibrium points $\bar{x}_1 = 0$ for $\alpha + \beta < \gamma + \theta$ and $\bar{x}_2 \in$ □ for $\alpha + \beta = \gamma + \theta$ of (1.1) are local asymptotically stable.

Proof. From Theorem 1.1 and (2.3),

$$a_2 = -\frac{\alpha + \beta}{\gamma + \theta}, \quad a_1 = \frac{\beta\gamma - \alpha\theta}{(\gamma + \theta)^2}, \quad a_0 = \frac{\alpha\theta - \beta\gamma}{(\gamma + \theta)^2}.$$

So

$$\begin{aligned}|a_2+a_0|-a_1 &= \left|\frac{\alpha\theta-\beta\gamma}{(\gamma+\theta)^2}-\frac{\alpha+\beta}{\gamma+\theta}\right|-\frac{\beta\gamma-\alpha\theta}{(\gamma+\theta)^2}\\ &= \frac{\alpha\gamma+\alpha\theta+\beta\theta+\beta\gamma}{(\gamma+\theta)^2}\\ &= \frac{(\alpha+\beta)(\gamma+\theta)}{(\gamma+\theta)^2}\\ &\le 1\end{aligned}$$

since $\alpha+\beta\le\gamma+\theta \Rightarrow \frac{\alpha+\beta}{\gamma+\theta}\le 1$.

$$\begin{aligned}|a_2-3a_0|+a_1 &= \left|-\frac{\alpha+\beta}{\gamma+\theta}-3\frac{\alpha\theta-\beta\gamma}{(\gamma+\theta)^2}\right|+\frac{\beta\gamma-\alpha\theta}{(\gamma+\theta)^2}\\ &= \frac{\alpha\gamma+3\alpha\theta+\beta\theta-\beta\gamma}{(\gamma+\theta)^2}\\ &= \frac{\alpha(\gamma+\theta)+\beta(\gamma+\theta)+2\alpha\theta+2\beta\gamma}{(\gamma+\theta)^2}\\ &= \frac{\alpha+\beta}{\gamma+\theta}+2\frac{\alpha\theta+\beta\gamma+\alpha\gamma-\alpha\gamma+\beta\theta-\beta\theta}{(\gamma+\theta)^2}\\ &= 3\frac{\alpha+\beta}{\gamma+\theta}-2\frac{\alpha\gamma+\beta\theta}{(\gamma+\theta)^2}\\ &< 3\end{aligned}$$

and

$$\begin{aligned}a_0^2+a_1-a_0a_2 &= \left(\frac{\alpha\theta-\beta\gamma}{(\gamma+\theta)^2}\right)^2+\frac{\beta\gamma-\alpha\theta}{(\gamma+\theta)^2}+\frac{\alpha\theta-\beta\gamma}{(\gamma+\theta)^2}\cdot\frac{\alpha+\beta}{\gamma+\theta}\\ &= \frac{\beta\gamma-\alpha\theta}{(\gamma+\theta)^2}\cdot\left(\frac{\beta\gamma-\alpha\theta}{(\gamma+\theta)^2}-\frac{\alpha+\beta}{\gamma+\theta}+1\right)\\ &= \frac{\beta\gamma-\alpha\theta}{(\gamma+\theta)^2}\cdot\left(1-\frac{\alpha\gamma+2\alpha\theta+\beta\theta}{(\gamma+\theta)^2}\right)\\ &< 1\end{aligned}$$

from

$$\begin{aligned}\alpha+\beta\le\gamma+\theta &\Rightarrow \alpha\gamma+\alpha\theta+\beta\gamma+\beta\theta\le(\gamma+\theta)^2\\ &\Rightarrow \beta\gamma-\alpha\theta<\alpha\gamma+\alpha\theta+\beta\gamma+\beta\theta\le(\gamma+\theta)^2\\ &\Rightarrow \frac{\beta\gamma-\alpha\theta}{(\gamma+\theta)^2}<1.\end{aligned}$$

By Theorem 1.1, $\overline{x}_1$ *and* $\overline{x}_2$ *are local asymptotically stable of* (1.1) *and the proof is complete.*

2.2. Global Attractor of $\bar{x}$ of (1.1)

Theorem 2.2. The equilibrium points of (1.1) is global attractor.

Proof. Let $[p,q]$ *be real numbers and assume that* $f:[p,q]^3 \to [p,q]$ *is a function defined by* $f(u,v,t)=\dfrac{\alpha uv+\beta ut}{\gamma v+\theta t}$. *Then we can easily see that the function is increasing in* u *and decreasing in* v,t.
Suppose that (m,M) *is a solution of the system*

$$M = f(m,M,M) \text{ and } m = f(M,m,m).$$

Since from (1.1)

$$m=\frac{\alpha Mm+\beta Mm}{\gamma m+\theta m} \text{ and } M=\frac{\alpha mM+\beta mM}{\gamma M+\theta M}$$

we have

$$(\gamma+\theta)m^2 = Mm(\alpha+\beta) \text{ and } (\gamma+\theta)M^2 = Mm(\alpha+\beta)$$

then

$$(\gamma+\theta)(M^2-m^2)=0.$$

Thus

$$M=m.$$

By Theorem 1.2, $\bar{x}_1$ *and* $\bar{x}_2$ *are global attractor of* (1.1) *and the proof is complete.*

2.3. Boundedness of Solutions of (1.1)

Theorem 2.3. Every solution of (1.1) is bounded.

Proof. Let $\{x_n\}_{n=-2}^{\infty}$ *be a solution of* (1.1). *Let* $M=max\{x_{n-1},x_{n-2}\}$. *From* (1.1)

$$x_{n+1}=\frac{\alpha x_n x_{n-1}+\beta x_n x_{n-2}}{\gamma x_{n-1}+\theta x_{n-2}} \le \frac{\alpha x_n M+\beta x_n M}{\gamma M+\theta M} < \frac{(\gamma+\theta)x_n M}{\gamma M+\theta M},$$

which implies that $x_{n+1}<x_n$ *for* $n\ge 0$. *Then*

$$\lim_{n\to\infty} x_n = \bar{x}.$$

Then, the proof is complete.

3. Computational examples

In this section, I perform computational examples to illustrate the validity of main results. In order to better express the numerical samples, a graph of the solutions was obtained by using matlab. These graphs are drawn with different parameters and different starting conditions.

- In Fig.1, The equilibrium $\bar{x}_1=0$ of (1.1) is shown to be global asymptotically stable under the initial conditions $x_{-2}=3.456, x_{-1}=7.879, x_0=-6.841$ and the parameters $\alpha=3,\beta=4,\gamma=5,\theta=6$ that meet the condition $\alpha+\beta<\gamma+\theta$.

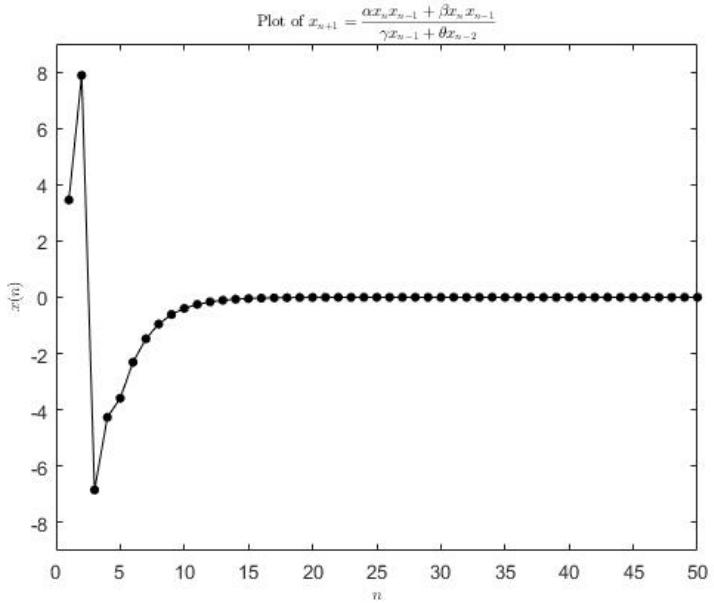

Figure 1. *Stability of the solutions of (1.1) under the condition* $\alpha + \beta < \gamma + \theta$.

- In Fig.2, The equilibrium $\overline{x}_2 = 15 \in$ of (1.1) is shown to be global asymptotically stable under the initial conditions $x_{-2} = -4.159, x_{-1} = 4.751, x_0 = -8.874$ and the parameters $\alpha = 3, \beta = 5, \gamma = 6, \theta = 2$ that meet the conditions $\alpha + \beta = \gamma + \theta$.

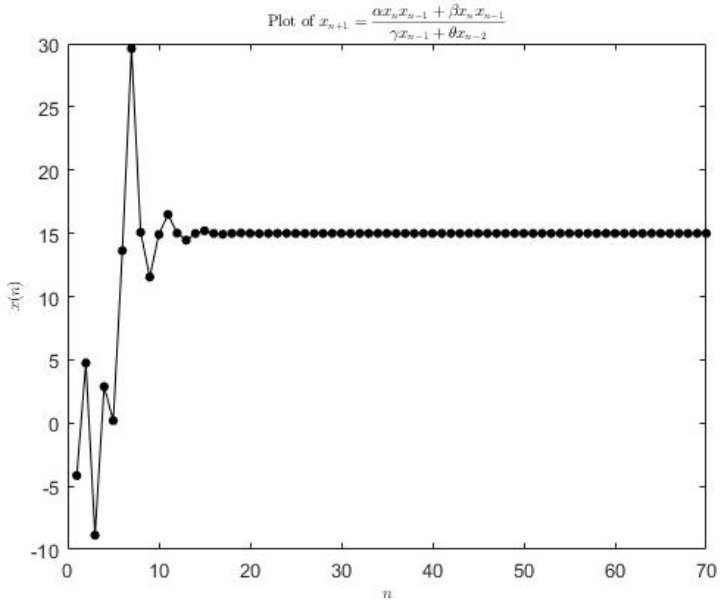

Figure 2. *Behavior of (1.1) under the condition* $\alpha + \beta = \gamma + \theta$.

- In Fig.3, (1.1) is shown to be not global asymptotically stable under the initial conditions $x_{-2} = -2.074, x_{-1} = 7.358, x_0 = -3.189$ and the parameters $\alpha = 3, \beta = 5, \gamma = 4, \theta = 3$ that meet the condition $\alpha + \beta > \gamma + \theta$.

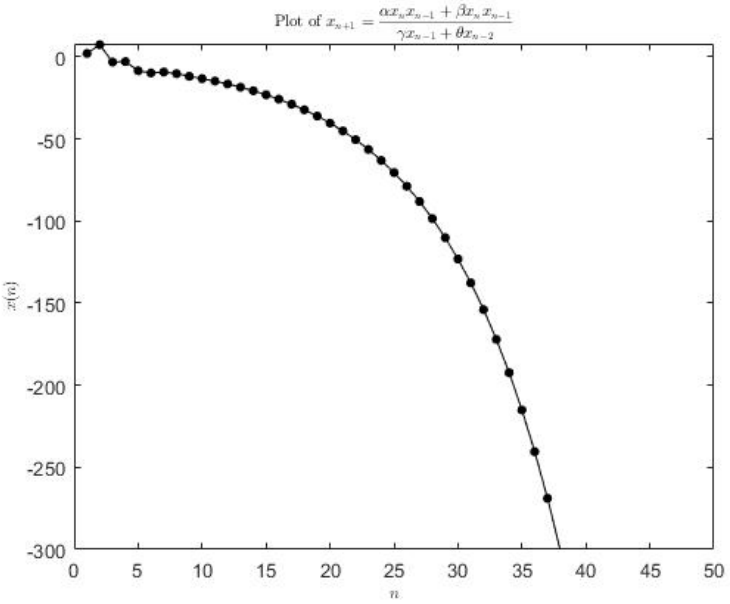

Figure 3. *Unboundness solutions of (1.1) under the condition* $\alpha + \beta > \gamma + \theta$.

References

[1]. Yang X., "On the global asymptotic stability of the difference equation $x_n = \frac{x_{n-1}x_{n-2} + x_{n-3} + a}{x_{n-1} + x_{n-2}x_{n-3} + a}$", Applied Mathematics and Computation, 171(2), (2005), 857–861.

[2]. Kulenović M.R.S., Ladas G., Sizer W.S., "On the recursive sequence $x_{n+1} = \frac{\alpha x_n + \beta x_{n-1}}{\gamma x_n + \delta x_{n-1}}$", Mathematical Sciences Research Hot-Line, 2(5), (1998), 1–16.

[3]. Elabbasy E.M., El-Metwally H.A., Elsayed E.M., "Global behavior of the solutions of some difference equations", Advances in Difference Equations, 1, (2011), 28.

[4]. Khaliq A., Elsayed E.M., "Qualitative study of a higher order rational difference equation", Hacettepe Journal of Mathematics and Statistics, 47(5), (2018), 1128–1143.

[5]. Erdogan M.E., Cinar C., Yalcinkaya I., "On the dynamics of the recursive sequence $x_{n+1} = \frac{x_{n-1}}{\beta + \gamma x_{n-2}^2 x_{n-4} + \gamma x_{n-2} x_{n-4}^2}$", Computers & Mathematics with Applications, 61(3), (2011), 533-537.

[6]. Erdogan M.E., Cinar C., Yalcinkaya I., "On the dynamics of the recursive sequence $x_{n+1} = \frac{\alpha x_{n-1}}{\beta + \gamma \sum_{k=1}^{t} x_{n-2k} \prod_{k=1}^{t} x_{n-2k}}$", Mathematical and Computer Modelling, 54(5), (2011), 1481-1485.

[7]. Erdogan M.E., Cinar C., "On the dynamics of the recursive sequence $x_{n+1} = \frac{\alpha x_{n-1}}{\beta + \gamma \sum_{k=1}^{t} x_{n-2k}^p \prod_{k=1}^{t} x_{n-2k}^q}$", Fasciculi Mathematici, 50, (2013), 59-66.

[8]. Abo-Zeid R., Al-Shabi M.A., "Global Behavior of a third order difference equation", Tamkang Journal of Mathematics, 43(3), (2012), 375-383.

[9]. Agarwal R.P., Difference Equations and Inequalities: Theory, Methods, and Applications, Chapman \& Hall/CRC Pure and Applied Mathematics, (2000).

[10]. Karakostas G.L., "Convergence of a Difference Equation Via The Full Limiting Sequences Method", Differential Equations and Dynamical Systems, 1(4), (1993), 289–294.

[11]. Belhannache F., Touafek N., Abo-Zeid R., "Dynamics of a third-order rational difference equation". Bulletin Mathematique de La Societe Des Sciences Mathematiques de Roumanie, 59(1), (2016), 13–22.

[12]. Hamza A.E., Ahmed A.M., Youssef A.M., "On the recursive sequence $x_{n+1}=\frac{a+bx_n}{A+Bx_{n-1}^k}$", Arab Journal of Mathematical Sciences, 17(1), (2011), 31–44.

[13]. Hamza A.E., Elsayed E.M., "Stability problem of some nonlinear difference eqauations", International Journal of Mathematics and Mathematical Sciences, 21(2), (1998), 331–340.

[14]. Grove A.E., Ladas G., Predescu M., Radin M., "On the Gloval Character of the Difference Equation $x_{n+1}=\frac{\alpha+\gamma x_{n-(2k+1)}+\delta x_{n-2l}}{A+x_{n-2l}}$". Journal of Difference Equations and Applications, 9(2), (2003), 171–199.

[15]. Camouzis E., Ladas G., Dynamics of Third - Order Rational Difference Equations with Open Problems and Conjectures, Chapman and Hall/CRC, (2007).